LUND UNIVERSITY

Death, survival, and morphological development of hippocampal granule cells born in an inflammatory environment

Bonde, Sara

2009

Death, survival, and morphological development of hippocampal granule cells born in an inflammatory environment

Sara Bonde

LUNDS UNIVERSITET
Medicinska fakulteten
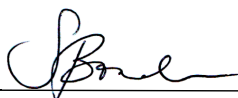
Organization LUND UNIVERSITY	Document name DOCTORAL DISSERTATION
Section of Restorative Neurology BMC A11 Sölvegatan 17 22184 Lund, Sweden	Date of issue January 16, 2009
Author(s) Sara Bonde	Sponsoring organization

Title and subtitle
Death, survival, and morphological development of hippocampal granule cells born in an inflammatory environment

Abstract

The brain continues to form new neurons throughout life. This process of adult neurogenesis has been thoroughly documented in several species including birds, rodents and humans. Adult neurogenesis is not a global process, but is confined to two subcompartments of the brain; the subventricular zone lining the lateral ventricles, and the subgranular zone (SGZ) in the hippocampal formation. A variety of stimuli such as voluntary exercise, epileptic seizure activity and inflammation can affect the basal level of neurogenesis. In the course of pathological conditions such as Alzheimer's disease, multiple sclerosis, epilepsy and stroke, an inflammatory response is initiated in the brain. Prolonged epileptic seizure activity, status epilepticus (SE), strongly imposes on the integrity of the delicate brain structure and cell communication. SE not only induces inflammation, but also neuronal death and a transient increase of basal adult neurogenesis in the hippocampal formation. What role inflammation plays in a disease such as epilepsy, and how it affects the neurons born in the aftermath of seizure activity, is largely unknown. The specific aim of the four studies included in this thesis was to investigate the effect inflammation has on the amount of basal and seizure-induced neurogenesis, and if the morphological development or functional characteristics of new neurons is affected when the neuron is born into an inflammatory environment. In brief, the purpose was to investigate the quantity and quality of the neurogenic outcome in inflammation. To comprehend the interplay between neurogenesis and inflammation would provide a valuable insight into disease progression, and could ultimately be part of the treatment or even a cure for pathological conditions involving seizure activity and inflammation.

Key words
Hippocampus, granule cells, adult neurogenesis, microglia, inflammation, status epilepticus, dendritic spines, gephyrin

Classification system and/or index terms (if any)

Supplementary bibliographical information	Language English

Distribution by (name and address)
Sara Bonde, Section of Restorative Neurology, Lund University, BMC A11, Sölvegatan 17, 221 84 Lund, Sweden

I, the undersigned, being the copyright owner of the abstract of the above-mentioned dissertation, hereby grant to all reference sources permission to publish and disseminate the abstract of the above-mentioned dissertation.

Signature _____   Date ___November 30, 2008___

Beauty often seduces us on the road to truth.
House M.D., 'Occam's Razor'

Contents

List of papers

A.

Inflammation is detrimental for neurogenesis in the adult brain.
Ekdahl CT, Claasen JH, Bonde S, Kokaia Z, Lindvall O.
PNAS 2003; 100 (23) 13632 - 37

B.

Long-term neuronal replacement in the adult rat hippocampus after status epilepticus despite chronic inflammation.
Bonde S, Ekdahl CT, Lindvall O.
Eur J Neurosci 2006; 23 (4) 965 - 74

C.

Environment matters: synaptic properties of neurons born in the epileptic adult brain develop to reduce excitability.
Jakubs K, Nanobashvili A, Bonde S, Ekdahl CT, Kokaia Z, Kokaia M, Lindvall O.
Neuron 2006; 52 (6) 1047 - 59

D.

Inflammation regulates functional integration of neurons born in the adult brain.
Jakubs K*, Bonde S*, Iosif R, Ekdahl CT, Kokaia Z, Kokaia M, Lindvall O.
*Authors contributed equally
J Neurosci 2008; 28 (47) 12477 - 88

Abbreviations and glossary

aCSF   **artificial cerebrospinal fluid**
              synthetic variety of the fluid circulating the brain and spine
BrdU   **bromodeoxyuridine**
              thymidine analogue
CNS   **central nervous system**
              brain and spinal cord
DG   **dentate gyrus**
              part of the hippocampal formation of the temporal lobe
EEG   **electroencephalogra (m/ph/phic)**
              measurement of brain activity
GC(s)   **granule cell(s)**
              main excitatory cell of the dentate gyrus
GCL   **granule cell layer**
              clearly outlined dense aggregation of granule cell somata in
              the dentate gyrus
IL   **interleukin**
              a family of cytokines
LPP   **lateral perforant path**
              neuronal connection between the entorhinal cortex and
              molecular layer
LPS   **lipopolysaccharide**
              potent trigger of bacteria-like inflammation, naturally
              occuring motif on gram-negative bacteria
ML   **molecular layer**
              part of the hippocampal formation, where the granule cells
              extend their dendrites
PTX   **picrotoxin**
              $GABA_A$ channel blocker that isolates excitatory currents
SE   **status epilepticus**
              long-lasting epileptic seizure
SGZ   **subgranular zone**
              strip between the granule cell layer and the hilus where the
              neural stem/progenitor cells are located and give rise to
              adult neurogenesis.
TTX   **tetrodotoxin**
              action potential blocker that isolates spontaneous cell
              membrane activity

Abstract

The brain continues to form new neurons throughout life. This process of adult neurogenesis has been thoroughly documented in several species including birds, rodents and humans. Adult neurogenesis is not a global process, but is confined to two subcompartments of the brain; the subventricular zone lining the lateral ventricles, and the subgranular zone (SGZ) in the hippocampal formation. A variety of stimuli such as voluntary exercise, epileptic seizure activity and inflammation can affect the basal level of neurogenesis. In the course of pathological conditions such as Alzheimer's disease, multiple sclerosis, epilepsy and stroke, an inflammatory response is initiated in the brain. Prolonged epileptic seizure activity, status epilepticus (SE), strongly imposes on the integrity of the delicate brain structure and cell communication. SE not only induces inflammation, but also neuronal death and a transient increase of basal adult neurogenesis in the hippocampal formation. What role inflammation plays in a disease such as epilepsy, and how it affects the neurons born in the aftermath of seizure activity, is largely unknown. The specific aim of the four studies included in this thesis was to investigate the effect inflammation has on the amount of basal and seizure-induced neurogenesis, and if the morphological development or functional characteristics of new neurons is affected when the neuron is born into an inflammatory environment. In brief, the purpose was to investigate the quantity and quality of the neurogenic outcome in inflammation. To comprehend the interplay between neurogenesis and inflammation would provide a valuable insight into disease progression, and could ultimately be part of the treatment or even a cure for pathological conditions involving seizure activity and inflammation.

Svensk sammanfattning

Det finns många myter kring vårt kanske viktigaste organ - hjärnan. Till exempel hör man ofta att vi bara använder 10 procent av vår hjärna, och att den vuxna hjärnan inte får några nya nervceller. Men båda dessa påståenden är just myter, vetenskapligt motbevisade. Redan i mitten av 1960-talet hittade forskare tecken på att den vuxna hjärnan bildar nya nervceller, och i slutet av 1990-talet visades det definitivt att människans hjärna får tillskott av nya nervceller under hela livet. Dock bildas det inte nya nervceller överallt i vår hjärna, utan intressant nog bara i två områden: subventrikulärzonen och subgranulärzonen. Den senare nämnda finns i hippocampus-regionen i hjärnan, ett område som är viktigt för minnet, och det spekuleras att det är för att öka hjärnans minneskapacitet det bildas nya nervceller just här. I normala fall bildas de nya nervcellerna med en jämn takt, men olika faktorer såsom motion, inflammation och epileptiska anfall kan påverka med vilken hastighet, och hur många nya nervceller som bildas.

Ungefär en procent av befolkningen har diagnosen epilepsi, vilket innebär återkommande, spontana krampanfall. Medicinerna som idag finns tillgängliga hjälper långt ifrån alla med epilepsi att bli helt anfallsfria. På grund av bland annat denna bristande effekt hos tillgänglig medicin, behövs mer kunskap om vad som händer i hjärnan vid epileptiska anfall. Efter ett kraftigt och långvarigt epileptiskt anfall, så kallat status epilepticus (SE), ökar nervcellsnybildningen i subgranulärzonen tillfälligt, och det uppstår även en lokal aktivering av immunsystemet (inflammation) i området. Man har tidigare inte vetat om de nervceller som bildas efter SE beter sig som normala nervceller, eller om den efterföljande inflammationen eventuellt påverkar hur de nya nervcellerna utvecklas. Målet med de fyra vetenskapliga studier som ingår i den här avhandlingen var att ta reda på hur inflammation och epileptiska anfall påverkar nya nervcellers död och överlevnad, och om de nya nervcellerna påverkas till utseende eller beteende av att bildas i en sjuk miljö med inflammation och/eller epileptiska anfall.

De fyra studier som presenteras i denna avhandling har bidragit till en utökad kunskap rörande det viktiga samspelet mellan nybildning av nervceller (neurogenes) och inflammation i hjärnan genom att studera dessa processer i djurmodeller av inflammation och SE. Den första studien (**Paper A**) visar hur både den normala och den SE-orsakade nervcellsnybildningen är negativt påverkade av inflammation. Förekomsten av inflammation minskar drastiskt antalet överlevande nya nervceller, och på motsvarande sätt leder en samtidig anti-inflammatorisk behandling till en ökad nervcellsöverlevnad. Fastän inflammation därför kan anses vara negativt för nya nervceller, samt att den andra studien (**Paper B**) visar att

inflammationen efter SE blir kroniskt långvarig, ser vi att många av de nya nervceller som bildats direkt efter SE faktiskt överlever, trots att de har bildats och mognat i en inflammatorisk miljö. Sex månader efter ett SE-anfall är de nya nervcellerna fortfarande kvar i subgranulärzonen, och utgör så många som 10 procent av det totala antalet nervceller i området. I de två sista studierna påvisas att miljön som nya nervceller bildas i spelar en avgörande roll för deras beteende och signalering till andra nervceller, trots att de utseendemässigt inte går att skilja från äldre mogna nervceller. Nervceller som bildas i en miljö med epileptiska anfall (**Paper C**) eller i en miljö med enbart inflammation (**Paper D**) har en ökad benägenhet till minskad nervcellssignalering, och en samtidig minskad benägenhet till ökad signalering. Detta resultat är spännande eftersom epileptiska anfall just är karaktäriserade av bland annat en ökad nervcellssignalering. Att dessa nya nervceller då alltså bidrar till att minska nervcellsignaleringen i hjärnan, skulle kunna tyda på att de nervceller som bildas efter ett epileptiskt anfall försöker motverka att fler anfall uppstår. Förhoppningar finns om att denna vetskap på längre sikt ska kunna utgöra en grund för en ny typ av behandling mot epilepsi, och även i förlängningen kunna öka förståelsen kring andra sjukdomar med inflammation och nervcellspåverkan, t.ex. Alzheimers sjukdom och multipel skleros.

Introduction

The Brain

In ancient Egypt the brain was regarded as nothing more than cranial stuffing, and hence removed – through the nose – before mummification. It was in the heart intelligence was thought to lie. This belief did not change for 2500 years, even Aristotele (300 B.C.) agreed with this notion. Then along came Herophilos; a pioneer in basing medical conclusions on actual dissections of the human body. Through his novel work, he recognized that intelligence was located in the brain, the centre of the nervous system. He was among the first to consider it essential to base knowledge on empiric experimental study, and not religious belief, as did many of his predecessors, thereby laying the foundation to the scientific method in use today.

Hippocampus

Memory is a complex process of imprint, storage, and retrieval of information, involving a network of anatomical structures throughout the brain. Memory is a process that declines during normal ageing and in diseases such as Alzheimer's. The frontal lobes and basal ganglia play important roles in memory, as does the amygdala, which is further involved in the emotional component. However, it is the seahorse-shaped structure located in the temporal lobe, the hippocampus, that perhaps plays the most crucial role in memory processing. In a case study from the 1950s, it was demonstrated that the hippocampus is responsible for imprinting new memories, but not the actual site of memory storage. The patient HM underwent a surgical procedure, removing both hippocampi and medial parts of the right and left temporal lobe. Afterwards, he was diagnosed with anterograde amnesia, meaning that his old memories were unaffected and available to him, but he could not form any new memories after the surgery.

The hippocampal structure comprises the dentate gyrus (DG) with granule cell (GC) neurons arranged in a compact granule cell layer (GCL), partially enclosing the hilus. The part of the GCL closest to the hilus, and the part of hilus closest to the GCL are collectively referred to as the subgranular zone (SGZ), a structure involved in adult neurogenesis. Other parts of the hippocampal structure mentioned in this thesis are the inner and outer molecular layer (iML and oML) where the entorhinal axons connect to GC dendrites, and the CA1 and CA3 part of the information-processing pathway of the hippocampus (**FIGURE** 1). The temporal lobes and

especially the hippocampal structure are particularly vulnerable and often affected in diseases such as epilepsy.
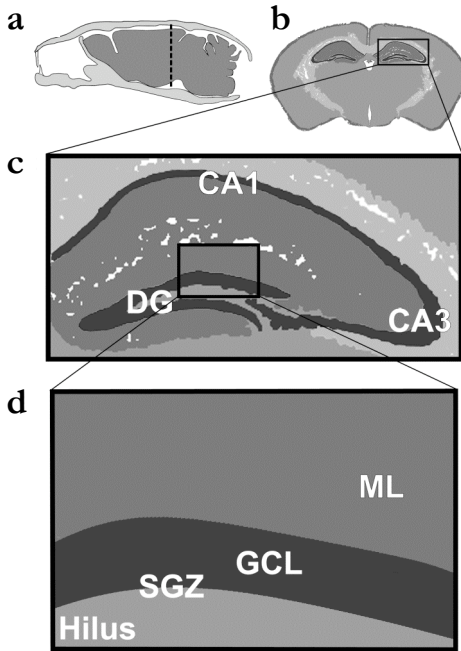
FIGURE 1. Schematic layout of relevant rat brain anatomy. The rat brain (a) is cut along the black dashed line forming a coronal section (b). The hippocampus (rectangle, b) is comprised of the CA1, CA3 and dentate gyrus (DG, c). A further magnification (rectangle, c) reveals granule cell layer (GCL) where granule cell (GC) somata are located, the subgranular zone (SGZ) on the GCL-hilus border where new neurons are born in the adult brain, and the molecular layer (ML) into which the GCs extend their dendritic trees, and the hilus into which the GCs extend their axons toward CA3 (d).

Neurons

All cells are surrounded by a hydrophobic cell membrane that prevents free passage of molecules and ions. This restricted in- and outflux converts free energy, ultimately from oxygen-<dependent cell metabolism, into a membrane potential. Keeping the membrane potential at steady state is essential for the survival of each cell. Reduced oxygen supply to cells, such as seen in stroke, will disrupt the membrane potential and cause promiscuous in- and outflux across the membrane, and necrotic cell death. Leaky necrotic cells will release energy-rich compounds such as ions and molecules into the extra-cellular space in an uncontrolled manner, which in turn may propagate the damage to neighbouring cells.

In the case of neurons, the cytoplasm close to the membrane is negatively charged relative to the outside the cell. This potential is maintained by energy-requiring ion exchange through sodium-potassium pumps in the cell membrane. Energy is delivered to the pumps as adenosine triphosphate (ATP) molecules, formed in the process of cell metabolism. For each ATP, three sodium (Na^+) ions are transported out and two

potassium (K$^+$) ions are transported into the neuron. This causes a relative reduction of positive charge inside the cell, due to imbalance of ions, and forms the basis for the electrical charge of −70 mV across neuronal cell membranes. Furthermore, the sodium-potassium transport causes a chemical imbalance over the cell membrane, which together with the ion-imbalance is known as the electrochemical potential.

Neurons have a unique communicatory system based on the electrochemical potential, where rapid electrical discharges are passed from cell to cell within the neuronal network. In general, a neuron is composed of a dendritic tree, through which it receives signals from other neurons; a cell soma containing the nucleus with the DNA for neuronal proteins; the axon through which the electrical signal is quickly conveyed; and finally a synaptic bouton where it connects by a synapse onto the next neuron and conveys the electric impulse (**FIGURE 2**).
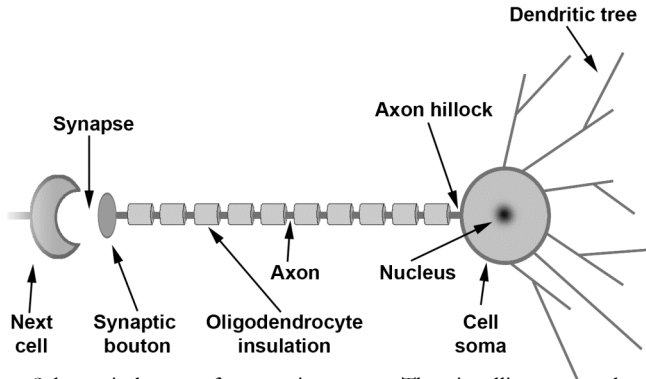
FIGURE 2. Schematic layout of a generic neuron. The signalling enters through the dendritic tree, through the soma, to the axon hillock where it converts to an action potential that travels the length of the axon to the synaptic bouton where vesicles containing a transmitter substance are released into the synaptic cleft and induce a response in the postsynaptic (next) cell.

Several neurons connect to the dendritic tree of a single neuron and release inhibitory or excitatory transmitter substance into the synaptic cleft. Excitatory transmitter substances such as glutamate bind to ion-channels in the postsynaptic membrane, causing them to open and allow Na$^+$ to flow into the next neuron along the electrochemical gradient and depolarize the membrane potential (< −70 mV). In contrast, inhibitory transmitter substances such as GABA cause negatively charged chloride ions to enter the next cell and hyperpolarize the membrane potential (> −70 mV). If enough positive charge enters the connection between the dendritic tree and the axon (or 'axon hillock'), and ultimately the next cell soma, an electrical impulse is initiated. The electrical impulse is an 'all-or-none' response

known as the action potential, which in turn opens voltage-sensitive channels that allow more Na^+ into the cell, propagating the signal along the axon to the synaptic bouton. Once in the presynaptic bouton, the axon potential causes influx of Ca^{2+} ions, which allow transmitter substance-containing vesicles to fuse with the cell membrane and release their content into the synaptic cleft. These transmitter substances cause de- or hyperpolarization of the next postsynaptic membrane, and hence the communicated electrical impulse continues within the neuronal network.

Glia

Knowledge of glial cells has been limited, and they have long had to suffice for being merely supportive of the *important* cell of the brain – the magnificent neuron. Although the phrase 'brain cell' commonly refers to a neuron, glial cells actually outnumber neurons immensely. Interest in glial cells has greatly increased in recent research, which has acknowledged their crucial presence and function.

Glial cells of the CNS are divided into macroglia (astrocytes and oligodendrocytes) and microglia. Astrocytes help maintain tissue homeostasis by removing excess transmitter substance from neuronal synaptic clefts, partaking in communication by emitting and responding to growth factors and cytokines, and protecting the brain by lining CNS blood vessels with large end-feet, thus forming the blood-brain barrier. Oligodendrocytes are crucial for high-speed neuronal signalling since they insulate most neuronal axons. Microglia, on the other hand, form a primary defence against invading pathogens and damage, and are described in further detail in the next chapter 'Inflammation'.

Inflammation

The concept of inflammation is complex, and trying to precisely specify which cells and molecules define it is difficult. Inflammation can be beneficial or harmful, or both, and depending on the type of stimuli the inflammatory outcome can vary greatly. One hallmark of inflammation in the brain is increased quantity and altered quality of the microglia cells. The number of microglia can increase either through proliferation of endogenous microglia, or invasion of microglia across the blood-brain barrier, while the quality of microglia alters in respect to cell morphology and to the level and type of factors secreted.

Microglia

The microglial cell was originally discovered and described by Del Rio-Hortega in early 1930's (Del Rio-Hortega 1932). Microglia are the immunocompetent brain-resident macrophages (Kreutzberg 1996). Macrophages are able to remove tissue debris by internalising it, a process important for maintaining tissue homeostasis. Unlike neurons and all other brain cells, the microglia are of mesodermal origin. This means microglia are formed outside the brain during embryonic development, and perinatally invade the rodent brain parenchyma to establish the endogenous microglial population (Ling and Wong 1993, Chan *et al.* 2007). Microglia comprise about 13 percent of glial cells in the CNS white matter (Hayes *et al.* 1987), the rest being predominately astrocytes and oligodendrocytes. In the CNS microglia are the primary surveillance and effector cells of the immune system. They help maintain homeostasis by serving as a primary defence against invading pathogens and damage, both by engulfing cellular debris through vesicular phagocytosis and by their intimate relationship with the immune system.

Quiescent microglia form a non-overlapping three-dimensional grid of cell somata territorially fixed in space. The cells are ramified, with several highly branched processes protruding from each soma (Kreuzberg 1996). These processes are dynamic, constantly extending and retracting within their designated perimeter; randomly scanning the entire extracellular space every few hours. This process allows the 'quiescent' microglia to maintain an active vigilance for abnormalities in the extra-cellular space. Microglia cells refrain from making physical contact with each other, but commonly contact astrocytes, neurons, and blood vessels, which suggests an important microglial role in cell-to-cell communication within the CNS (Nimmerjahn *et al.* 2005).

Microglia detect a variety of potentially harmful stimuli through surface receptors such as complement factors, immunoglobulins, purines, neurotransmitters, growth factors, and cytokines (for review, see Hanisch and Kettenmann 2007). Upon detection of a harmful stimulus, microglia undergo a series of morphological and functional changes, the extent of which depends on the nature of the threat/trigger. When activated the highly ramified, rod-shaped microglia cell somata will become increasingly rounded while the processes will shorten and thicken (Kreutzberg 1996). The microglia become polarized, as they extend their processes towards the site of injury, shielding the injured area through accumulation of microglial extensions (Nimmerjahn *et al.* 2005). The microglia somata will subsequently start to migrate and/or proliferate following activation, along with phenotypic and functional changes such as increased expression of major histocompatibility complex II (MHC-II), and a wide variety of complement proteins, cytokines, trophic factors, and cytotoxins (Gehrmann *et al.* 1995, de Simoni *et al.* 2000, Butovsky *et al.* 2005, Gibbons and Dragunow 2006, Ziv *et al.* 2006b). Resting microglia show a low density of ion channels, but when becoming increasingly active, the electrophysiological properties change with addition of inward rectifying potassium currents, and later outward potassium currents (Boucsein *et al.* 2000, Lyons *et al.* 2000). In a final state of microglial activation, the microglia become phagocytic, internalising and breaking down potentially toxic debris (Streit and Kreutzberg 1988).

To avoid adverse effects of inflammation, it is crucial for the organism that the ongoing inflammatory process is fine-tuned and balanced, and it has been suggested that microglia are down-regulated and removed through apoptosis after a threat has been cleared (Gehrmann 1995, Gehrmann and Banati 1995). If the inflammatory process is not balanced the immune system could attack surrounding healthy host cells, a phenomenon seen in autoimmune diseases such as multiple sclerosis and diabetes. Following CNS injury, a highly complex cellular and molecular interplay occurs, an inflammatory communication that involves most CNS cells (e.g. microglia, neurons, astrocytes, and oligodendrocytes; see **FIGURE 3**).

FIGURE 3. An illustration of parts of the complex neuron-glia communication in CNS health and injury. Further information is provided and discussed in recent reviews (Ziv and Schwartz 2008, Pocock and Kettenmann 2007, Ekdahl *et al.* 2008, Barres 2008, Chen and Palmer 2008)
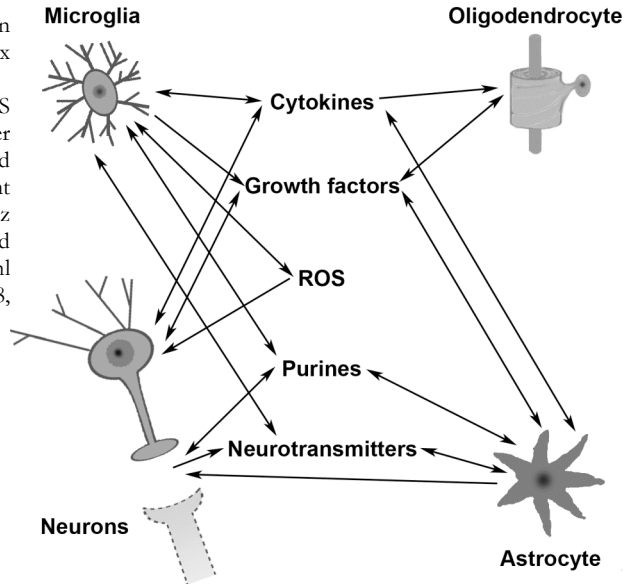
Neurogenesis

The notion that new neurons are continuously being born in the adult brain was reported already in the mid 1960's by Josef Altman and Gopal Das (Altman and Das 1965). However, their findings were controversial and therefore largely neglected for decades. Nevertheless, during the 1990s, their data was verified and supported, when repeated in several new publications using modern techniques (Gould and Cameron 1996, Gage *et al.* 1998). Today, the presence of adult neurogenesis is largely accepted, and has been documented in several non-mammalian species and a wide variety of mammals, including humans (Kaplan and Hinds 1977, Goldman and Nottebohm 1983, Gould *et al.* 1997, Eriksson *et al.* 1998). Neurogenesis has controversially been implicated to occur in multiple structures throughout the adult brain, but to date, only truly accepted to occur from neural stem/progenitor cells in two discrete regions: the subventricular zone of the lateral ventricle wall and in the subgranular zone (SGZ) of the dentate gyrus (DG), part of the hippocampal formation located within the temporal lobe (**FIGURE 1**) (Taupin and Gage 2002).

Adult neurogenesis in the granule cell layer

The process of adult hippocampal neurogenesis largely resembles the corresponding perinatal process (Espósito *et al.* 2005), where developing granule cells go through distinct electrophysiological and morphological

stages, and express a variety of cellular markers. In the DG, radial glia-like precursor (type-1) cells in the SGZ, located on the border between DG and hilus, give rise to transiently amplifying progenitor (type-2) cells. The round type-2 cells express DCX, a marker for proliferating neuronal progenitors. DCX+ cells become hyperpolarized by ambient GABAergic input, which drives the process of maturation further through an intermediate (type-3) cell type, before the cell becomes postmitotic and unable to further divide (eds. Gage *et al.* 2008). Maturing GCs migrate further into the GCL and start sprouting appropriate dendritic projections towards the inner molecular layer (ML) (Shapiro *et al.* 2007, Zhao *et al.* 2006). Within 10 days after cell birth, the axons projecting from the immature GCs through the hilus start reaching their CA3 target area, the dendritic tree continues to branch while reaching the outer ML (Shapiro *et al.* 2007, Zhao *et al.* 2006).

The early depolarizing GABAergic input onto adult-born granule cells becomes increasingly hyperpolarizing during maturation, and the maturing granule cells progressively receive more glutamatergic synaptic input (Espósito *et al.* 2005, Overstreet-Wadiche and Westbrook 2006). An abundance of new granule cells are born, out of which a minority survives in a glutamate-dependent way (Tashiro *et al.* 2006). Within 16 days after granule cell birth, appropriate axonal connections have been made, the dendritic tree has branched even further, and GCs display the four types of dendritic spines onto which predominately excitatory glutamatergic input connects (Zhao *et al.* 2006). This connection between entorhinal cortex and GC dendritic spines is the first synapse in the trisynaptic pathway of hippocampal information processing, whereas the second synapse is between the GC axon and CA3 pyramidal cell dendrites, and the third between axons of CA3 pyramimdal cells and CA1 neuronal dendrites. Subsequently, the CA1 cell conveys the information back to the entorhinal cortex (Witter and Amaral 2004). Within two months after adult birth, the new GCs become electrophysiologically and morphologically indistinguishable from neighbouring, older GCs in the GCL (van Praag *et al.* 2002, Espósito *et al.* 2005).

Regulation of neurogenesis

Adult neurogenesis is strictly controlled and limited to the neurogenic niche, a confined subcompartment within the hippocampus, which permits the neural stem cells to proliferate and continuously give rise to new neurons throughout life. The hippocampal neurogenic niche is comprised of neurons, astrocytes, microglia, transmitters, cytokines, and blood vessels, all of which contribute in a complex manner to the delicate balance of neurogenesis. Under physiological conditions, adult rodent

neurogenesis produces a steady amount of around 9000 new GC neurons on a daily basis (Cameron and McKay 2001). A change within the neurogenic niche can potentially alter any stage of the neurogenic process; the proliferation, survival, migration, maturation, or functional integration of the new GCs. Factors such as stress (Gould *et al.* 1998), ageing (Kuhn *et al.* 1996), and depression (Brezun and Daszuta 1999) can ultimately reduce neurogenesis. On the contrary, voluntary exercise (van Praag *et al.* 1999), enriched environment (Kempermann *et al.* 1997), learning (Gould *et al.* 1999) and epileptic seizures (Parent *et al.* 1997) have been shown to increase neurogenesis.

Results

Status epilepticus and bacteria-like infection cause acute and chronic inflammation

Following detection of bacteria-like infection through LPS infusion (**Paper A, D**) or trauma caused by SE seizure (**Paper A, B, C**), microglia become activated in the dentate gyrus and initiate removal of tissue debris through vesicular phagocytosis (**FIGURE 4**). The cell processes become shorter, fewer, and thicker, whilst the homogenous three-dimensional grid of microglial somata is disrupted when the cells cluster in the SGZ-GCL and the hilus (**Papers A, B, C, D**). The activation of microglia is rapid, and about four times more microglia are phagocytotically active one week after SE (**Paper C**) and LPS-infusion (**Paper D**) as compared to the respective control treatments. The acute activation of microglia becomes chronic, and is still present within both SGZ-GCL and hilus at least six months after an SE insult (**Paper B**) and seven weeks after a single LPS-infusion (**Paper C**).

Non-resident microglia are known to infiltrate the brain across the blood-brain-barrier at two, six, and sixteen weeks after experimental stroke (Thored *et al.*, 2008), a feature that does not occur five weeks or six months following SE (**Paper B**). In pilocarpine-induced SE, astrogliosis is prominent in the hippocampus ten and thirty-one days after the insult (Borges *et al.* 2003), but in our studies not present at five or six weeks, or six months, after electrically induced SE (**Paper B** unpublished observation, **Paper C**).

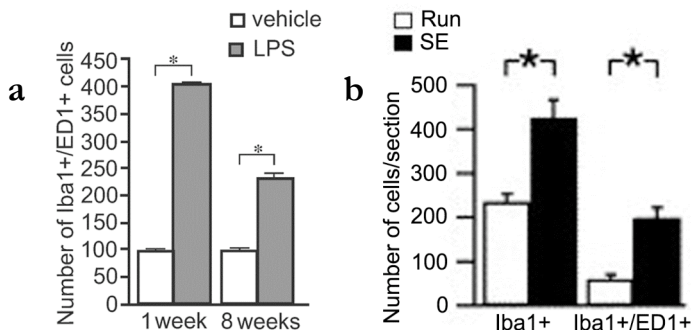**FIGURE 4.** Inflammation following status epilepticus (SE) and lipopolysaccharide (LPS) injection. The number of microglia (Iba1+) in active phagocytosis (Iba1+/ED1+) is upregulated at one and eight weeks after LPS injection (a), and at seven weeks after SE (b), as compared to respective controls (vehicle/run). Error bars indicate SEM. Adapted from Paper C: figure 1 h; and Paper D: figure 1 c.

Microglia react to pathological disturbances of their microenvironment by aforementioned responses, along with concomitant modifications to gene expression and their profile of secreted cytokines and growth factors. A full account of this is not within the scope of this thesis, but briefly IGF-1, IL-1β, IL-6, inducible nitric oxide synthase (iNOS) and TNF-α are upregulated acutely after SE (de Simoni *et al.* 2000, Choi *et al.* 2008), and IL-6, IL-1, IL-1β and TNF-α after LPS-mediated microglial activation (Vallieres *et al.* 1997, Cacci *et al.* 2008). Neurons respond to cytokines secreted from microglia, and conversely microglia respond to neuronal signals. Thus, there exists an intimate connection and communication between microglia and neurons in the CNS both under physiological and pathological conditions (**FIGURE 3**).

Inflammation can be detrimental to granule cell neurogenesis

An intense trauma like severe SE naturally affects the delicate balance in the hippocampal neurogenic niche, and neurons die within the hilus at one and five weeks after SE **(Paper A, C)**, and within the CA1 and CA3 fields of the hippocampus at five weeks after SE (Mohapel *et al.* 2004). For many years, inflammation has been regarded as nothing but negative for the survival of neurons and recovery after trauma to the CNS (Bracken 1991, Popovich *et al.* 1999, Ghirnikar *et al.* 2001). In support of this, an inflammatory response is attained when the brain is subjected to LPS-infusion (**FIGURE 5 a**) or electrically induced SE (**FIGURE 5 b**), accompanied with greatly reduced survival of those neurons born following the insult (**FIGURE 5 c** and **d**, respectively). After continuous LPS-infusion for 28 days, only as few as one-seventh of the neurons born into the inflammatory environment have survived and matured as compared to the control environment. The number of surviving neurons is negatively correlated with the number of microglia in active phagocytosis following LPS infusion (**FIGURE 5 e**).
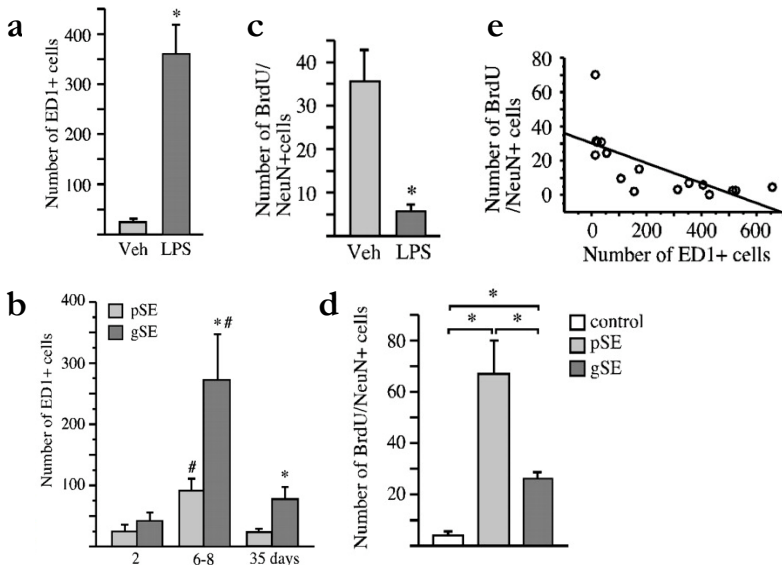
FIGURE 5. Inflammation impairs basal and status epilepticus (SE)-induced hippocampal neurogenesis. The number phagocytotic microglia (ED1+) and newborn neurons (BrdU/NeuN+) after four weeks of intracortical lipopolysaccharide (LPS) (a, c) or five weeks after SE insult (b, d). Both LPS-infusion and SE-insult give rise to a dramatic increase in the number of ED1+ microglia (a, b) and reduced number of surviving neurons (c, d) as compared to respective control environment (veh/control). Follwoing LPS-infusion, the number of BrdU/NeuN+ cells is negatively correlated with the number of ED1+ microglia (c). Error bars indicate SEM. Adapted from Paper A: figure 1 c, e, f; figure 2 f, g.

Anti-inflammatory treatment with minocycline reduces the number of microglia in active phagocytosis both six and 35 days after SE-induced inflammation (**FIGURE 6 a, b**). This reduced inflammation is accompanied by increased number of surviving insult-induced newborn neurons (**FIGURE 6 c**). The detrimental effect inflammation exerts on neurogenesis was confirmed in an independent contemporary study (Monje *et al.* 2003). Together, these results show that both basal and SE-induced neurogenesis is negatively regulated by LPS-induced inflammation, and that the number of surviving neurons can be restored through anti-inflammatory treatment.
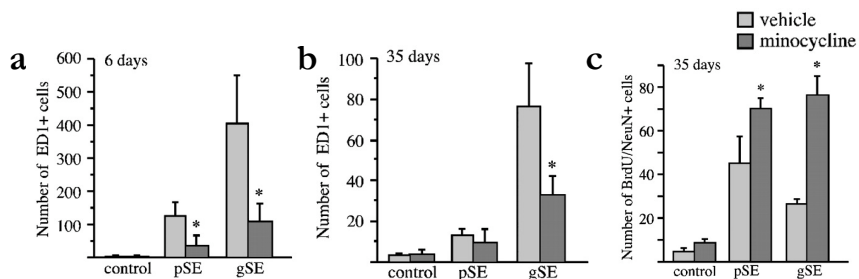
FIGURE 6. Minocycline prevents inflammation-mediated suppression of hippocampal neurogenesis. Reduced number of microglia in active phagocytosis (ED1+) at six days (a) and five weeks (b) following electrically induced SE. The reduction of ED1+ cells increases the survival of neurons born after the initial SE-insult (c). Adapted from Paper A: figure 4 a, b, e.

Granule cells survive despite being born into an inflammatory environment

Status epilepticus causes a transient increase of neurogenesis that can be detected three days after the SE insult, peaking seven days after the initial insult (Parent *et al* 1997). Before, the long-term survival of these neurons had not been investigated, but was only monitored for four-five weeks following the initial insult (**Paper A**, Mohapel *et al*. 2004). In the next study the long-term neurogenic outcome after electrically induced SE was investigated. Acute inflammation becomes chronic after SE, and is still present even six months after the initial insult (**FIGURE 7 a**). Despite the previously described detrimental effects of inflammation, an impressive amount of the neurons born after both partial and generalized SE had survived for six months (**FIGURE 7 b**) and comprised about nine percent of the total number of neurons within the SGZ-GCL, compared to two percent in the control environment. The neurons born into the inflammatory environment incorporate into the GCL without giving rise to a subsequent increase in GCL volume, suggesting they replace neurons that died following the insult (**FIGURE 7 c**). At four weeks after severe generalized SE, fewer newborn neurons are detected in the SGZ-GCL, as compared to after milder partial SE (Mohapel *et al*. 2004). This initial difference in neuronal survival depending on seizure severity is no longer present at six months, where the number of surviving seizure-induced neurons is at equal levels in partial and generalized SE profiles (**FIGURE 7 c**).

A previous study has reported that the ongoing neurogenesis is decreased at four months after kainic acid-induced SE as compared to basal control level of neurogenesis (Hattiangady *et al*. 2004). However, this is a result the present studies were unable to replicate, where instead it was

found that the level of ongoing neurogenesis returned to control levels six months after SE (**FIGURE 7 d**). Moreover, granule cells are found to aberrantly migrate into the hilus following SE (Parent *et al.* 1997), which was confirmed and furthermore showed that these aberrant newborn granule cells were still migrating into the hilus even six months after their SE-induced birth (**FIGURE 7 e**).
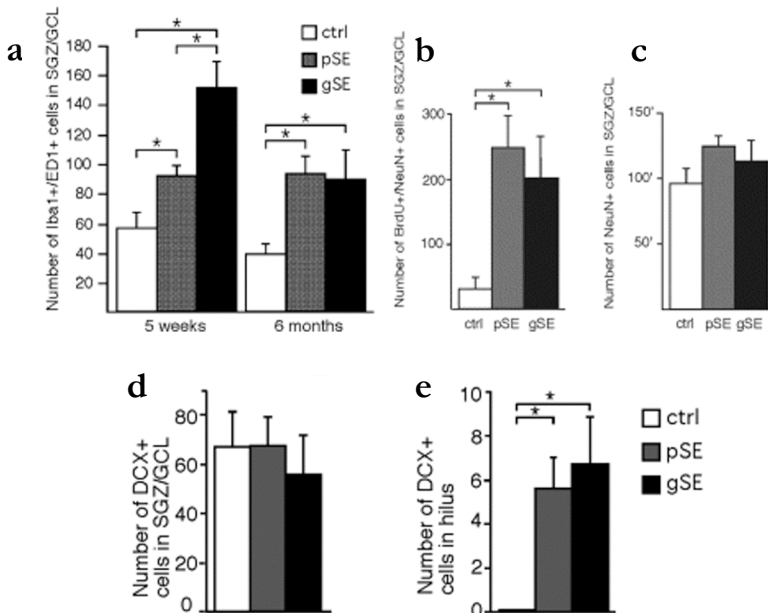
FIGURE 7. Neurogenesis after an acute and chronic status epilepticus (SE)-induced inflammation. After electrically induced SE, the number of microglia in active phagocytosis (Iba1+/ED1+) is rapidly increased, and remains increased five weeks and six months after the initial insult (a). SE induces increased neurogenesis, and many of these neurons are still present within the subgranular zone (SGZ) – granule cell layer (GCL) six months after the insult (b) without causing a subsequent increase in the total number of granule cells in the SGZ-GCL (c). The number of proliferating neuroblasts (DCX+) has returned to basal levels in the SGZ-GCL (d), but there are still more newborn neurons migrating into the hilus (e) six months after SE, as compared to controls. Error bars indicate SEM. Adapted from Paper B: figure 4c; 5 c, d; 6 e, g.

17

Granule cells born in an inflammatory environment do not exhibit altered membrane properties or morphological development

The granule cell intrinsic membrane properties – resting membrane potential, membrane time constant, input resistance, and action potential threshold, amplitude and duration – were investigated. Despite being born into a pathological inflammatory environment after electrically induced SE (**Paper C**) or LPS-injection (**Paper D**), the newborn neurons developed similar intrinsic membrane properties as the granule cells born in the physiological control environment, and resembled those of older granule cells born before the inflammatory stimuli. The morphological development of the granule cells born into the inflammatory environment was thoroughly investigated at time of decapitation five weeks after SE (**Paper C**), or throughout their development (10, 17, and 23 d after LPS) and at the time of decapitation eight weeks after LPS-injection (**Paper D**) (i.e. four weeks and three days, 10 days, 16 days, seven weeks after retroviral labelling following SE and LPS-injection respectively). At five weeks after SE, the newborn granule cells throughout the GCL exhibited small cell somata and dendritic trees extending well into the molecular layer, characteristics typical of dentate granule cells (**Paper C**). The granule cells born into the LPS-provoked inflammatory environment (**Figure 4 b**) show similar morphotemporal development as the granule cells born into a physiological control environment. The dendrites extend into the ML within the first three days, axons reach towards the CA3 within the first 10 days, branched dendritic trees with spines reach even further into the ML within the first 16 days, and finally the new granule cells become morphologically indistinguishable from their neighbouring mature granule cells within seven weeks after their birth (**Paper D**).

It has been previously described that about 10 percent of granule cells born up to 60 weeks after pilocarpine-induced SE display aberrant dendrites, projecting into the hilus (hilar basal dendrites, HBD) and sometimes subsequently projecting trough the GCL into the molecular layer (recurrent basal dendrites, RBD), a feature very rarely found in granule cells born in a physiological control environment and suggested to contribute to pathological network excitability following SE (Ribak *et al.* 2000). Granule cells born around one week after kainic acid-induced SE display dendrites still aberrantly projecting into the hilus several weeks later (Jesssberger *et al.* 2007). However, in granule cells born one week after an SE insult (**Paper C**) or LPS injection (**Paper D**), only very few hilar basal dendrites were detected at four or six weeks later, respectively, with no difference from granule cells born in the physiological control environment.

A detailed analysis of the morphological characteristics of the granule cells (GFP+) born into an LPS-induced inflammatory environment was conducted six weeks after their birth. However, the morphology of the granule cells born in an inflammatory environment did not differ from those born in a physiological control environment in regards to distribution of GFP+ granule cells in the GCL (inner, mid, and outer GCL) (**FIGURE 8 a**), the polarity of the GFP+ cells (parallel, 45° angle, or perpendicular to the direction of the GCL) (**FIGURE 8 a**), the number of dendrites per GFP+ cell, the number of branching points along the dendritic tree (**FIGURE 8 c**), or the axonal exit point (basal, medial, apical). Furthermore, the density of GFP+ dendritic spines in general (**FIGURE 8 d, e**), and the density of mushroom spines in particular (associated with strong excitatory connectivity; ref) was not different for the granule cells born into an inflammatory environment compared to the control environment (**Paper D**).
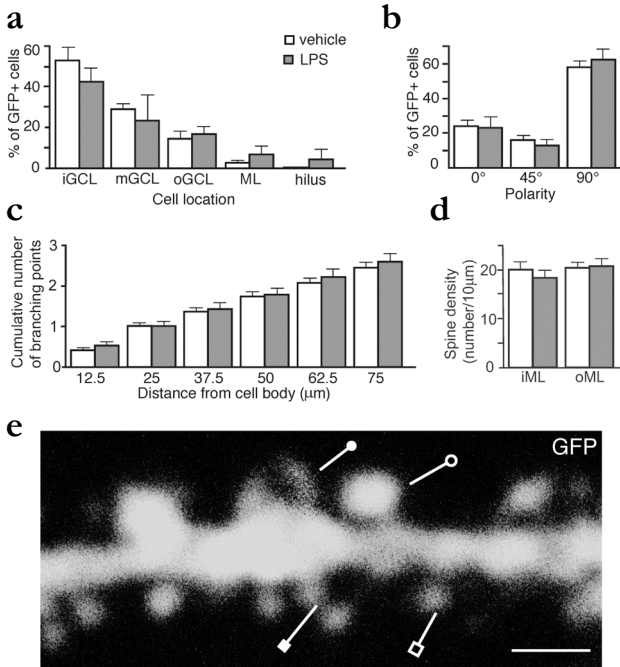
FIGURE 8. The morphological properties characteristic of granule cells are not affected when the granule cell is born into an inflammatory environment. A detailed study of morphological parameters of granule cells were conducted revealing no difference in location (a), cell soma polarity (b), dendritic branching (c), or spine density in the inner and outer molecular layer (d; iML and oML, respectively) on newborn granule cells (GFP+) in LPS- or vehicle-treated animals respectively. Morphological appearance of the four types of dendritic spines (e); mushroom (open circle), filopodia (filled circle), thin (open square), and stubby (closed square). Scale bar: 1 μm. Error bars indicate SEM. Adapted from Paper D: figure 2 f, g, h and figure 8 a, b.

Granule cells born into an inflammatory environment show altered excitatory and inhibitory synaptic properties

Despite that the neurons born into an SE- (**Paper C**) or LPS-induced (**Paper D**) inflammatory environment developed into mature granule cells morphologically indistinguishable from those born in respective physiological control environment, we have shown that they actually display altered excitatory and inhibitory synaptic connectivity. The granule cells born into the inflammatory environment one week after electrically induced SE (**Paper C**) or LPS-injection (**Paper D**), develop decreased excitatory connectivity along with increased inhibitory connectivity.

Accumulation of the cytoplasmic protein gephyrin is required for stability of GABAergic synapses (Kneussel and Betz 2000, Yu *et al.* 2007). Following LPS-induced inflammation, the gephyrin cluster density remained unaltered (**FIGURE 9 a**), but the increased inhibitory synaptic connectivity was accompanied with significantly larger GABAergic inhibitory gephyrin clusters on the dendritic trees in the ML as compared controls (**FIGURE 9 b**).
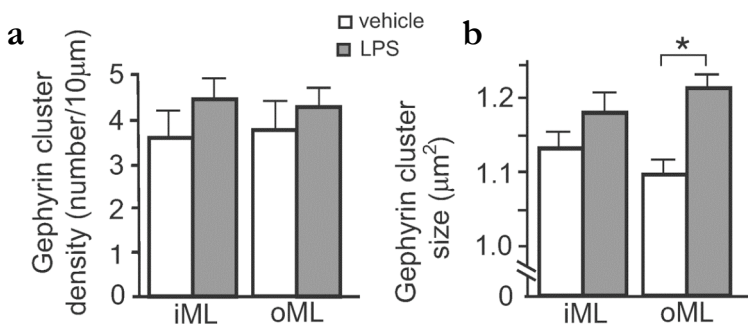
FIGURE 9. Inhibitory synaptic connections on granule cell dendrites. The density of inhibitory GABAergic synaptic clusters (gephyrin+) remained unaltered in both inner and outer molecular layer (a; iML and oML), but the gephyrin clusters were significantly larger in the outer ML (b) at seven weeks following lipopolysaccharide (LPS) induced inflammation as compared to in control environment. Error bars indicate SEM. Adapted from Paper D: figure 8 f, g.

Discussion

Together, the results from the four studies presented in this thesis illustrate the spectrum of the impact inflammation poses on adult hippocampal neurogenesis. It ranges from detrimental to permissive, and can even dictate the functional properties of neurons born into the inflammatory environment. Inflammation reduces the number of surviving newborn neurons in both basal and SE-induced inflammation, a condition reversed by anti-inflammatory treatment. However, despite both an acute and chronic inflammation following SE, a substantial number of the granule cells born following the insult survived on a long-term basis and comprised nine percent of the total number of neurons within the hippocampus. Neurons born in an inflammatory environment induced by SE or bacteria-like infection responded to their pathological environment with reduced excitatory and increased inhibitory synaptic connectivity. Also, while the new neurons developed along the same detailed morphotemporal course as in a control environment, the increased inhibitory synaptic connectivity following bacteria-like infection was accompanied with larger inhibitory synapses on the new neurons.

Inflammation affects the quantity of neurons

That inflammation has an impact on the outcome of adult neurogenesis is clear from the results presented in this thesis, yet how and to what extent appears to be highly variable, depending on factors such as the type of inflammatory trigger, whether it be seizure activity or bacteria-like infection.

Upon activation, microglia migrate towards the affected area, an effect potentially mediated through monocyte chemoattractant protein-1 (MCP-1) expressed by already activated microglia at the site of injury (Deng *et al.* 2008). This explains why inflammation causes the highly organized grid of microglia cell bodies to be disrupted, and how microglial cells can accumulate at sites of damage. Pathogen-associated LPS is a potent trigger of microglia activation, and a subsequent cytokine release that produces an unfavourable environment for neurons *in vivo* and *in vitro* (**Paper A**, Cacci *et al.* 2005, Liu *et al.* 2005). However, when microglia are cultured with LPS for longer periods, instead of an acute exposure, a different state of microglial activation and cytokine expression pattern is reached, characterized by reduced expression of proinflammatory molecules like IL-6, TNF-α and nitric oxide, and increased expression of anti-inflammatory cytokines like IL-10 and PGE-2 (Ajmone-Cat *et al.* 2003, Cacci *et al.* 2008). This work is further supported by an *in vivo* study revealing a variable inflammatory

outcome dependent on timing and magnitude of intrahippocampal LPS-infusion (Herber *et al.* 2006) Furthermore, subsets of inflammatory microglia and macrophages within the same structure can express different levels and types of cytokines, illustrated following experimental stroke where the same inflammatory cell rarely expresses both IL-1β and TNF-α (Clausen *et al.* 2008). TNF-α is a potent inflammatory cytokine released by microglia, acting either neuroprotective or pro-apoptotic through TNF-receptors 1 and 2 (TNF-R1 and -R2) located on neuronal progenitors. Signalling via TNF-R2 has a neuroprotective role on basal hippocampal neurogenesis, while TNF-R1 is a negative regulator of basal neurogenesis, and insult-induced neurogenesis in both the hippocampus after SE and in the subventricular zone following experimental stroke (Heldmann *et al.* 2005, Iosif *et al.* 2006, 2008). Infusion of insulin-like growth factor 1 (IGF-1) has been shown to promote neurogenesis, while depletion attenuates the neurogenic effect of environmental enrichment (Aberg *et al.* 2000, Trejo *et al.* 2001). When microglial cells are stimulated by INF-γ or TGF-β, neurogenesis is increased, while oligodendrogensis is favoured when the microglia are stimulated with IL-4, showing that microglia can actually dictate and increase the neurogenic outcome (Battista *et al.* 2006, Butovsky *et al.* 2006).

That the same trigger can cause different subsets of microglia to display different cytokine profiles, that the state of microglia activation is dependent on the timing of the inflammatory trigger, and that the neurogenic outcome is affected differently by a variety of inflammatory cytokines, describes the dynamic and highly variable function of microglia in inflammation. In turn, it also describes how inflammation can have an impact on neurons and the neurogenic outcome of granule cells born in the inflammatory environment.

Inflammation affects neuronal distribution and function

The evolutionary basis and functional relevance of adult hippocampal neurgenesis remains elusive, as do the reasons for inflammation-mediated and seizure-induced changes to the neurogenic process. Not only does SE cause death of neurons while transiently increasing neurogenesis, but it also alters the distribution and functional properties of the newborn neurons (Mohapel *et al.* 2004, Parent *et al.* 1997, **Paper C**).

GCs aberrantly migrate into the hilus following SE, and remain there long-term (Parent *et al.* 1997, **Paper B**). The hilus is an area of cell death and inflammation following SE (Mohapel *et al.* 2004, **Paper B**), and neuroblasts have previously been shown to migrate towards sites of damage

following experimental stroke and experimental multiple sclerosis (Arvidsson *et al.* 2002, Picard-Riera *et al.* 2002). The inflammatory response following SE produces a plethora of molecules which can attract the neural progenitor cells through expression of a variety of cytokine receptors such as CCR1, CCR2 and CXCR3 (Tran *et al.* 2007, Belmadani *et al.* 2006). Inflammatory cytokines like INF-γ and TNF-α are potential mediators of the NPC attraction, through their induction of local microglial production of monocyte chemoattractant protein-1 (MCP-1), which attracts NPCs through CCR2 receptor (Belmadani *et al.* 2006).

Earlier studies have suggested that the SE-induced neurogenesis contributes to the maintenance of epilepsy based on studies showing granule cells located aberrantly within the hilar formation, granule cell dendrites projecting aberrantly into the hilar formation, and granule cell axons projecting aberrantly into the molecular layer (Ribak *et al.* 2000, Scharfman *et al.* 2000, 2002, Buckmaster *et al.* 2002, Pierce *et al.* 2005). Here, the fate of the majority of the SE-induced new neurons, i.e. those that (non-aberrantly) integrate into the GCL, was investigated (**Paper C**). Previous studies have shown that granule cells can have different morphological characteristics in a pathological environment, and showed altered numbers of dendritic spines (Suzuki *et al.* 1997), dendritic length and extent of dendritic tree branching (von Campe *et al.* 1997), aberrant hilar basal dendrites and recurrent basal dendrites (Ribak *et al.* 2000), and mossy fiber sprouting into the molecular layer (Houser *et al.* 1990). We performed extensive studies of morphological characteristics, without finding any differences between the cells born into either the SE-exposed or LPS-induced inflammatory environments, compared to respective physiological control environment. Interestingly, the present experiments found that new cells born into either of the two inflammatory environments showed reduced excitatory- and increased inhibitory synaptic connectivity of the neurons born into the SE-exposed GCL. These findings suggest that the majority of the newborn neurons following SE, the ones that integrate into the GCL, actually tended to counteract the pathologically excitable SE-environment. However, spontaneous seizures do occur despite the presence of seizure-induced newborn neurons within the GCL following SE (Parent *et al.* 1997, **Paper B, C**). The reason for these spontaneous seizures may be the aforementioned aberrant hilar basal dendrites and mossy-fiber sprouting, two phenomena that possibly contribute to an immense network suceptibility and epileptogenesis following SE. Also, many inhibitory GABAergic interneurons die following the SE insult, reducing the inhibitory capacity of the hippocampal network, potentially contributing to subsequent epileptogenesis. Furthermore, the decreased excitatory and increased inhibitory synaptic connectivity onto the new granule cells born into the

LPS-induced inflammatory environment, suggest a possible mechanism for these granule cells to precautionarily reduce the risk for subsequent seizure activity to occur as a secondary effect of brain inflammation.

The research presented in this thesis has shown for the very first time that synaptic connectivity is altered in the new granule cells born into a pre-existing pathologic environment (**Paper C, D**). Both SE and LPS create an inflammatory environment that promotes plastic changes through cytokines and growth factors such as TNF-α and brain-derived neurotrophic factor (BDNF), which are capable of modulating excitatory and inhibitory synaptic transmission, and altering dendritic spine morphology (Ajmone-Cat *et al.* 2006, Pickering *et al.* 2005, Henneberger *et al.* 2005, von Bohlen und Halbach *et al.* 2006). In conjunction with increased inflammatory-induced inhibitory synaptic connectivity following LPS-injection, we found larger $GABA_A$ receptor-clusters (gephyrin+) on the dendrites of newborn granule cells (**Paper D**), potentially mediated by the ability of BDNF to regulate the transcription of $GABA_A$ receptors (Lund *et al.* 2008).

Is inflammation good or bad?

Following trauma such as SE, it now seems unlikely that simultaneous local inflammation and neurogenesis are merely coincidental, but instead, in cohort, serve the increased tissue demand for maintenance and repair. Depending on the type and intensity of the trigger, along with the duration of exposure, different states of microglial activation and subsequent neurogenic outcome will result. In light of such a complex relationship between pro- and anti-inflammatory cytokines, to suggest that microglia merely perform a *dual* role, or are either good or bad for the process of neurogenesis, would be to over-simplify. For a recent review of the intimate relationship between inflammation and adult neurogenesis see Ekdahl *et al* (2008).

Here, while we have demonstrated that inflammation can be detrimental to neurogenesis (**Paper A**), permit long-term survival of neurons (**Paper B**), and dictate the excitatory and inibitory synaptic connectivity of the newborn neurons (**Paper C, D**), yet other studies have shown the immune system can actually instruct neurogenesis to occur. In spinal cord injury simultaneously treated with neural progenitors and inflammatory T-cells directed towards a CNS antigen, the T-cells recruit the exogenously applied neural progenitors to migrate to the site of injury, thus improving the functional recovery (Ziv *et al.* 2006a). Also, in animals depleted of T-cells, neurogenesis was clearly decreased, and when restoring the system with T-cells interacting specifically with microglia in the brain,

progenitor proliferation was again increased (Ziv *et al.* 2006b). Furthermore, depending on whether microglia are activated by either of the T cell-derived cytokines IL-4 or IFN-γ, microglia contribute to hippocampal neurogenesis and oligodendrogenesis respectively (Butovsky *et al.* 2006). This shows that the inflammatory-mediating microglia, previously associated primarily with exerting negative effects on neurogenesis, can in association with immune system T-cells actually participate in instructing adult neurogenesis.

Together, our results show that not all newborn neurons will respond to an inflammatory environment by dying, even when exposed to inflammation under the crucial period of their development. Rather, some will survive, mature, and integrate into a chronically inflamed hippocampus, both after SE and after LPS-injection.

Future perspective

The four studies included in this thesis have significantly increased the knowledge of the effect an inflammatory environment poses on the neurons. However, as always when questions are answered, inevitably, more will arise. To date, it has been very difficult, if not impossible, to discuss inflammatory effects in general terms. The discourse is rather more emphasized when results are specified as 'under these exact conditions', 'in this strain of animal', and 'in this amount, type and time of exposure results in', etc. It will be important to continue the mapping of specific stages of microglial activation, and also, what provokes and defines them. **Papers C and D** have shed light on how neurons are affected by being born into an inflammatory environment. Obviously, it would be of great value to know how newborn neurons in different stages of maturation respond to an onset of inflammation: to understand when the neurons are sensitive to inflammatory exposure, and subsequent events. Finally, the very interesting results from **Paper C** suggest that the SE-induced newborn neurons might actually counteract the excitable environment they are born into, an approach that could be taken much further by trying to increase the number of surviving neurons following SE, perhaps using inflammatory mediators to attract the neurons to the desired location and monitor the effects on the environment excitability. In order to someday translate these pre-clinical data in a therapeutic manner in human conditions such as seizure disorders, and also other CNS disorders where the immune system is involved, such as multiple sclerosis, Alzheimer's disease, and stroke, it is my opinion that one must consider both neuronal and inflammatory properties for the greatest success.

Methodology

Animal models

To reach our specific aim of elucidating the impact a pre-existing inflammatory environment poses on neuronal birth, survival, migration, and integration into the neuronal network, two animal models have been used throughout the four papers included in this thesis. The models mimic two types of inflammatory environment formed as a response to bacterial infection and epileptic seizure, respectively, whereupon the neurogenic outcome is analysed. The animal models and subsequent analyses are reviewed in this chapter, and for specific information on concentrations, provider etc., I refer to **Papers A-D**.

Model for bacterial infection

Almost all Gram-negative bacteria are pathogens, meaning they cause disease when infecting a host organism. Gram-negative bacteria have an outer layer mainly comprised of lipopolysaccharide (LPS), a motif conserved throughout bacteria evolution due to its protective function. In the simultaneous evolution of the immune system e.g. in rat and human, it has proven useful to be able to respond to bacterial infection in order to fight it and survive. To accomplish this, the innate immune system in the brain has taken advantage of pathogen-associated motif patterns like LPS. The main immune cells of the brain are microglia, further described in the previous chapter ('Inflammation'). Through toll-like receptors (TLRs) on microglia membranes, pathogen invasion causes activation of microglia cells, a process known as inflammation.

To mimic bacteria-induced inflammation in an animal model, LPS endotoxin is delivered to the hippocampus, either continuously through a micro-osmotic pump (**Paper A**), or by a single microcapillary injection (**Paper D**). The LPS causes a prominent inflammatory response with increased numbers of microglia throughout the period of continuous micro-osmotic delivery (**Paper A**), and both acutely and seven weeks after the single-dose injection (**Paper B**). Thus, the LPS animal model provides a local and stable inflammatory environment, enabling the study of survival and morphological development of hippocampal neurons born therein.

Model for status epilepticus

Normal brain function is based on a delicate balance of factors stimulating or inhibiting nerve cell signalling. An altered balance favouring

excitation over inhibition, can give rise to uncontrolled signalling commonly referred to as epileptic seizures. Epilepsy is a collective name of a heterogeneous group of recurrent, unprovoked seizures. The extent of a single seizure varies widely depending on where in the brain the seizure originates and whereto it spreads. A seizure manifests itself along a spectrum: from creating a few seconds of absence, to a long-lasting full-blown seizure called status epilepticus (SE). Severe SE is a condition that causes uni- or bilateral cramps of peripheral limb muscles, loss of consciousness, and an increased risk of death due to heart failure. About one percent of the western population suffers chronically from epilepsy, primarily affecting children and the elderly. Some cases of epilepsy are hereditary. These are often caused by mutations affecting neurotransmitter communication towards increased excitation or reduced inhibition, which lowers the threshold for seizure occurrence. Furthermore, an array of conditions affecting the brain can secondarily give rise to epilepsy, such as tumours, stroke, infection, malformation and trauma. Nonetheless, despite the modern techniques available, about 50 percent of the cases remain idiopathic, meaning a plausible underlying cause of the disease cannot be determined. In the brain, the temporal lobes seem particularly prone to seizure activity, and are often affected in epilepsy. Apart from seizure activity *per se*, human temporal lobe epilepsy (TLE) can give rise to cognitive decline and abnormal changes of the hippocampal granule cell layer (GCL). Change can include reorganisation of granule cell (GC) mossy fibers (axons), dispersion of the GCL, loss of GCs, appearance of aberrantly located GCs, along with occurrence of activated microglia, astrogliosis, and increased levels of inflammatory cytokines like interleukin-1 (IL-1), and cytokine receptors like IL-1 receptor type 1 (IL-1R1) (Houser 1990, Ozbas-Gerçeker *et al.* 2004, Oyegbile *et al.* 2004, Ravizza *et al.* 2008).
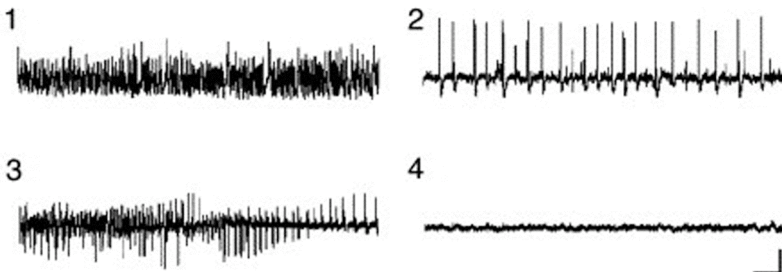
FIGURE 10. Electroencephalographic (EEG) recordings of status epilepticus (SE) activity in an animal model. From the electrode implanted into the hippocampus measured EEG shows SE seizure activity (1), abnormal interictal spiking (2), activity during a spontaneous seizure four weeks after initial SE insult (3), and normal control EEG activity at one week after running (4; control). Scale bar: 2 s, 1 mV. Adapted from Paper C: figure 1 a.

To mimic severe human TLE in an animal model, an electrode is implanted into the rodent hippocampus through which SE is induced electrically (**Paper A, B, C**). Animals develop either mild partial or more severe generalized SE, involving one or both hemispheres, respectively. Spontaneous seizures will continue to occur throughout life with concomitant changes to electroencephalogram (EEG) recordings of brain activity (**FIGURE 10**), and with behavioural manifestations including akinesia, automatisms, limb cramps, salivation, and loss of balance (Mello *et al.* 1993). As in human TLE, the SE-treated rodent hippocampus show GCL dispersion, aberrantly located GCs within the hilus and ML, GC loss, reorganisation of GC mossy fibers, astrogliosis and a pronounced inflammatory response (Mello *et al.* 1993, Parent *et al.* 1997, Borges *et al.* 2003).

Techniques for detecting neurogenesis and inflammation

A number of methods have been developed to study the processes of neurogenesis and inflammation in the brain. The technical goal is to label cells or cell structures specifically and efficiently, detecting as many as possible of nothing but the desired cell type. For the papers included in this thesis, newborn cells have been detected with bromodeoxyuridine (BrdU; **Paper A, B**) and retrovirus (**Paper C, D**) *in vivo*, along with *in situ* immunohistochemical labelling with antibodies for specific visualisation of the inflammatory and neurogenic processes (**Paper A, B, C, D**).

Bromodeoxyuridine labelling

The blueprint for an organism is stored in its genes made of deoxyribonucleic acid (DNA) strands inside the nucleus of each and every cell. The DNA is folded into 42 and 46 chromosomes in rat and human cells respectively. The DNA molecule has only four building blocks: cytosine, guanine, adenosine and thymidine. Different combinations of these are the basis for building all types of molecules and cells, and by extension, whole organisms. When a cell divides to form two daughter cells, the pattern of cytosine-guanine and adenosine-thymidine block-order is copied; giving the newborn cells a clone of the mother-cell DNA. Bromodeoxyuridine (BrdU) is a molecule analogous to thymidine, meaning that when BrdU is injected at the time of cell division it will incorporate into the newborn cells at thymidine sites along the DNA molecule. The BrdU-molecule is associated with a bromide-group, allowing for subsequent antibody-based specific detection of newborn BrdU-labelled cells, using a standard protocol for immunohistochemistry (see below).

As for all techniques, it is important to critically evaluate the efficiency and specificity of the method at hand. Detecting dividing cells by incorporating thymidine analogues into DNA has been used for several decades, but the specificity of the method is to some extent still debated. One risk using the method is that damaged cells repairing their DNA could also incorporate BrdU, thus falsely labelling a repairing cell as a new cell. Moreover, by incorporating BrdU into its DNA, the cell risks that the modified thymidine interferes with normal cell function and potentially induce cell death. However, the technique has been highly refined (for references, see Christie and Cameron 2006). It is now known that low-dose injections of BrdU (50 mg/kg for rat) are not lethal, and cells are not damaged by the uptake of BrdU. Also, BrdU+ and BrdU- cells show similar functional characteristics. To ascertain BrdU-specificity, other techniques for labelling newborn cells, such as retrovirus based approaches or using antibodies such as Ki67 and DCX, have been utilised to show overlap of newborn cells and cells labelled with BrdU. Also, none of the approaches label a large population of cells in areas of damage, where many cells are expected to undergo DNA repair. Furthermore, cells in need of DNA repair only restore small portions of the whole DNA molecule, which renders the BrdU content of a repairing cell too minute to detect with antibody-based immunohistochemistry. Additionally, for the papers included in this thesis, only completely and homogenously stained nuclei were analysed and regarded as part of a truly newborn cell.

Replication-deficient retroviral labelling

Another efficient way to label dividing cells is to infect them with replication-incompetent oncoretrovirus particles carrying the gene for green-fluorescent protein (GFP; **Papers C, D**). This approach allows for easy detection of newborn cells in live slices during electrophysiological patch-clamp recordings (see chapter 'Electrophysiology'). The retrovirus (RV) particles are injected locally, and enter host cells through interaction between viral surface glycoprotein and host cell membrane receptors. The single-stranded viral RNA is reversely transcribed into double-stranded DNA in the host cell cytoplasm. If the infected cell undergoes mitosis, viral DNA enters through a transiently open nuclear envelope into the host cell nucleus, where it randomly integrates into the host DNA. Regulated by a promoter on the viral DNA, the viral gene becomes transcribed and translated into GFP, which stably labels the entire newborn cell. Essential parts have been removed from the viral genome prior to infection, rendering the replication-incompetent RV unable to spread and infect neighbouring cells. For papers C and D included in this thesis, Moloney

Murine Leukemia virus (Mo-MLV) backbone inserted with a GFP-coding sequence under either of the ubiquitous promoters NIT (**Paper C**) or CAG (**Paper D**) has been utilized to efficiently label cells born around the time of viral infection.

The efficiency of transducing viral DNA into host cells may vary depending on intracellular half-life of the RV vector and the number of infectious units delivered. The concentration of the RV solution injected in Paper C and D was approximately $1.1 - 1.3 \times 10^8$ transducing units per milliliter, and the half-life of Mo-MLV-derived retroviral vectors has been estimated to 5.5 - 7.5 hours inside the host cell cytoplasm (Andreadis *et al.* 1997). An estimated 250 transducing units are required for successful labelling of one neuron using GFP-carrying RV under the CAG-promoter (Zhao *et al.* 2006). Thus, it can be deduced that only a negligible number of neurons (about eight) may still be retrovirally infected 48 hours (six half-lives) after the 1.5-ml injection in Paper C and D. Another factor limiting the number of host cells expressing GFP after viral infection is the type of promoter associated with the RV. As aforementioned, RV with either NIT (**Paper C**) or CAG (**Paper D**) promoters have been used, and the CAG promoter transduces a much higher number of GFP-expressing neurons as compared to the NIT promoter. Furthermore, the random incorporation of retroviral DNA into host DNA during mitotic cell division can potentially cause irreparable damage to the infected cell if incorporated into a crucial host gene. Another risk is that modified retroviral particles may be or become replication competent and consequently spread to and infect neighbouring host cells uncontrollably. Nevertheless, the biology of retroviral vector is well known, and has successfully been used in gene therapy since 1989 without reports of serious side effects (Vile *et al.* 1996).

Immunohistochemistry

The technique of immunohistochemistry is based on use of antibodies ('immuno-') recognizing specific antigens on the cell surface, in the cytosol or inside the cell nucleus when added to thinly sliced tissue ('histo-').

To ensure tissue morphology and stability during the immunohistochemical staining procedure and subsequent analysis, the soft brain tissue is treated with the formalin-derived fixative paraformaldehyde (PFA). Exposing tissue to PFA disables endogenous proteolytic enzymes, protects from bacterial damage, and lends stability by creating strong covalent bonds between serine-residues in proteins throughout the tissue. The added rigidity enables the tissue to be thinly sliced, a requirement for adequate antibody penetration. Antibody penetration is further improved by

addition of the membrane rupturing detergent Triton X-100. For antigen located within the cell nucleus, additional treatment may be required to open the nuclear envelope. By heating tissue in either warm hydrochloric acid or boiling citrate buffer (both pH < 7), specific antibodies can reach and efficiently label nuclear BrdU and Ki67-antigen respectively (Paper A, B).

In immunohistochemistry, a specific antibody binding directly to the antigen of interest is called a primary (1°) antibody (**FIGURE 11**). Once the primary antibody is in contact with its antigen, they strongly bind together. A primary antibody can be either monoclonal or polyclonal, depending on how it is produced. A monoclonal antibody is produced by infusing the desired antigen into a mouse, where the murine immune system will respond by making antibodies against the infused antigen. Antigen-producing spleen cells are then fused with myeloma cells and cultured individually, while the surrounding medium is tested for the desired antibody. When a positive culture is found (one that produces the desired antibody) the antibody is cloned and propagated *in vivo* or *in vitro*, followed by the harvesting of the specific monoclonal antibody. Monoclonal antibodies all bind to exactly the same epitope (location) on a corresponding antigen. For production of polyclonal antibodies, the antigen is similarly infused into an animal and the activated immune system produces antibodies against the antigen. The serum from the animal is thereafter purified to obtain a mix of polyclonal antibodies. Thus, a polyclonal antibody is produced by a variety of immune cells that all recognise the same antigen, but do so by binding to different epitopes on that specific antigen. Monoclonal antibodies are generally regarded more specific than polyclonal antibodies.

In immunohistochemistry, when the primary antibody has bound to the desired antigen, excess antibodies are rinsed away from the tissue, before a secondary (2°) antibody is introduced. The secondary antibody binds to the Fc heavy-chain part of the primary antibody (**FIGURE 11**). The secondary antibody can be conjugated with FITC (green) or Cy3 (red) fluorophores, or non-fluorescent biotin. When conjugated with a fluorophore, the stained cells will light up in a fluorescent microscope when excited with the complementary wavelength. Biotin-conjugated secondary antibodies can either be made green-fluorescent by adding Alexa fluor 488, or making them brown for light microscopy by adding avidin-biotin-complex (ABC), and subsequently exposing the complex to 3,3'diaminobenzidine (DAB) and hydrogen peroxide (**FIGURE 11**)
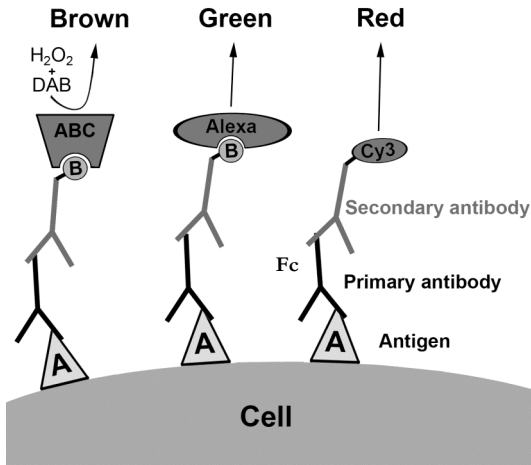
Figure 11. Illustration of the basis for immunohistochemical labelling technique. A specific primary antibody binds to an antigen. In turn, the primary antibody is bound by a secondary antibody for light microscopy (brown) or fluorescence microscopy (green, red).

The technical drawbacks of immunohistochemistry include a risk for labelling of unspecific antigens, and general labelling of the background tissue reducing the contrast between specific and non-specific staining. However, specificity of antibodies can be assessed by use of positive and negative controls. A positive control is obtained by staining tissue with an antibody where the corresponding antigen should be present, e.g. BrdU-antigen in areas of continuous cell division (e.g. SGZ of adult hippocampi) in BrdU-injected animals. Absence of BrdU-positive staining under these circumstances should be interpreted as inadequacy of the antibody. Either by staining tissue with an antibody whose antigen should not be present, or by omitting the primary antibody from the staining protocol, one can obtain a negative control. If staining is detected under these circumstances, the specificity of the antibody is inadequate. A further control for labelling specificity occurs during subsequent microscopical analysis. Knowledge of where and in which cell type an antigen should be located allows for identification of the morphology of a specific, and thereby a non-specific, labelling outcome (**EXAMPLE 1**). Furthermore, antigen detection with rat primary antibody (e.g. rat anti-BrdU; **Paper A, B**) on rat tissue is complicated by high levels of background staining due to secondary anti-rat antibody (Cy3 donkey anti-rat) binding not only to the primary antibody but also unspecifically to endogenous rat tissue immunoglobulin like IgG. However, this problem is common only in tissue like muscle, skin, and kidney, but not in brain tissue since it is devoid of IgG-antibodies (Peress *et al.* 1989) apart from areas with close association to the cerebrospinal fluid such as periventricular tissue (Peress *et al.* 1987).

Example 1. When analysing an immunohistochemical staining made with ED1 antibody, specific labelling is solely confined to phagocytic vesicles inside microglia cell bodies. Active and quiescent microglia cell bodies can be stained specifically with Iba1-antibody. If ED1+ labelling is found outside Iba1+ cell bodies, the specificity of the labelling technique and/or antibody used should be questioned. Also, if the exact morphological structure is fluorescent in several wavelengths (colours), the stained structure is likely non-specific auto-fluorescence, and not a phagocytic vesicle.

Finally, measures can be taken to reduce labelling of background tissue by adding serum to the antibody solution, or by quenching the tissue with hydrogen peroxide and methanol before DAB-technique labelling for light microscopy.

Electrophysiology

This thesis is particularly focused on neuronal and inflammatory cell number and morphology. However, paper C and D are also based on electrphysiological patch-clamp recordings of neurons. In order to fully comprehend the conclusions drawn from these two studies, a basic understanding of neuronal electrophysiology is essential. The number of neurons and their morphological characteristics cannot provide a complete understanding of how a pathological condition affects neurons in the brain. Additionally, the functional characteristics of neurons must be taken into account. When neurons communicate, transmitter substances are released into the synaptic cleft, causing a flow of ions across the membrane of the postsynaptic cell. In the electrophysiological technique, electrical current in a single neuron is measured. The single-cell currents reflect neuronal function, and can be more broadly applied to understanding how single neurons integrate and communicate in the larger neuronal circuitry of the CNS.

To distinguish newborn neurons from adult neurons, the newborn cells are specifically labelled with a retrovirus carrying the gene for GFP (see 'Replication-deficient retroviral labelling' on pp 29-30). Functional properties were electrophysiologically recorded from newborn and adult neurons in live hippocampal tissue from animals exposed to SE or LPS, and their respective control animals. The hippocampal tissue was cut into thick slabs, and kept alive in aCSF for a few hours under a microscope connected to an advanced system for recording of electrophysiological activity. The technique is known as whole-cell voltage-clamp recording, where the patch micropipette seals onto the GC soma and ruptures the membrane. This

renders an open connection between the GC and micropipette interior, thus enabling recording of electrical currents within the patched cell.

When an action potential reaches the synaptic bouton it causes release of transmitter substances into the synaptic cleft (see 'Neurons' on pp 5-7). Depending on the type of transmitter substance released, it can either cause excitation or inhibition of the postsynaptic neuronal membrane. Excitation may lead to propagation of the action potential signal along the postsynaptic neuronal axon to further synaptic clefts, while inhibition reduces the likelihood of continued action potential propagation. Changes in cell excitation can be studied by blocking inhibitory $GABA_A$ receptors with picrotoxin (PTX), which allows for recording of purely excitatory currents. Blocking the inhibitory signalling enables monitoring of spontaneous and action potential-elicited excitatory glutamate release in the postsynaptic cell. The recorded currents are called spontaneous excitatory postsynaptic currents (sEPSCs). The effect of spontaneous presynaptic glutamatergic release alone can be recorded in the chosen cell by simultaneously blocking $GABA_A$ receptors with PTX and presynaptic action potentials with tetrodotoxin (TTX) added to the extracellular bath solution. The recorded currents in these conditions are referred to as miniature excitatory postsynaptic currents (mEPSCs). Reduced frequency of EPSCs (i.e. EPSCs occuring at longer inter-event intevals: IEIs) suggests reduced excitatory input onto the recorded cell. To normalize the dispersion of the EPSC responses recorded in the postsynaptic cells, the standard deviation is divided by the mean, rendering the coefficient of variation (CV). CV is a measurement that gives an estimation of the probability that glutamate will be released from the presynaptic terminal and subsequently cause postsynaptic EPSCs. By delivering extracellular stimulations to the afferent excitatory pathway, the lateral perforant path (LPP), coming from the entorhinal cortex synapsing onto the hippocampal granule cells, induces excitatory currents in the postsynaptic neuron. This approach can be used to study the way a synaptic response changes due to previous activity. Delivering two pulses in short succession to the LPP, induces paired-pulse facilitation (PPF), a form of presynaptically mediated short-term plasticity. PPF and CV of EPSCs are both inversely related to overall release probability of glutamate. This means that increased PPF or CV is indicative of the patched cell having presynaptic connections with an overall reduced probability of glutamate release (i.e. a reduced excitatory input onto the recorded cell).

As mentioned previously, neurotransmitter release can also induce inhibitory effects on the postsynaptic neuron. While excitatory effects are commonly mediated by the neurotransmitter glutamate, GABA typically mediates inhibitory effects. Changes in cell inhibition can be isolated by

34

blocking glutamate-mediated excitation with D-AP5 and NBQX, while studying the inhibitory postsynaptic currents (IPSCs). Under these conditions, spontaneous and action potential-dependent postsynaptic inhibition can be monitored through spontaneous inhibitory postsynaptic currents (sIPSCs). Furthermore, by blocking action potential generation in the presynaptic cells with TTX, inhibitory currents due to spontaneous GABA release can be monitored alone through miniature inhibitory postsynaptic currents (mIPSCs). IPSCs occuring at shorter IEIs with higher amplitudes are indicative of the recorded cell receiving enhanced inhibitory input. A slow rise and decay of the IPSCs suggest activation of synapses on the dendrites, distal to the recording pipette, while faster kinetics are associated with signalling through proximal somatic synapses. Stimulating the molecular layer (ML) twice in short succession induces paired-pulse depression (PPD) of IPSCs. PPD occurs when the first stimulation releases GABA which, besides inducing IPSCs in the postsynaptic cell, gives rise to inhibition of GABA release following the second stimulation. Reduced PPD suggests that the postsynaptic cell receives more inhibitory input, since the second GABA release is not as reduced.

Microscopy and statistics

To analyse the immunohistochemically stained tissue, a variety of microscopical approaches have been used: regular light microscopy and light microscopy in a stereological setting to estimate the total number of neurons in the granule cell layer (**Paper B**), conventional fluorescence microscopy and confocal fluorescence microscopy to safely determine colocalisation of two antibodies or, to clearly visualise minute details of neuronal morphology, such as dendritic spines (**Paper D**).

Statistical analysis between experimental conditions, such as partial and generalized SE, and the corresponding control group (**Paper B**) was performed using analysis of variance (ANOVA) with Bonferroni post-hoc test. Single treatment conditions were analysed with t-tests, such as LPS-injected animals and their controls (**Paper D**). Both ANOVA and t-tests are based on analysing the variance of means, and require the data to follow normal distribution. T-tests can be either paired or unpaired. A paired t-test is used to compare data that are repeated measures, such as data from the same animal measured before and after a treatment. Unpaired t-tests are used to compare independent groups, such as separate control and experimental groups.

Data obtained from immunohistochemically labelled tissue was analysed with appropriate statistical tests and a p-value was obtained. If the p-value is greater than 0.05, one fails to reject the null-hypothesis, and it can

be concluded there is no statistically significant difference between the groups. With a *p*-value less than 0.05 the null-hypothesis is rejected, and it can be concluded there is a significant difference between the compared groups. A *p*-value is an arbitrarily, predetermined cut-off point, and a value of less than 0.05 suggests with 95 percent likelihood that the data from the compared distributions are different. A null hypothesis can be rejected with increasing certainty when *p*-values of 0.01 or 0.001 are set. Thus, a *p*-value is a measurement of credibility, how likely it is that the obtained result actually reflects a true difference between compared data groups.

Technical limitations

When studying a human disease like epileptic seizure and inflammation in a rodent model using a variety of markers to detect inflammatory cells and neurons, one must be careful with interpretation of the data. It is essential to remember that the present discussion is of rodent epilepsy and the data might not be clearly transferrable to the human condition. When labelling resected rodent tissue with an antibody against, for instance, Iba-1, it is crucial to keep in mind that what is visualized under the microscope are those Iba-1 antibodies that have successfully bound to Iba-1 antigen. The antigen should only be localized to microglia, excess antibody should have been rinsed off the tissue, and the Iba-1 antibody should have bound to all Iba-1 antigen within the tissue. When injecting a label like BrdU *in vivo*, it is possible that the BrdU might label other than dividing cells, and might not label all dividing cells. The issue of label uncertainty becomes even more evident when using a replication-deficient retrovirus like RV-GFP. Even though the label efficiency increased from **Paper C** to **Paper D** when switching viral promoter, the uptake and expression of a retroviral label is variable from one injection to another, making this labelling technique particularly unsuitable for quantitative comparisons. The low efficacy of transduction of GFP to newborn cells in **Paper C** prompted us to increase the neurogenesis in control animals, which is the reason that we used animals with voluntary exercise as a control group for this experiment. Finally, when analysing the stained tissue for positive labelling, there is always a risk for bias. To reduce the risk, the analyst should always be blind to treatment conditions. However, the treatment *per se* might sometimes alter the tissue integrity or labelling parameters in a clear and predictable way, making it difficult to blind the samples. For instance, experimental stroke induces a large lesion and tissue loss in the brain, where the control animals have no lesion at all. The same is true for analysing inflammatory environment following either SE- or LPS-treatment, where both cause a marked upregulation of microglia (increased

numbers and altered morphology). Under these conditions where the treatment results in obvious effects not found in the corresponding control animals, the risk of bias cannot be removed and therefore must be taken into account. However, drawbacks should not simply be viewed as arguments to avoid using a specific technique, since all techniques and models have drawbacks (along with their respective advantages), but rather be kept in mind when critically analysing the results, and also be a motivator for a continuous strive to improve the technique.

Acknowledgements

Although most are already well aware of how they have contributed to this particular PhD experience, and how I feel about their support – there is still nothing like an official, ISBN-numbered 'thank you', is there? This is I, humbly acknowledging the contribution of others, to a successful completion of my thesis.

Locked in the non-ergonomical position one faces when mounting brain slices onto objective glasses, I felt someting swoosh by the outer field of my right peripheral vision. I didn't recognise the pace and the posture. I had been at the lab on and off for a while, and was well aware of the constant out- and influx of people. Was it curly brown? Perhaps it was a new colleague? But I was wrong. It was not *a* colleague, it turned out to be *the* colleague. Her name was – and still is – Katie. Her warmth, charm and consideration was immediate and tangible. We bonded, and quickly became friends also outside the perimeter of the lab. Sweetie, since you left Sweden (and most importantly me!) a year ago, I feel a void. Your kind loving support, our talks behind shut doors, and your companionship still mean the world to me. Thanks for introducing me to America, and making me understand why you love it so. Thanks for all the bring-alongs from your trips and visits back home – VS, B&B, and that Porfidio. And thanks for that fun trip to Amsterdam, with all the jazz, diamonds, beer and chocolate! You are so kind. But I guess that should not come as a surprise, considering your 50 % Santa-genes.

And speaking of Santa makes me think of all those Christmas parties, especially that one lasting through the night, all that dancing, and something about me riding a red lab-trolley. Pär, you have made the working climate warm and a tad crazy, and thanks for keeping track of updated ugly-numbers. Keep on spreading your glowing atmosphere!

And speaking of ugly-numbers, I send a thanks to Robban for great fun at the lab, for reminding me to take lunch breaks, for updating me with great music culture and new releases I just had to listen to – who will let me know when Foo Fighters release their next album now? Thanks for sharing with me your kindness and friendship.

And speaking of music culture, Johan Hellsten you are a true music guru, and I cannot think of several huge artists, without immediately thinking of you too (that's a compliment, right?). In my mind, you and Springsteen will remain intertwined. Thanks for teaching me how to drink coffee, and for caring, for cheering me on, and for the entertainment during

so many hours of tedious microscopy. And for breaking the stereological microscope that time, so I got a good week's break from it.

And speaking of stereological microscopy, every time I start thinking about that, I hear a voice in my head telling me that 'volume does not matter' and instructing me how easy and uncomplicated the whole thing is. Andreas, thanks for making me feel immensely appreciated at the lab, for making me feel smart, for all those dinners, hours of listening to your lovely music, and for personifying impatience. For being crazy with me (like opening that bottle of gin in the middle of the Tuna-Tornavägen intersection after the Christmas party), for hanging out on my balcony, for all the gifts, and for letting me talk you into doing stuff you hate – like step-aerobics and drinking tequila. You are an amazing friend!

Not only is he himself a great friend, you see, he has done the ingenious thing of shacking up with another magnificent person – sweet, fun, insane, brilliant Elisabet. Thanks for all the parties, all the hours analysing weird people, for the shopping, for making me feel special, for standing by me, for all the beer and soup, for all the romantic comedies, for all the text messages, for being honest and supportive, and for being perfect just the way you are.

When on the subject of standing by me I want to tell you all the story of Sofie. Her and me met randomly during high school, and have been hanging out ever since. She is sweet, fun, supportive, loving, with just the right amount of crazy. She will hate me for acknowledging her in English, but I love how upset she can get sometimes. Thanks for being my conscience, for reminding me to go to Gerdahallen (although I ignore the invitations much of the time), for being my McD-friend, for sharing everything with me, for truly being there, and for co-planning our Seilbahn. Du bist doch am Besten!

Und wo ich schon beim Thema Deutsch bin (tack Sofie), hätte ich gern ein bisschen über Irene mitteilen. If you haven't met her, I must say you have definitely missed something special. She is quite the girl! Only few can measure up with her dedication and efficiency. She's spontaneous, funny, caring, kind, and honest. Irene, you are my crocodile, and I am your alligator.

And while on the subject of dedication, Olle, you have shown me what it's like to really stick to your calling, to never settle but making everything top-notch, or even a notch over that. I thank you for answering that first naïve e-mail I sent more than 7 years ago now; "I am a biomedicine student and I am like, sort of, interested in the brain". Thanks for seeing that spark in me, and introducing me to the whirlwind Christine.

Christine, to me you are ambition from top to toe. Thanks for instantly making me feel part of the lab, for your patience during all those

hours of teaching techniques and theory. For really taking your time, and trusting in me – even when I wiped off all those brain slices, just because you left-handedly mount them on the 'wrong' side of the objective glass. I can still remember that feeling of panic when so clumsily ruining your staining. Thank you for quickly letting go, and allowing me to try everything on my own: the surgeries, the microscopy, and the stainings. Thanks also for your contagious enthusiasm, and for your much-appreciated friendship.

Another person I got to meet during my studies has taught me a great deal about everything. I now know that it is very important to take a vacation from work, to go for coffee and lunch with my colleagues, to strictly separate work time and spare time, and that I am great. Richard, I still often think of you, and I want to make sure that you realise how thankful I am for your help.

And speaking of spending time with my colleagues, Ursula, I just love hanging out with you. You have a wonderful outgoing, happy spirit. You're full of spontaneity, hugs and cheerful words. You are true, honest and a colourful inspiration, and all this I thank you for sharing with me! Thanks also for hosting all those dinners, and for always making me smile.

And speaking of smiles, I have a friend with the most beautiful smile! Malin, to find you living just a few doors down from my own was one of the best discoveries I've ever made. How we connected, and quickly shared everything, talked into the small hours, studied, interpreted boys and their ways (or at least tried to), went for coffee, cried, and laughed. And we still do all of that, which means so much to me.

While on the matter of laughs, Litsa, that wonderful laugh of yours instantly gets me smiling, it's great with a new force like you close by. And all sweet colleagues, contributing with your special traits: Andreas TS with always having an answer to any question; Therese with kind caring friendliness combined with wearing inspiring fashion making me think: "damned, I wish I could dress like that!"; the really cool Marco pulling off eyeliner tremendously well; Marie for your positive attitude, always a smile on your face and those happy bouncing curls; Zaza for keeping me on my toes and being helpful and supportive; Jan for being so incredibly relaxed and always up for a tease; Carlo for your sensitive and caring side; Linda for caring and listening; Henrik for your initiative and drive, for your commitment to the lab, and for being inspiringly smart; Malin W for being so much fun and making me feel useful and important by asking me questions that I know the answer to; James for being a trustworthy collaborator and always up for a laugh; Merab for being positive, very helpful and kind, and always greeting me with a smile on your face; Karin for being sweet and fun; Stefanie (honey!) for being such a great friend, you inspire me with your vast range of skills; Anders for being so supportive and

helpful – scientifically and personally – you are special to me; Salina for your lovely relaxed attitude, for showing me around San Diego and bringing me to that wonderful sushi place, and for all those great girls' dinners; sweet Johanna for your lovely British accent, for entertaining hours in the basement and for contributing with a new-found friendship; Tomas for your kindness, the lunches and the chats; Daniel for being the sweetest there is. To the here specifically mentioned, and to all other BMC:ers I've interacted with, I would like to say: we're a heterogeneous group of people pushed together, which has made the lab a diverse, interesting and fun place for me to work. Thank you all so very much for that!

And needing your own paragraph, Ramiro and Joakim, in my head you are located within the same compartment. That is the compartment of being slightly insane, always teasing and being charmingly weird! You two are a rare kind, and I will definitely miss having you both around.

Another charmingly weird person is you, sweet Peter. And if I could choose, you'd stop the ridiculous silliness living in stupid Stockholm. But much of your charm is that there's no way I could change anything about you, had I wanted to. You're as stubborn as I am, which is terribly annoying. You always win the wrestles, and you always seem to *enjoy* my threats (I lovingly hate you for that!). Thanks for listening, even if it's virtual, day and night. And saying all those supportive, kind and very bright things.

Someone else online during the night, willing to listen, is of course my one and only sister Emma. She has gone off to Japan, yet again, forcing me to settle for a virtual sisterhood. Oh, how I miss you. You are my morality, and my immorality. You once taught me to read, and there's absolutely no way I could have finished this thesis had I been illiterate! What would I be without you? Even though you are across the globe doing your thing, you always remember me, you always support me, and you are always the best sister I could dream of. I will never stop being your imoto. Oh, and also, thanks for taking an interest in my lab work (mounting those slides, and meeting the rats), and for introducing me to your in-Sweden replacement – sweet Daniel.

I want you all to know how lucky I am – I seriously have *the* most amazing family. They are always routing for me, spoiling me, calling me on the phone, and being my concrete foundation, with underfloor heating and a fuzzy carpet on top. Dad and Mum, you already know what you do, and how I feel about you both, and to you I pass my deepest gratitude. You are the best parents one could wish for. To my lawfully acquired family Per-Olof, Gunilla, Jimmy, and Anna; thank you for caring, and for all the nice things you say and do. I feel privileged, and worth a million around you.

And while on the topic of worth a million. Johan "Joding" Svensson Bonde, I am the luckiest of lucky – loving a terrific guy like you,

and being loved in return! I too am happy about those first drinks, and all that has come to follow. You are silly, crazy, loving, caring, relaxed, and sweet – with all those brown eyes! Thanks for the sweet tokens of love, for cooking me dinners, and putting lunch boxes in my bag. For keeping track of everything I seem to lose, and specifically in this context – padding my way through the finalisation of this thesis. And not the least, making (from my weird scribbles) figures 1, 2, 3 and 11, and assisting with the thesis layout along with software (and my own) breakdowns.

Finally, I wish to give an extra special thanks to my wonderful proofreaders: Stefanie, Johanna, Christine and Katie – thanks for not letting me get away with any mistakes. Your help was truly invaluable. Also thanks to Keith Layson, and The Journal of Neuroscience for letting me reproduce Paper D.

To one and all making it through this final chapter of the book, I want to say: I realise you might not have read *all* the pages leading up to this final one, and it doesn't matter. But if per chance you actually did read the rest, I really do hope you enjoyed it, and an extra thanks, and a mental gold star to you!

References

Aberg MA, Aberg ND, Hedbäcker H, Oscarsson J, Eriksson PS (2000) Peripheral infusion of IGF-I selectively induces neurogenesis in the adult rat hippocampus. *J Neurosci* 20, 2896-903.

Ajmone-Cat MA, Nicolini A, Minghetti L (2003) Prolonged exposure of microglia to lipopolysaccharide modifies the intracellular signalling pathways and selectively promotes prostaglandin E_2 synthesis. *J Neurochem* 87, 1193-203.

Ajmone-Cat MA, Iosif RE, Ekdahl CT, Kokaia Z, Minghetti L, Lindvall O (2006) Prostaglandin E_2 and BDNF levels in rat hippocampus are negatively correlated with status epilepticus severity: no impact on survival of seizure-generated neurons. *Neurobiol Dis* 23, 23-35.

Altman J, Das GD (1965) Autoradiographic and histological evidence of postnatal hippocampal neurogenesis in rats. *J Comp Neurol* 124, 319-35.

Andreadis ST, Brott D, Fuller AO, Palsson BO (1997) Moloney murine leukemia virus-delivered retroviral vectors decay intracellulary with a half-life in the range of 5.5-7.5. *J Virol* 71, 7541-48.

Arvidsson A, Collin T, Kirik D, Kokaia Z, Lindvall O (2002) Neuronal replacement from endogenous precursors in the adult brain after stroke. *Nat Med* 8, 963-70.

Battista D, Ferrari CC, Gage FH, Pitossi FJ (2006) Neurogenic niche modulation by activated microglia: transforming growth factor β increases neurogenesis in the adult dentate gyrus. *Eur J Neursci* 23, 83-93.

Barres BA (2008) The mystery and magic of glia: a perspective on their roles in health and disease. *Neuron* 60, 430-40.

Belmadani, A, Tran PB, Ren D, Miller RJ (2006) Chemokines regulate the migration of neural progenitors to sites of neuroinflammation. *J Neurosci* 26, 3182-91.

Borges K, Gearing M, McDermott DL, Smith AB, Almonte AG, Wainer BH, Dingledine R (2003) Neruonal and glial pathological changes during epileptogenesis in the mouse pilocarpine model. *Exp Neurol* 182, 21-34.

Bracken MB (1991) Treatment of actue spinal cord injury methyl prednisolone: results of a multicenter, randomized clincal trial. *J Neurotrauma* Suppl 1, S47-50.

Brezun JM, Daszuta A (1999) Depletion in serotonin decreases neurogenesis in the dentate gyrus and the subventricular zone of adult rats. *Neurosci* 89, 999-1002.

Buckmaster PS, Zhang GF, Yamawaki R (2002) Axon sprouting in a model of temporal lobe epilepsy creates a predominately excitatory feedback circuit. *J Neurosci* 22, 6650-58.

Butovsky O, Talpalar AE, Ben-Yaakov K, Schwartz M (2005) Activation of microglia by aggregated beta-amyloid or lipopolysaccharide impairs MHC-II expression and renders them cytotoxic whereas IFN-gamma and IL-r render them protective. *Mol Cell Neursci* 29, 381-93.

Butovsky O, Ziv Y, Schwartz A, Landa G, Talpalar AE, Pluchino S, Martino G, Schwartz M (2006) Microglia activated by IL-4 or INF-γ differentially induce neurogenesis and oligodendrogenesis from adult stem/progenitor cells. *Mol Cell Neurosci* 31, 149-60.

Boucsein C, Kettenmann H, Nolte C (2000) Electrophysiological properties of microglial cells in normal and pathologic rat brain. *Eur J Neurosci* 12, 2049-58.

Cacci E, Claasen J-H, Kokaia Z (2005) Microglia-derived tumor necrosis factor-alpha exaggerates death of newborn hippocampal progenitor cells in vitro. *J Neurosci Res* 80, 789-97.

Cacci E, Ajmone-Cat MA, Anelli T, Biagioni S, Minghetti L (2008) In vitro neuronal and glial differentiation from embryonic or adult neural precursor cells are differently affected by chronic or acute activation of microglia. *Glia* 56, 412-25.

Cameron HA, McKay RD (2001) Adult neurogenesis produces a large pool of new granule cells in the dentate gyrus. *J Comp Neurol* 435, 406-17.

<center>REFERENCES</center>

Chan WY, Kohsaka S, Rezaie P (2007) The origin and cell lineage of microglia: new concepts. *Brain Res Rev* 53, 344-54.

Chen Z, Palmer TD (2008) Cellular repair of CNS disorders: an immunological perspective. *Human Mol Gen* 17, R84-R92

Choi YS, Cho HY, Hoyt KR, Naegele JR, Obrietan (2008) IGF-1 receptor-mediated ERK/MAPK signaling couples status epilepticus to progenitor cell proliferation in the subgranular layer of the dentate gyrus. *Glia* 56, 791-800.

Christie BR, Cameron HA (2006) Neurogenesis in the adult hippocampus. *Hippocampus* 16, 199-207.

Clausen BH, Lambertsen KL, Babcock AA, Holm TH, Dagnaes-Hansen F, Finsen B (2008) Interleukin-1beta and tumor necrosis factor-alpha are expressed by different subsets of microglia and macrophages after ischemic stroke in mice. *J Neuroinflammation* 5, epub ahead of print.

Del Rio-Hortega (1932) Microglia. *Cytology and cellular pathology of the nervous system.* Penfield W (editor), New York, 481-534.

Deng YY, Lu J, Ling EA, Kaur C (2008) Monocyte chemoattractant protein-1 (MCP-1) produced via NF-kappaB signaling pathway mediates migration of amoeboid microglia in the periventricular white matter in hypoxic neonatal rats. *Glia*, epub ahead of print.

de Simoni MG, Perego C, Ravizza T, Moneta D, Conti M, Marchesi F, De Luigi A, Garattini S, Vezzani A (2000) Inflammatory cytokines and related genes are induced in the rat hippocampus by limbic status epilepticus. *Eur J Neurosci* 12, 2623-33

Ekdahl CT, Kokaia Z, Lindvall O (2008) Brain inflammation and adult neurogenesis: the dual role of microglia. *Neuroscience*, epub ahead of print.

Eriksson PS, Perfilieva E, Bjork-Eriksson T, Alborn AM, Nordborg C, Peterson DA, Gage FH (1998) Neurogenesis in the adult human hippocampus. *Nat Med* 4, 1313-17.

Espósito MS, Piatti VC, Laplagne DA, Morgenstern NA, Ferrari CC, Pitossi FJ, Schinder AF (2005) Neuronal differentiation in the adult hippocampus recapitulates embryonic developoment. *J Neurosci* 25, 10074-86.

Gage FH, Kempermann G, Palmer TD, Peterson DA, Ray J (1998) Multipotent progenitor cells in the adult dentate gyrus. *J Neurobiol* 36, 249-266.

Gage FH, Kempermann G, Song H (editors) (2008) Adult neurogenesis. *Cold Spring Harbor Laboratory Press*, ISBN 978-087969784-6.

Gehrmann J (1995) Colony stimulating factors regulate programmed cell death of rat microglia / brain macrophages in vitro. *J Neuroimmunol* 63, 55-61.

Gehrmann J, Banati RB (1995) Microglial turnover in the injured CNS: activated microglia undergo delayed DNA fragmentation following peripheral nerve injury. *J Neuropathol Exp Neurol* 54, 680-88.

Gehrmann J, Banati RB, Wiessner C, Hossmann KA, Kreutzberg GW (1995) Reactive microglia in cerebral ischaemia: an early mediator of tissue damage? *Neuropathol Appl Neurobiol* 21, 277-89.

Ghirnikar RS, Lee YL, Eng LF (2001) Chemokine antagonist infusion promotes axonal sparing after spinal cord contusion injury in rat. *J Neurosci Res* 64, 582-89.

Gibbons HM, Dragunow M (2006) Microglia induce neural cell death via a proximity-dependent mechanism involving nitric oxide. *Brain Res* 1084, 1-15,

Goldman SA, Nottebohm F (1983) Neuronal production, migration, differentiation in a vocal control nucleus of the adult female canary brain. *PNAS* 80, 2390-94.

Gould E, Cameron HA (1996) Regulation of neuronal birth, migration and death in the rat dentate gyrus. *Dev Neurosci* 18, 22-35.

Gould E, McEwen BS, Tanapat P, Galea LA, Fuchs E (1997) Neurogenesis in the dentate gyrus of adult tree shrew is regulated by psychosocial stress and NMDA receptor activation. *J Neurosci* 17, 2492-98.

REFERENCES

Gould E, Tanapat P, McEwen BS, Flugge G, Fuchs E (1998) Proliferation of granule cell precursors in the dentate gyrus of adult monkeys is diminished by stress. *PNAS* 95, 3168-71.

Gould E, Beylin A, Tanapat P, Reeves A, Shors TJ (1999) Learning enhances adult neurogenesis in the hippocampal formation. *Nat Neurosci* 2, 260-65.

Hanisch UK, Kettenmann H (2007) Microglia: active sensor and versatile effector cells in the normal and pathologic brain. *Nat Neurosci* 10, 1387-94.

Hattiangady B, Muddanna RS, Shetty AK (2004) Chronic temporal lobe epilepsy is associated with severely declined dentate neurogenesis in the adult hippocampus. *Nbiol Dis* 17, 473-90.

Hayes GM, Woodroofe MN, Cuzner ML (1987) Microglia are the major cell type expressing MHC class II in the human white matter. *J Neurol Sci* 80, 25-37.

Heldmann U, Thored P, Claasen JH, Arvidsson A, Kokaia Z, Lindvall O (2005) TNF-alpha antibody infusion impairs survival of stroke-generated neuroblasts in adult rat brain. *Exp Neurol* 196, 204-8.

Henneberger C, Kirischuk S, Grantyn R (2005) Brain-derived neurotrophic factor modulates GABAergic synaptic transmission by enhancing presynaptic glutamic acid decarboxylase 65 levels, promoting asynchronous release and reducing the number of activated postsynaptic receptors. *Neuroscience* 135, 749-63.

Herber DL, Maloney JL, Roth LM, Freeman MJ, Morgan D, Gordon MN (2006) Diverse microglial responses after intrahippocampal administration of lipopolysaccharide. *Glia* 53, 382-91.

Houser CR (1990) Granule cell dispersion in the dentate gyrus of humans with temporal lobe epilepsy. *Brain Res* 535, 195-204.

Iosif RE, Ekdahl CT, Ahlenius H, Pronk CJ, Bonde S, Kokaia Z, Jacobsen SE, Lindvall O (2006) Tumor necrosis factor receptor 1 is a negative regulator of progenitor proliferation in adult hippocampal neurogenesis. *J Neurosci* 26, 9703-12.

Iosif RE, Ahlenius H, Ekdahl CT, Darsalia V, Thored P, Jovinge S, Kokaia Z, Lindvall O (2008) Suppression of stroke-induced progenitor proliferation in adult subventricular zone by tumor necrosis factor receptor 1. *J Cereb Blood Flow Metab* 28, 1574-87.

Jessberger S, Zhao C, Toni N, Clemenson GD Jr, Li Y, Gage FH (2007) Seizure-associated, aberrant neurogenesis in adult rats characterized with retrovirus-mediated cell labeling. *J Neurosci* 27, 9400-7.

Kaplan MS, Hinds JW (1977) Neurogenesis in the adult rat: electron microscopic analysis of light radioautographs. *Science* 197, 1092-94.

Kempermann G, Kuhn HG, Gage FH (1997) More hippocampal neurons in adult mice living in an enriched environment. *Nature* 386, 493-95.

Kreutzberg GW (1996) Microglia: a sensor for pathological events in the CNS. *Trends Neurosci* 19, 312-18.

Kneussel M, Betz H (2000) Receptors, gephyrin and gephyrin associated proteins: novel insights into the assembly of inhibitory postsynaptic membrane specialisations. *J Physiol* 525, 1-9.

Kuhn HG, Dickinson-Anson H, Gage FH (1996) Neurogenesis in the dentate gyrus of the adult rat: age-related decrease of neuronal progenitor proliferation. *J Neurosci* 16, 2027-33.

Ling EA, Wong WC (1993) The origin and nature of ramified and amoeboid microglia: a historical review and current concepts. *Glia* 7, 9-18.

Liu YP, Lin HI, Tzeng SF (2005) Tumor necrosis factor-alpha and interleukin-18 modulate neuronal cell fate in embryonic neural progenitor culture. *Brain Res* 1054, 152-58.

Lund IV, Hu Y, Raol YH, Benham RS, Faris R, Russek SJ, Brooks-Kayal AR (2008) BDNF selectively regulates GABAA receptor transcription by activation of the JAK/STAT pathway. *Sci Signal* 1, ra9.

Lyons SA, Pastor A, Ohlemeyer C, Kann O, Wiegand F, Prass K, Knapp F, Kettenmann H, Dirnagl U (2000) Distinct physiologic properties of microglia and blood-borne cells in the rat brain slices after permanent middle cerebral artery occlusion. *J Cereb Blood Flow Metab* 20, 1537-49.

Mello LE, Cavalheiro EA, Tan AM, Kupfer WR, Pretorius JK, Babb TL, Finch DM (1993) Circuit mechanisms of seizures in the pilocarpine model of chronic epilepsy: cell loss and mossy fiber sprouting. *Epilepsia* 34, 985-95.

Mohapel P, Ekdahl CT, Lindvall O (2004) Status epilepticus severity influences the long-term outcome of neurogenesis in the adult dentate gyrus. *Neurobiol Dis* 15, 196-205.

Monje ML, Toda H, Palmer TD (2003) Inflammatory blockade restores adult hippocampal neurogenesis. *Science* 302, 1760-65.

Nimmerjahn A, Kirchoff F, Helmchen F (2005) Resting microglial cells are highly dynamic surveillants of brain parenchyma in vivo. *Science* 308, 1314-18.

Overstreet-Wadiche L, Westbrook GL (2006) Functional maturation of adult-generated granule cells. *Hippocampus* 16, 208-15.

Oyegbile TO, Dow C, Jones J, Bell B, Rutecki P, Sheth R, Seidenberg M, Hermann BP (2004) The nature and course of neuropsychological morbidity in chronic temporal lobe epilepsy. *Neurology* 62, 1736-42.

Ozbas-Gerçeker F, Gorter JA, Redeker S, Ramkema M, van der Valk P, Baayen JC, Ozgüç M, Saygi S, Soylemezoglu F, Akalin N, Troost D, Aronica E (2004) Neurotrophin receptor immunoreactivity in the hippocampus of patients with mesial temporal lobe epilepsy. *Neuropathol Appl Neurobiol* 30, 651-64.

Parent JM, Yu TW, Leibowitz RT, Geschwind DH, Sloviter RS, Lowenstein DH (1997) Dentate granule cell neurogenesis is increased by seizures and contributes to aberrant network reorganization in the adult rat hippocampus. *J Neurosci* 17, 3727-38.

Peress NS, Siegelman J, Fleit HB (1987) High avidity periventricular IgG-Fc receptor activity in human and rabbit brain. *Clin Immunol Immunopathol* 42, 229-38.

Peress NS, Siegelman J, Fleit HB, Fanger MW, Perillo E (1989) Monoclonal antibodies identify three IgG Fc receptors in normal human central nervous system. *Clin Immunol Immunopathol* 53, 268-80.

Picard-Riera N, Decker L, Delarasse C, Goude K, Nait-Oumesmar B, Liblau R, Pham-Dinh D, Evercooren AB (2002) Experimental autoimmune encephalomyelitis mobilizes neural progenitors from the subventricular zone to undergo oligodendrogenesis in adult mice. *PNAS* 99, 13211-16.

Pickering M, Cumiskey D, O'Connor JJ (2005) Actions of TNF-alpha on glutamatergic synaptic transmission in the central nervous system. *Exp Physiol* 90, 663-70.

Pierce JP, Melton J, Punsoni M, McCloskey DP, Scharfman HE (2005) Mossy fibers are the primary source of afferent input to ectopic granule cells that are born after pilocarpine-induced seizures. *Exp Neurol* 196, 316-31.

Pocock JM, Kettenmann H (2007) Neurotransmitter receptors on microglia. *Trends Neurosci* 30, 527-35.

Popovich PG, Guan Z, Wei P, Huitinga I, van Rooijen N, Stokes BT (1999) Depletion of hematogenous macrophages promotes partial hindlimb recovery and neuroanatomical repair after experimental spinal cord injury. *Exp Neurol* 158, 351-65.

Ravizza T, Gagliardi B, Noe F, Boer K, Aronica E, Vezzani A (2008) Innate and adaptive immunity during epileptogenesis and spontaneous seizures: Evidence from experimental models and human temporal lobe epilepsy. *Neurobiol Dis* 29, 142-60.

Ribak CE, Tran PH, Spigelman I, Okazaki MM, Nadler JV (2000) Status epilepticus-induced hilar basal dendrites on rodent granule cells contribute to recurrent excitatory circuitry. *J Comp Neurol* 428, 240-53.

REFERENCES

Scharfman HE, Goodman JH, Sollas AL (2000) Granule-like neurons at the hilar/CA3 border after status epilepticus and their synchrony with area CA3 pyramidal cells: functional implications of seizure-induced neurogenesis. *J Neurosci* 20, 6144-58.

Scharfman HE, Sollas AL, Goodman JH (2002) Spontaneous recurrent seizures after pilocarpine-induced status epilepticus activate calbindin-immunoreactive hilar cells of the rat dentate gyrus. *Neuroscience* 111, 71-81.

Shapiro LA, Upadhyaya P, Ribak CE (2007) Spatiotemporal profile of dendritic outgrowth from newly born granule cells in the adult dentate gyrus. *Brain Res* 1149, 30-37.

Streit WJ, Kreutzberg GW (1988) Response of endogenous glial cells to motor neuron damage induced by toxic ricin. *J Comp Neurol* 268, 248-63.

Suzuki F, Makiura Y, Guilhem D, Sørensen JC, Onteniente B (1997) Correlated axonal sprouting and dendritic spine formation during kainate-induced neuronal morphogenesis in the dentate gyrus of adult mice. *Exp Neurol* 145, 203-13.

Tashiro A, Sandler VM, Toni N, Zhao C, Gage FH (2006) NMDA-receptor-mediated, cell-specific integration of new neurons in the adult dentate gyrus. *Nature* 442, 929-33.

Taupin P, Gage FH (2002) Adult neurogenesis and neural stem cells of the central nervous system in mammals. *J Neurosci Res* 69, 745-49.

Thored P, Heldmann U, Gomes-Leal W, Gisler R, Darsalia V, Taneera J, Nygren JM, Jacobsen SW, Ekdahl CT, Kokaia Z, Lindvall O (2008) Long-term accumulation of microglia with proneurogenic phenotype concomitant with persistent neurogenesis in adult subventricular zone after stroke. *Glia*, in press.

Tran PB, Banisadr G, Ren D, Chenn A, Miller RJ (2007) Chemokine receptor expression by neural progenitor cells in neurogenic regions of mouse brain. *J Comp Neurol* 20, 1007-33.

Trejo JL, Carro E, Torres-Aleman I (2001) Circulating insulin-like growth factor I mediates exercise-induced increases in the number of new neurons in the adult hippocampus. *J Neurosci* 21, 1628-34.

Vallières L, Rivest S (1997) Regulation of the genes encoding interleukin-6, its receptor, and gp130 in the rat brain in response to the immune activator lipopolysaccharide and the proinflammatory cytokine interleukin-1beta. *J Neurochem* 69, 1668-83.

van Praag H, Kempermann G, Gage FH (1999) Running increases cell proliferation and neurogenesis in the adult mouse dentate gyrus. *Nat Neurosci* 2, 266-70.

van Praag H, Schinder AF, Christie BR, Toni N, Palmer TD, Gage FH (2002) Functional neurogenesis in the adult hippocampus. *Nature* 415, 1030-34.

Vile RG, Tuszynski A, Castleden S (1996) Retroviral vectors: from laboratory tools to molecular medicine. *Mol Biotechnol* 5, 139-58.

von Bohlen und Halbach O, Krause S, Medina D, Sciarretta C, Minichiello L, Unsicker K (2006) Regional and age-dependent reduction in trkB receptor expression in the hippocampus is associated with altered spine morphologies. *Biol Psychiatry* 59, 793-800.

von Campe G, Spencer DD, de Lanerolle NC (1997) Morphology of dentate granule cells in human epileptogenic hippocampus. *Hippocampus* 7, 472-88.

Witter MP, Amaral DG (2004) Chapter 21: Hippocampal formation. In: Paxinos G, editor. *The rat nervous system*, Academic Press, San Diego, pp 635-704

Yu W, Jiang M, Miralles CP, Li R-W, Chen G, de Blas AL (2007) Gephyrin clustering is required for the stability of GABAergic synapses. *Mol Cell Neurosci* 36, 484-500.

Zhao C, Teng ME, Summers RG, Ming G-L, Gage FH (2006) Distinct morphological stages of dentate granule neuron maturation in the adult mouse hippocampus. *J Neurosci* 26, 3-11.

Ziv Y, Avidan H, Pluchino S, Martino G, Schwartz M (2006a) Synergy between immune cells and adult neural stem/progenitor cells promotes functional recovery from spinal cord injury. *PNAS* 103, 13174-79.

REFERENCES

Ziv Y, Ron N, Butovsky O, Landa G, Sudai E, Greenberg N, Cohen H, Kipnis J, Schwartz M (2006b) Immune cells contribute to the maintenance of neurogenesis and spatial learning abilities in adulthood. *Nat Neurosci* 9, 268-75.
Ziv Y, Schwartz M (2008) Orchestrating brain-cell renewal: the role of immune cells in adult neurogenesis in health and disease. *Trends in Mol Med* 14, 471-78

Original Papers A-D

A

Inflammation is detrimental for neurogenesis in adult brain

Christine T. Ekdahl*, Jan-Hendrik Claasen†, Sara Bonde*, Zaal Kokaia†, and Olle Lindvall*‡

*Laboratory of Neurogenesis and Cell Therapy, Section of Restorative Neurology, Wallenberg Neuroscience Center, Biomedical Center A-11, and †Laboratory of Neural Stem Cell Biology, Section of Restorative Neurology, Stem Cell Institute, Biomedical Center B-10, Lund University Hospital, SE-221 84 Lund, Sweden

New hippocampal neurons are continuously generated in the adult brain. Here, we demonstrate that lipopolysaccharide-induced inflammation, which gives rise to microglia activation in the area where the new neurons are born, strongly impairs basal hippocampal neurogenesis in rats. The increased neurogenesis triggered by a brain insult is also attenuated if it is associated with microglia activation caused by tissue damage or lipopolysaccharide infusion. The impaired neurogenesis in inflammation is restored by systemic administration of minocycline, which inhibits microglia activation. Our data raise the possibility that suppression of hippocampal neurogenesis by activated microglia contributes to cognitive dysfunction in aging, dementia, epilepsy, and other conditions leading to brain inflammation.

In the adult mammalian brain, neural progenitor cells located in the subgranular zone (SGZ) of the dentate gyrus (DG) generate thousands of new neurons each day (1). These neurons develop the morphological and functional properties of dentate granule cells and become integrated into existing neuronal circuitries (2). The role of neurogenesis for hippocampal function is still unclear, but some experimental evidence suggests its involvement in memory formation (3) and mood regulation (4). Impairment of hippocampal neurogenesis may be linked to the cognitive decline in aging, Alzheimer's disease (AD), and major depression (5–7).

Brain inflammation probably plays an important role in the pathogenesis of chronic neurodegenerative disorders like AD and Parkinson's disease (8, 9). Neurodegeneration caused by inflammation involves activation of the brain's resident immune cells, the microglia, which produce a large number of proinflammatory factors (10–12). Also, acute brain insults, e.g., stroke and status epilepticus (SE), are linked to inflammation (13, 14), which contributes to the propagation of the neuropathological events (9, 15). These insults trigger increased neurogenesis in the SGZ (16–19). After severe SE, there is an 80% loss of newly formed dentate neurons (20), which raises the possibility that the associated inflammatory response is deleterious for hippocampal neurogenesis.

Here, we show that the microglia activation associated with inflammation impairs both basal and insult-induced hippocampal neurogenesis. We find that systemic administration of the tetracycline derivative minocycline, which specifically inhibits microglia activation, is an effective treatment to restore neurogenesis suppressed by inflammation.

Materials and Methods

Surgery and Induction of SE. Male Sprague–Dawley rats were implanted with a stimulating/recording electrode into the right ventral hippocampus [coordinates: 4.8 mm caudal and 5.2 mm lateral to bregma, 6.3 mm ventral to dura, and toothbar at −3.3 mm (21)] under pentobarbital or halothane anesthesia. In 37 animals, a brain infusion cannula (Alzet, Palo Alto, CA) was also placed intracortically on the right side of the brain (2 mm caudal and 1.2 mm lateral to bregma and 2.6 mm ventral to dura). Twenty-five rats were implanted only with the infusion cannula.

Ten days after surgery, all rats with implanted electrodes, except nonstimulated controls, were subjected to electrically induced SE with 60–90 min of suprathreshold stimulation followed by 2 h of self-sustained continuous ictal electroencephalographic (EEG) activity (22). Seizures were interrupted with i.p. injections of pentobarbital. Forty SE animals were subjected only to SE and perfused 2, 6–8 (pooled), or 35 days later.

BrdUrd Labeling. Six days after SE, rats were given four injections (every 2 h during a 6-h period) of BrdUrd (50 mg/kg, i.p; Sigma). Animals subjected to 4 weeks of intracortical infusions of lipopolysaccharide (LPS) or vehicle were injected with BrdUrd twice daily for 1 week, starting 6 days after the initiation of infusions. Rats receiving only 6 days of intracortical infusions were given four injections of BrdUrd (every 2 h during a 6-h period) at day 6 and perfused 2 h thereafter.

LPS and Minocycline Treatment. A miniosmotic pump (28-day pump, 0.25 µl/h; Alzet) was connected to the brain infusion cannula. The pump contained either LPS from *Escherichia coli* (serotype 055:B5; 20 µg/µl artificial cerebrospinal fluid; Sigma) or vehicle. Infusions were continued for 6 or 28 days.

Minocycline (Sigma) dissolved in potassium PBS (KPBS), pH 7–7.4, or vehicle was injected i.p. during 6 days or 35 days after SE or in nonstimulated controls. Animals received minocycline (50 mg/kg) twice daily for the first 2 days and once daily for the next 5 days (4 days for the short-term survival group), followed by 25 mg/kg once daily (23).

Immunohistochemistry. Rats were transcardially perfused with saline followed by 4% paraformaldehyde. Brains were postfixed overnight in the same medium and placed in 20% sucrose for 24 h, before sectioning (30 µm). For BrdUrd/NeuN, BrdUrd/doublecortin, and BrdUrd/ED1 double-label immunofluorescence, the sections were pretreated with 1 M HCl for 30 min at +67°C and then preincubated with appropriate serum, followed by incubation with primary antibodies overnight at +4°C. Sections were incubated for 2 h in the dark with secondary antibodies, followed by 2 h with Streptavidin Alexa Fluor 488 (1:200, Molecular Probes). The following antibodies were used: rat anti-BrdUrd (1:100, Oxford Biotechnology, Oxfordshire, U.K.), mouse anti-NeuN (1:100, Chemicon), mouse anti-ED1 (1:200, Serotec), goat anti-doublecortin (1:400, SC-8066, Santa Cruz Biotechnology), Cy3-conjugated donkey anti-rat (1:400, Jackson ImmunoResearch), and biotinylated horse anti-mouse or anti-goat (1:200, Vector Laboratories). Single labeling for NeuN, ED1, and Ki67 (mouse anti-Ki67 antibody, 1:200, NovoCastra, Newcastle, U.K.) were performed with biotinylated horse anti-mouse antibody and visualized with avidin-biotin-peroxidase
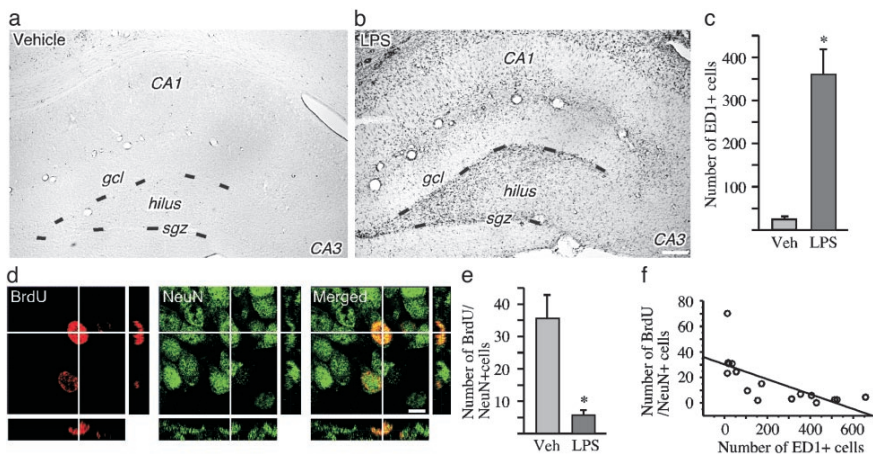
Fig. 1. Inflammation impairs basal hippocampal neurogenesis. (*a–c*) Immunohistochemical staining for ED1-positive activated microglia in the DG after 28 days of intracortical vehicle (*a*) or LPS (*b*) infusions, and number of activated microglia in the SGZ/GCL in the same treatment groups (*c*). (*d*) A newly formed BrdUrd/NeuN double-labeled neuron in the SGZ is visualized by using confocal microscopy in an orthogonal projection composed of 19 optical *z*-planes (0.5 μm thick). (*e*) The number of BrdUrd/NeuN double-labeled new neurons in the SGZ/GCL after 28 days of LPS or vehicle infusion (14 days after the last BrdUrd injection). (*f*) Correlation between number of ED1-positive and BrdUrd/NeuN double-labeled cells. Data are the number of cells per section. *n* = 6 and 10 for vehicle- and LPS-treated rats, respectively. Shown are means ± SEM. ∗, *P* < 0.05. Hilus, dentate hilus. Dotted lines depict SGZ. (Scale bar = 20 μm in *b* and 7.2 μm in *d*.)

complex, followed by diaminobenzidine reaction. For the Fluoro-Jade staining, the sections were rehydrated, pretreated in 0.06% potassium permanganate for 15 min, rinsed in distilled water, incubated in 0.001% Fluoro-Jade working solution (Histo-Chem, Jefferson, AR) for 30 min, rinsed in distilled water, immersed in xylene, and cover-slipped.

Microscopical Analysis. By using light microscopy, all single-labeled BrdUrd-, ED1-, and Ki67-positive cells were counted in the granule cell layer (GCL) and within two cell diameters below this region in the SGZ. Single-labeled NeuN-positive cells were counted in the dentate hilus, outlined by the GCL and an imaginary border between the lateral endings of the GCL. The number of labeled cells was calculated in 3–6 coronal sections from each rat, located between 3.3 mm and 4.3 mm posterior to bregma (encompassing dorsal hippocampus), and expressed as the mean number of cells per section. The numbers of BrdUrd/doublecortin and BrdUrd/NeuN double-labeled cells were quantified by using Olympus AX-70 epifluorescent and confocal scanning (Kr/Ar 488 nm and 568 nm excitation filter; Bio-Rad MRC1024UV) microscopes, respectively. Fifty BrdUrd-positive cells were analyzed from each rat, and the percentage was used to calculate the total number of BrdUrd/NeuN-positive cells per section.

Statistical Analysis. Values are means ± SEM. Comparisons were performed by using one-way analysis of variance (ANOVA) followed by post hoc Bonferroni test. Differences were considered significant at *P* < 0.05. A correlation *z* test was used to assess the relation between number of ED1-positive cells and BrdUrd/NeuN double-labeled cells.

Results

Inflammation Impairs Basal Neurogenesis. We first explored whether inflammation influences the formation of new neurons

in the SGZ in the intact brain. LPS is a potent activator of the inflammatory response, particularly of microglia. It acts via the CD14 receptor to trigger a kinase cascade in microglia, resulting in cytokine gene transcription (10). After 28 days of intracortical infusion of LPS, we observed a substantial number of ED1-immunopositive, activated microglia in the dentate SGZ/GCL and hilus whereas very few such cells were detected in control brains (Fig. 1 *a–c*). To label new cells, we used BrdUrd, a thymidine analogue that is incorporated into DNA during its synthesis, i.e., cell division, DNA replication, and to less extent DNA repair (24). Several lines of evidence strongly indicate that BrdUrd-labeled cells in the SGZ/GCL, both in the intact brain and after insults such as cerebral ischemia and SE, are not mature neurons undergoing DNA repair but cluster-forming, dividing cells that subsequently pass through distinct neuronal differentiation steps (16, 25–27).

The LPS-induced inflammation caused an 85% reduction in the number of new neurons, i.e., BrdUrd-immunoreactive cells double-labeled for the neuron-specific marker NeuN, in the SGZ/GCL (Fig. 1 *d* and *e*). There was a significant negative correlation between the number of new neurons and the number of activated microglia (correlation coefficient = −0.7; *P* = 0.0019; Fig. 1*f*). We observed no loss of mature hilar neurons (compare ref. 28), indicating a specific detrimental effect of inflammation on the newly formed neurons.

We then explored whether the LPS-induced inflammation suppressed basal hippocampal neurogenesis by inhibiting cell proliferation. Six days of intracortical LPS infusion followed by BrdUrd injections and perfusion 2 h thereafter did not significantly alter the number of BrdUrd-positive cells (LPS: 48 ± 20.2 vs. vehicle: 26.8 ± 5.3) or of cells double-labeled with BrdUrd and doublecortin (LPS: 6.9 ± 1.8 vs. vehicle: 10.6 ± 2.5), a marker for immature neuroblasts, in the SGZ/GCL. Also, the number of newly proliferated Ki67-positive cells did not differ between LPS- and vehicle-treated animals (data not shown).

Ekdahl *et al.*

Fig. 2. Hippocampal neurogenesis is impaired after brain insult associated with tissue damage and inflammation. (*a–d*) Neurodegeneration as visualized with Fluoro-Jade staining (*a* and *c*) and NeuN immunoreactivity (*b* and *d*) in the DG 35 days after SE. Note more damage and fewer remaining neurons in the dentate hilus after generalized SE (gSE) as compared with partial SE (pSE). (*e*) The distribution of ED1-positive, activated microglia in the DG 6 and 35 days after partial or generalized SE. (*Left Inset*) Shown are higher magnification of activated microglia. (*Right Inset*) Shown are ED1-positive (green) cells surrounding BrdUrd-positive (red) cells in the SGZ. (*f*) The number of ED1-positive microglia in the SGZ/GCL 2, 6–8, and 35 days after SE. (*g*) The number of BrdUrd/NeuN double-labeled new neurons in the SGZ/GCL 35 days after SE (28 days after BrdUrd injections). Data are number of cells per section. Shown are means ± SEM. *, $P < 0.05$ (compared with pSE in *f*). #, $P < 0.05$ compared with 35 days. In *f*, $n = 6$ (3 + 3), 21 (14 + 7), and 13 (8 + 5) for the 2-day, 6- to 8-day, and 35-day groups, respectively, with individual numbers for pSE and gSE in parentheses. In *g*, $n = 5$, 8, and 5 for nonstimulated controls, pSE, and gSE, respectively. Hilus, dentate hilus. Dotted lines depict SGZ. (Scale bar = 100 μm in *a–e* and 10 μm in *Right Inset* in *e*.)

Inflammation Attenuates Increased Neurogenesis After Brain Insult.
We then assessed whether the magnitude of neurogenesis in the SGZ after a brain insult is affected by the degree of concomitant inflammation in the tissue environment. We induced SE of two different severities, partial and generalized, respectively, by applying electrical stimulation to the hippocampus (22). Gen-

eralized SE caused more damage in the DG hilus compared with partial SE, as shown both with Fluoro-Jade staining (Fig. 2 *a* and *c*) and counts of NeuN-positive cells 35 days after the insult (Fig. 2 *b* and *d*; cells per section: generalized SE, 385 ± 49.5; partial SE, 578.1 ± 39.8). Animals with generalized SE also had significantly higher numbers of activated microglia in the SGZ/

GCL and dentate hilus (Fig. 2f). Six to eight days after the insult, many of the ED1-positive cells had swollen cell bodies and processes and were often found in close proximity to clusters of newly formed BrdUrd-labeled cells (Fig. 2e). Over the subsequent 28 days, the number of ED1-positive cells markedly declined but was still higher in generalized as compared with partial SE animals (Fig. 2f). The ED1-positive cells also became smaller with fewer processes (Fig. 2e).

Hippocampal neurogenesis clearly differed between partial and generalized SE. At 35 days, there was a 15-fold increase in the number of new neurons in the SGZ/GCL of partial SE animals. Also, rats with generalized SE showed increased neurogenesis, but the number of new neurons was 60% lower as compared with the partial SE group (Fig. 2g). This difference was not due to reduced formation of new neurons because cell proliferation in the SGZ is similar after partial and generalized SE (P. Mohapel, C.T.E., and O.L., unpublished results). These data indicated that the severity either of the hippocampal damage or of the inflammatory response determined the magnitude of neurogenesis after SE. To distinguish between these two mechanisms, LPS was infused intracortically during 28 days in animals that had exhibited partial SE. Such animals normally show only minor damage and inflammation. LPS caused no loss of NeuN-positive cells in the DG hilus after partial SE (cells per section: partial SE plus vehicle, 422.1 ± 37.3; partial SE plus LPS, 446.4 ± 41.2). Also, with LPS treatment, the damage in partial SE animals was significantly less than that in vehicle-treated, generalized SE animals (259.0 ± 76.7 NeuN-positive cells per section).

The LPS infusion increased the numbers of ED1-positive cells in the SGZ/GCL (Fig. 3 a–d). Importantly, both the number of ED1-positive cells in the SGZ/GCL and their morphology in these rats were similar to what was observed in the vehicle-treated generalized SE rats (Fig. 3 c and d).

The LPS-induced inflammation was accompanied by a reduced number of new neurons in the SGZ/GCL (Fig. 3e). There was a significant negative correlation between the numbers of new neurons and activated microglia (correlation coefficient = −0.6, P = 0.0001). Thus, without aggravating the damage, the inflammation caused by LPS infusion in the partial SE animals resulted in a similar low number of new neurons as observed in vehicle-treated, generalized SE animals (Fig. 3e).

Minocycline Restores Neurogenesis in Inflammation. We finally investigated whether the inflammation-mediated suppression of hippocampal neurogenesis can be prevented by specific inhibition of microglia activation. Minocycline readily passes the blood–brain barrier and suppresses the microglial response in neurodegenerative disease models (23, 29). In both partial and generalized SE animals that received minocycline systemically for 6 days and were perfused immediately thereafter, the number of activated microglia in the SGZ/GCL was dramatically reduced compared with vehicle-treated rats (Fig. 4a). Also, 35 days of minocycline treatment led to a decreased number of ED1-positive cells in the generalized SE animals whereas the low number of ED1-positive cells at this time point after partial SE was unchanged (Fig. 4b).

Minocycline treatment gave rise to increased numbers of new neurons in the SGZ/GCL 35 days after SE (Fig. 4 c–e). The effect of minocycline was more pronounced in generalized SE animals, and therefore, similar numbers of new neurons were now found in partial and generalized SE rats. Minocycline did not act through stimulation of SGZ cell proliferation because we observed no increase in the number of newly proliferated, Ki-67-positive cells in the minocycline-treated rats. Also, minocycline did not alter the degree of neuronal differentiation from the proliferating cells because the percentage of BrdUrd-positive cells double-labeled with NeuN was similar in minocycline- and
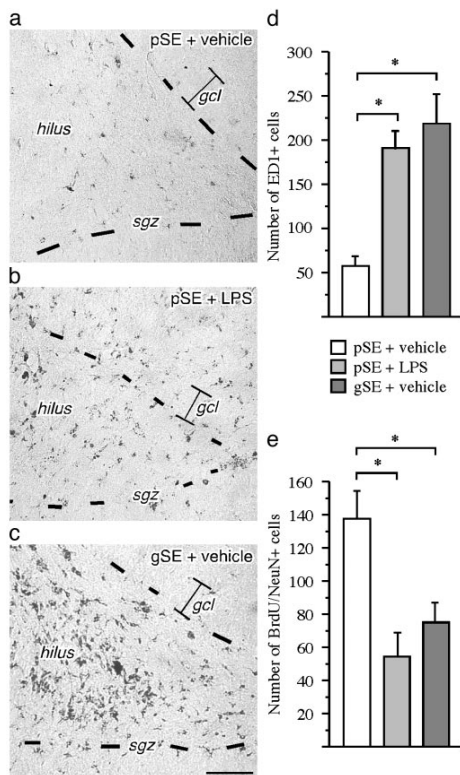
Fig. 3. Inflammation causes impairment of hippocampal neurogenesis after brain insult not associated with tissue damage. (a–c) Immunohistochemical staining of ED1-positive activated microglia in the SGZ/GCL after intracortical vehicle or LPS infusions during 28 days after partial SE (pSE) or generalized SE (gSE). (d) The number of ED1-positive cells in the DG after SE. Note that the distribution and number of ED1-positive microglia in the SGZ is similar in partial SE plus LPS and generalized SE plus vehicle animals whereas there are very few cells in the partial SE plus vehicle rats. (e) The number of BrdUrd/NeuN-positive new neurons in the SGZ/GCL 28 days after LPS or vehicle treatment after SE (21 days after BrdUrd injections). Data are number of cells per section. Shown are means ± SEM. *, P < 0.05. n = 16, 15, and 5 for pSE plus LPS, pSE plus vehicle, and gSE plus vehicle, respectively. Hilus, dentate hilus. Dotted lines depict SGZ. (Scale bar = 100 μm.)

vehicle-treated rats. The degree of epileptic damage to dentate hilar neurons was unaltered after minocycline treatment (NeuN-positive cells per section: partial SE plus vehicle, 505.3 ± 72.7 vs. partial SE plus minocycline, 401.3 ± 39.9; generalized SE plus vehicle, 286.5 ± 56.7 vs. generalized SE plus minocycline 170.5 ± 41.4).

We also found that minocycline did not influence neurogenesis in nonstimulated control animals, which had very few activated microglia in the SGZ/GCL (Fig. 4 a and b). Thus, administration of minocycline did not significantly alter either the number of Ki67-positive cells after 6 days (cells per section: minocycline, 20.4 ± 1.1 vs. vehicle, 26.6 ± 7.8) or the number of
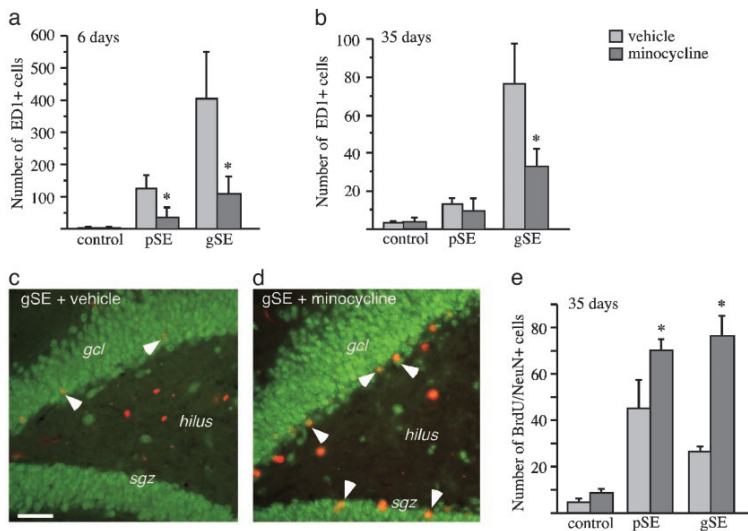
Fig. 4. Minocycline prevents inflammation-mediated suppression of hippocampal neurogenesis. (*a* and *b*) The number of ED1-positive, activated microglia in the SGZ/GCL in nonstimulated controls, and 6 days (*a*) and 35 days (*b*) after generalized SE (gSE) and partial SE (pSE) with or without minocycline treatment. (*c* and *d*) The distribution of BrdUrd (red) and NeuN (green) cells in the DG at 35 days after gSE with and without minocycline treatment. Arrowheads depict BrdUrd/NeuN-double-labeled new neurons. (*e*) The number of new neurons in the SGZ/GCL in nonstimulated controls and 35 days after gSE and pSE (28 days after BrdUrd injections). In *a*, *n* = 19 (5 + 9 + 5) and 14 (4 + 7 + 3); in *b*, *n* = 13 (4 + 5 + 4) and 14 (5 + 4 + 5); and in *e*, *n* = 13 (4 + 5 + 4) and 14 (5 + 4 + 5) for minocycline and vehicle, respectively, with individual numbers for nonstimulated controls, pSE, and gSE in brackets. Data are number of cells per section. Shown are means ± SEM. *, $P < 0.05$ compared with vehicle-treated animals. Hilus, dentate hilus. Scale bar = 50 μm.

BrdUrd/NeuN-double labeled new neurons after 5 weeks of treatment (Fig. 4*e*).

Discussion

Our data show that brain inflammation causes inhibition both of the basal, continuous formation of new neurons in the intact hippocampal formation and of the increased neurogenesis in response to a brain insult. We provide direct *in vivo* evidence for a cellular mechanism underlying the detrimental action of inflammation on neurogenesis. Thus, we find that activated microglia are localized in close proximity to the newly formed cells and, also, that the impairment of neurogenesis depends on the degree of microglia activation, irrespective of whether there is damage or not in the surrounding tissue. We demonstrate a significant negative correlation between the number of activated microglia in the neurogenic zone and the number of surviving new hippocampal neurons. Finally, we show that a selective inhibitor of microglia activation, minocycline, restores hippocampal neurogenesis in inflammation without affecting neurogenesis in control animals. The microglia activation specifically compromises the survival of the new hippocampal neurons whereas there is no evidence for suppression of cell proliferation or neuronal differentiation in either basal or insult-induced neurogenesis. The deleterious effect of activated microglia on the newly formed neurons is most likely mediated through the action of cytokines, such as IL-1β or IL-6, tumor necrosis factor α, nitric oxide, and reactive oxygen species (10–12, 30). These molecules can be released from microglia and are neurotoxic *in vitro*.

Brain inflammation and microglia activation are believed to be involved in many disorders associated with cognitive impairment such as AD, Lewy body dementia, and AIDS dementia (8, 31, 32). Antiinflammatory treatment can protect from onset or progression of AD in patients (33). Cranial irradiation leads to inflammation in the SGZ and progressive cognitive deterioration (34). There is now growing evidence that systemic inflammation, triggered by peripheral infection or injury, can cause activation of already primed microglia in the brains of AD patients, as well as in the normal aging brain, leading to delirium and aggravation of the cognitive decline (32). Our data are consistent with a model in which inflammation-mediated suppression of hippocampal neurogenesis plays a pathophysiological role for the cognitive dysfunction in these conditions.

The high vulnerability to inflammation observed here for newly generated neurons could have implications also for neurogenesis in other brain areas. Generation of dopamine neurons was recently reported to occur in the adult mouse substantia nigra (35). Inflammatory changes in this region, which are common in Parkinson's disease patients (9), could suppress neurogenesis and contribute to disease progression. Also, >80% of the new striatal neurons that are generated from the subventricular zone after stroke in rats die within the first weeks after the insult (36). Ischemic insults are associated with inflammation (37) that, based on the data reported here, is likely to compromise the survival of newly formed neurons. Our findings suggest antiinflammatory treatment as a possible novel strategy to improve the efficacy of neuronal replacement from endogenous precursors in stroke and other neurodegenerative disorders.

Here, we have demonstrated that an inflammatory response in the tissue environment that encounters newborn neurons during neurogenesis in the adult brain is detrimental for their survival. However, microglia activation after brain damage can probably also have beneficial effects by promoting other aspects of regeneration, e.g., through the release of neurotrophic molecules (38, 39). It is conceivable that the relative importance of the harmful and helpful actions of microglia under various circumstances will determine the behavioral consequences of brain inflammation and its inhibition by drugs like minocycline.

1. Cameron, H. A. & McKay, R. D. (2001) *J. Comp. Neurol.* **435,** 406–417.
2. van Praag, H., Schinder, A. F., Christie, B. R., Toni, N., Palmer, T. D. & Gage, F. H. (2002) *Nature* **415,** 1030–1034.
3. Shors, T. J., Miesegaes, G., Beylin, A., Zhao, M., Rydel, T. & Gould, E. (2001) *Nature* **410,** 372–376.
4. Santarelli, L., Saxe, M., Gross, C., Surget, A., Battaglia, F., Dulawa, S., Weisstaub, N., Lee, J., Duman, R., Arancio, O., Belzung, C. & Hen, R. (2003) *Science* **301,** 805–809.
5. Zitnik, G. & Martin, G. M. (2002) *J. Neurosci. Res.* **70,** 258–263.
6. Jacobs, B. L. (2002) *Brain Behav. Immun.* **16,** 602–609.
7. Haughey, N. J., Nath, A., Chan, S. L., Borchard, A. C., Rao, M. S. & Mattson, M. P. (2002) *J. Neurochem.* **83,** 1509–1524.
8. Nelson, P. T., Soma, L. A. & Lavi, E. (2002) *Ann. Med.* **34,** 491–500.
9. Liu, B. & Hong, J. S. (2003) *J. Pharmacol. Exp. Ther.* **304,** 1–7.
10. Pocock, J. M. & Liddle, A. C. (2001) *Prog. Brain Res.* **132,** 555–565.
11. Hanisch, U. K. (2002) *Glia* **40,** 140–155.
12. Gebicke-Haerter, P. J. (2001) *Microsc. Res. Tech.* **54,** 47–58.
13. Stoll, G., Jander, S. & Schroeter, M. (1998) *Prog. Neurobiol.* **56,** 149–171.
14. Andersson, P. B., Perry, V. H. & Gordon, S. (1991) *Neuroscience* **42,** 201–214.
15. Ling, E. A., Ng, Y. K., Wu, C. H. & Kaur, C. (2001) *Prog. Brain Res.* **132,** 61–79.
16. Parent, J. M., Yu, T. W., Leibowitz, R. T., Geschwind, D. H., Sloviter, R. S. & Lowenstein, D. H. (1997) *J. Neurosci.* **17,** 3727–3738.
17. Liu, J., Solway, K., Messing, R. O. & Sharp, F. R. (1998) *J. Neurosci.* **18,** 7768–7778.
18. Bengzon, J., Kokaia, Z., Elmer, E., Nanobashvili, A., Kokaia, M. & Lindvall, O. (1997) *Proc. Natl. Acad. Sci. USA* **94,** 10432–10437.
19. Arvidsson, A., Kokaia, Z. & Lindvall, O. (2001) *Eur. J. Neurosci.* **14,** 10–18.
20. Ekdahl, C. T., Mohapel, P., Elmer, E. & Lindvall, O. (2001) *Eur. J. Neurosci.* **14,** 937–945.
21. Paxinos, G. & Watson, C. (1997) *The Rat Brain in Stereotaxic Coordinates* (Academic, San Diego).
22. Ekdahl, C. T., Mohapel, P., Weber, E., Bahr, B., Blomgren, K. & Lindvall, O. (2002) *Eur. J. Neurosci.* **16,** 1463–1471.
23. Brundula, V., Rewcastle, N. B., Metz, L. M., Bernard, C. C. & Yong, V. W. (2002) *Brain* **125,** 1297–1308.
24. Selden, J. R., Dolbeare, F., Clair, J. H., Nichols, W. W., Miller, J. E., Kleemeyer, K. M., Hyland, R. J. & DeLuca, J. G. (1993) *Cytometry* **14,** 154–167.
25. Tonchev, A. B., Yamashima, T., Zhao, L., Okano, H. J. & Okano, H. (2003) *Mol. Cell. Neurosci.* **23,** 292–301.
26. Yagita, Y., Kitagawa, K., Sasaki, T., Miyata, T., Okano, H., Hori, M. & Matsumoto, M. (2002) *J. Neurosci. Res.* **69,** 750–756.
27. Iwai, M., Sato, K., Omori, N., Nagano, I., Manabe, Y., Shoji, M. & Abe, K. (2002) *J. Cereb. Blood Flow Metab.* **22,** 411–419.
28. Kim, W. G., Mohney, R. P., Wilson, B., Jeohn, G. H., Liu, B. & Hong, J. S. (2000) *J. Neurosci.* **20,** 6309–6316.
29. Tikka, T., Fiebich, B. L., Goldsteins, G., Keinanen, R. & Koistinaho, J. (2001) *J. Neurosci.* **21,** 2580–2588.
30. Vallieres, L., Campbell, I. L., Gage, F. H. & Sawchenko, P. E. (2002) *J. Neurosci.* **22,** 486–492.
31. Katsuse, O., Iseki, E. & Kosaka, K. (2003) *Neuropathology* **23,** 9–15.
32. Perry, V. H., Newman, T. A. & Cunningham, C. (2003) *Nat. Rev. Neurosci.* **4,** 103–112.
33. McGeer, P. L., Schulzer, M. & McGeer, E. G. (1996) *Neurology* **47,** 425–432.
34. Monje, M. L., Mizumatsu, S., Fike, J. R. & Palmer, T. D. (2002) *Nat. Med.* **8,** 955–962.
35. Zhao, M., Momma, S., Delfani, K., Carlén, M., Cassidy, R. M., Johansson, C. B., Brismar, H., Shupliakov, O., Frisén, J. & Janson, A. (2003) *Proc. Natl. Acad. Sci. USA* **100,** 7925–7930.
36. Arvidsson, A., Collin, T., Kirik, D., Kokaia, Z. & Lindvall, O. (2002) *Nat. Med.* **9,** 963–970.
37. Nencini, P., Sarti, C., Innocenti, R., Pracucci, G. & Inzitari, D. (2003) *Cerebrovasc. Dis.* **15,** 215–221.
38. Streit, W. J., Walter, S. A. & Pennell, N. A. (1999) *Prog. Neurobiol.* **57,** 563–581.
39. Schwartz, M. (2003) *J. Cereb. Blood Flow Metab.* **23,** 385–394.

NEUROSCIENCE

B

Long-term neuronal replacement in adult rat hippocampus after status epilepticus despite chronic inflammation

Sara Bonde,[1,2] Christine T. Ekdahl[1,2] and Olle Lindvall[1,2]

[1]Laboratory of Neurogenesis and Cell Therapy, Section of Restorative Neurology, Wallenberg Neuroscience Center, University Hospital, SE-221 84, Lund, Sweden
[2]Lund Strategic Research Center for Stem Cell Biology and Cell Therapy, Lund, Sweden

Abstract

Dentate gyrus (DG) neurogenesis is transiently increased during the first weeks after status epilepticus (SE). Survival of the new neurons is initially compromised by an acute inflammatory response, but the long-term fate of the remaining ones in the post-SE environment is unknown. Here adult rats were subjected to 2 h electrically evoked self-sustained SE and perfused after 5 weeks or 6 months. Rats exhibited partial or generalized SE followed by spontaneous behavioural seizures and abnormal electroencephalographic activity during 6 months. Numbers of activated microglia in the dentate subgranular zone (SGZ)-granule cell layer (GCL) and in the hilus declined after 5 weeks, but were still elevated at 6 months after SE, with no differences between the milder partial and the more severe generalized SE. At 6 months, partial and generalized SE rats showed a seven-fold increase in the number of mature SGZ–GCL neurons formed during the first 2 weeks along with aberrant neurons in the hilus. Total numbers of mature neurons in SGZ–GCL were unaltered, indicating that SE-generated neurons replaced dead granule cells. Neuroblast formation had returned to normal levels in SGZ–GCL but generation of aberrant neurons in the hilus was still ongoing at 6 months. Our data indicate that long-term impairment of neurogenesis, as reported previously after kainic acid-induced SE, is not a general feature of chronic epilepsy. We have found that a substantial proportion of the mature granule cells at 6 months are generated during the first 2 weeks after SE and survive despite chronic inflammation, and that SE triggers continuous production of aberrant hilar neurons.

Introduction

In the adult brain, neuroblasts are continuously generated from multipotent progenitor cells in the subgranular zone (SGZ) of the dentate gyrus (DG; Gage *et al.*, 1998). The new neurons develop into functional granule cells (van Praag *et al.*, 2002) but can also differentiate into inhibitory interneurons (Liu *et al.*, 2003). The formation of neurons in the SGZ is modulated by physiological stimuli, and circumstantial evidence suggests a link between hippocampal neurogenesis and cognitive function (Lie *et al.*, 2004). Brain insults also trigger increased neurogenesis in SGZ (Bengzon *et al.*, 1997; Parent *et al.*, 1997; Arvidsson *et al.*, 2001; Jin *et al.*, 2001; Liu *et al.*, 2003). Following status epilepticus (SE), SGZ cell proliferation is elevated for 2 weeks and seizure-generated mature neurons can survive for at least 4 weeks (Parent *et al.*, 1997). The magnitude of survival seems to be dependent on the severity of SE. In rats exhibiting partial SE, induced by electrical stimulation in the hippocampus, new neurons formed at 1 week showed no decrease over the subsequent 4 weeks. In contrast, there was a 65% loss of new neurons in rats with generalized SE (Mohapel *et al.*, 2004).

One important mechanism determining whether SE-generated neurons will survive or not is the magnitude of inflammatory changes in the tissue environment. We have shown that acute inflammation

after SE, as reflected by microglial activation, has detrimental effects on the survival of new neurons shortly after their birth (Ekdahl *et al.*, 2003a). Microglial activation occurs in the hippocampus within the first 24 h after SE induced by administration of kainic acid (Rizzi *et al.*, 2003), pilocarpine (Rosell *et al.*, 2003), or by electrical stimulation (De Simoni *et al.*, 2000). Increased numbers of activated microglia were observed in the hippocampus up to 1 month after pilocarpine-induced SE (Borges *et al.*, 2003). In our previous study (Ekdahl *et al.*, 2003a), poor survival of insult-generated neurons at 5 weeks was associated with more pronounced inflammatory changes in the SGZ and granule cell layer (GCL) after generalized as compared to partial SE.

Recently, hippocampal neurogenesis has been reported to be suppressed at 5 months after kainic acid administration in a rat model of temporal lobe epilepsy (Hattiangady *et al.*, 2004). New neurons were identified using immunohistochemistry for doublecortin (DCX), a reliable marker of neurogenesis which is transiently expressed (for ~ 2–3 weeks) in newly formed neuroblasts in both the intact and injured brain (Brown *et al.*, 2003; Couillard-Despres *et al.*, 2005). It has been proposed that the marked reduction in DCX-positive cells in the SGZ–GCL as compared to controls, observed at 5 months after SE, contributes to the persistent increase in seizure susceptibility. It is unclear, though, whether a long-term decrease in neurogenesis also characterizes other SE models.

In the present study, rats were subjected to electrically induced SE and allowed to survive for 5 weeks or 6 months thereafter. The objectives were three-fold: firstly, to determine whether SE leads to

long-lasting inflammatory changes in the dentate SGZ–GCL (i.e. GCL and within two cell diameters below this region in the SGZ) and hilus; secondly, to determine whether neurons generated during the first 2 weeks after SE can exhibit long-term survival in the SGZ–GCL and hilus and, if this is the case, whether they constitute a significant proportion of mature granule cells at 6 months; and thirdly, to clarify whether electrically induced SE causes suppression of hippocampal neurogenesis several months after the initial insult.

Materials and methods

Animals and surgery

Forty-three male Sprague-Dawley rats (Möllegaard's Breeding Center, Copenhagen, Denmark) weighing 230–270 g at the time of surgery were housed separately under 12-h light−12-h dark conditions with *ad libitum* access to food and water. All rats were anaesthetized with halothane (1–2%) and implanted unilaterally with a twisted insulated stainless-steel stimulating and recording electrode (Plastics One, Roanoke, VA, USA) into the right ventral hippocampal CA1–CA3 region (coordinates: 4.8 mm caudal and 5.2 mm lateral to bregma, 6.3 mm ventral from dura; toothbar at −3.3 mm; (Paxinos & Watson, 1997). Electrodes were collected in a plastic pedestal and covered with a dust cap (Plastics One). Rats were then either subjected to electrically induced SE ($n = 33$) or used as nonstimulated controls ($n = 10$). The animals were divided into two groups which survived for either 5 weeks ($n = 9$ SE and $n = 4$ control rats) or 6 months ($n = 24$ SE and $n = 6$ control rats). All experiments followed guidelines set by the Malmö-Lund Ethical Committee for use and care of laboratory animals, and were conducted in accordance with European Union directive on the subject of animal rights.

Induction of SE

Seven days after electrode implantation, SE was induced as originally described by Lothman *et al.* (1989). Afterdischarge (AD) threshold was determined for each rat through a 1-s 50-Hz electrical current, starting at 10 μA and increasing in 10-μA increments at 1-min intervals until an AD lasting 5 s or more was registered (Chart 3.6.3, PowerLab/MacLab; AD Systems, Hastings, UK). Thirty minutes later, rats received a 1-h suprathreshold stimulation with 10-s trains of 1-ms biphasic square wave pulses, at a frequency of 50 Hz. Every 10 min, stimulations were interrupted for 1 min of electroencephalogram (EEG) recordings and AD measurements. After 1 h of stimulation, all rats exhibited continuous, self-sustained ictal EEG activity. Based on the severity of behavioural convulsions, two different SE profiles were distinguished (Mohapel *et al.*, 2004): partial SE (including grade 1–2 according to Racine's scoring system for kindled seizures: Racine, 1972) and generalized SE (including grade 3–4). Behavioural convulsions and ictal EEG activity were arrested with pentobarbital (65 mg/kg i.p.) 2 h after cessation of stimulation.

Bromodeoxyuridine administration

Beginning on day 3 after the induction of SE and continuing for 14 days, all animals in the 6-month survival group, including nonstimulated controls, were given injections twice daily of the thymidine analogue 5-bromo-2′-deoxyuridine (BrdU; 50 mg/kg, i.p.;

Sigma) dissolved in potassium phosphate-buffered saline (KPBS) for labelling of mitotic cells (Dolbeare, 1995).

Recording of electroencephalogram

In order to estimate the spontaneous spiking frequency in the SE animals of the 6-month survival group, EEG recordings were sampled for 3 min weekly from the hippocampal electrode throughout the survival period. A longer, continuous 2-h EEG recording was performed immediately prior to perfusion.

Tissue preparation and sectioning

Five weeks or six months after SE, rats were weighed, received an overdose of pentobarbital anaesthesia (250 mg/kg i.p.) and were transcardially perfused with 100 mL ice-cold saline followed by 250 mL ice-cold paraformaldehyde (PFA; 4% in 0.1 M PBS, pH 7.4). Brains were removed and postfixed for 24 h in PFA, and then placed for at least 24 h in 20% sucrose in 0.1 M phosphate buffer. Brains were subsequently cut into 30-μm-thick coronal sections on a freezing microtome and stored in cryoprotective solution at −20 °C.

Immunohistochemistry

The primary antibodies used for the immunohistochemical stainings were: rat anti-BrdU (1 : 100; Oxford Biotechnology Ltd, Oxford, UK), mouse anti-Ki67 (1 : 50; Novocastra, Newcastle upon Tyne, UK), goat anti-DCX (1 : 1000; Santa Cruz Biotechnology Inc., Santa Cruz, CA, USA; Collin *et al.*, 2005; Thored *et al.*, 2005) mouse anti-neuron-specific nuclear protein NeuN (1 : 100; Chemicon, Temecula, CA, USA), rabbit anti-Iba1 (1 : 1000; Wako Chemicals, Osaka, Japan), mouse anti-ED1 (1 : 200; Serotec Ltd, Oxford, UK) and mouse anti-CD45 (1 : 50; BD Biosciences, San Jose, CA, USA). The secondary antibodies used were: biotin horse anti-mouse, biotin horse anti-goat, biotin goat anti-rabbit (all 1 : 200; Vector, Burlingame, CA, USA), and Cy3 donkey anti-rat and Cy3 donkey anti-rabbit (both 1 : 200; Jackson Immuno-Research, West Grove, PA, USA). All single labellings started with quenching for 30 min in 3% hydrogen peroxide and 10% methanol, except for the Ki67 staining which also included a high-temperature antigen-retrieval procedure before the quenching procedure, i.e. boiling for 10 min in citrate buffer (0.01 M, pH 6), cooling for 25 min, rinsing twice in Tris hydroxymethylaminoethane buffer (50 mM, pH 7.6) and finally in KPBS. The BrdU–NeuN double labelling started with an acidic antigen retrieval procedure with HCl (1 M) for 30 min at +67 °C. For both single and double labelling, preincubation followed for 1 h in blocking solution, i.e. 0.25% Triton-X100 in KPBS with 2% normal goat, donkey or horse serum, before incubation with a single or a combination of two primary antibodies at +4 °C overnight. The sections were then rinsed three times in blocking solution and incubated with secondary antibodies for 2 h in blocking solution. For single labelling, the sections were thereafter incubated with the avidin–biotin–peroxidase complex (ABC 8 μL/mL; Elite ABC kit, Vector Laboratories) for 1.5 h and treated with 3,3′-diaminobenzidine (0.5 mg/mL) and hydrogen peroxide. The sections were mounted on microscope slides, sequentially dehydrated in increasing concentrations of ethanol, processed in xylene and coverslipped with Pertex mounting medium (HistoLab products AB) for light microscopy. In order to improve visualization, the sections single-labelled with Iba1 and NeuN antibody were counterstained with

Cresyl Violet. For double stainings, the sections were incubated for 2 h in streptavidin-conjugated Alexa Fluor 488 (1 : 200; Molecular Probes, the Netherlands) and mounted and coverslipped with glycerol-based mounting medium for fluorescence microscopy.

Fluoro-Jade staining

Free-floating brain sections were mounted in KPBS and allowed to dry overnight. As described in detail elsewhere (Schmued *et al.*, 1997), the sections were rehydrated, pretreated with 0.06% potassium permanganate for 15 min, rinsed in distilled water, incubated in 0.01% Fluoro-Jade working solution (Histo-Chem, Jefferson, AR, USA) for 30 min, rinsed in distilled water, immersed in xylene and coverslipped.

Cell counting

The Iba1, BrdU and DCX stainings were performed on three or four coronal sections from each rat located between −3.2 and −4.5 mm from bregma (dorsal hippocampal region). The number of immunoreactive cells (i.e. Iba1-positive cell soma, nuclei and processes, BrdU-positive nuclei and DCX-positive cell soma and processes) was counted in the SGZ–GCL. Cells were also counted in the dentate hilus. We found no differences in number of cells between ipsilateral (stimulated) and contralateral side, either in SGZ–GCL or in dentate hilus, for any of the stainings, and cell numbers are therefore presented as average number per section. Double-labelling with Iba1–CD45 and Iba1–ED1 was examined in 100 Iba1-positive cells per rat and structure (SGZ–GCL and dentate hilus) using an Olympus BX61 epifluorescence and light microscope. Double-labelling of BrdU–NeuN was assessed in 50 BrdU-positive cells per rat and structure (SGZ–GCL and dentate hilus) using a confocal scanning light microscope (Bio-Rad MRC1021UV, UK) with Kr–Ar 488 and 568 nm excitation filter. A double-labelled BrdU–NeuN-positive cell was defined as having the strongest intensity of both stainings within the same or neighbouring 1-μm-thick optical section through the cell in a consecutive Z-series of at least 10 sections, in 200–400× magnification and with a resolution of 1024 × 1024 pixels. The percentages of double-labelled cells were multiplied by the total number of Iba1- or BrdU-positive cells, and are presented as average number of double-labelled cells per section. Stereological estimations of the total number of NeuN-positive cells in the SGZ–GCL was performed on four sections from each rat located between −3.2 and −4.5 mm from bregma, using a modified optical fractionator method on an Olympus BH-2 microscope with a 100× oil objective CCD-IRIS colour video camera, and CAST-GRID software (Olympus, Albertslund, Denmark). For systematic sampling, the frame area was set to 237.5 μm^2 with a counting interval of 100 μm in X and Y level, and the optical dissector constituted an 8-μm-thick fraction of the total section thickness (Heidenhain Microcator and CAST-GRID software). The counting frame area and counting interval were set to allow for at least 200 cells to be sampled, and the optical dissector was set to sample cells below the first 2 μm from the surface of the section.

Statistical analysis

An observer blind to treatment conditions performed all analyses. Comparisons were carried out using one-way ANOVA with subsequent Bonferroni–Dunn *post hoc* test. Results are presented as means ± SEM. Differences are considered significant at $P < 0.05$. Paired correlations were performed with the z-test. All statistical analyses were conducted using StatView software, version 5.0.1 (Abacus Concepts, Berkeley, CA, USA).

Results

Electrically induced SE lead to spontaneous seizure activity and hippocampal damage

In about two-thirds of the rats that had experienced partial or generalized SE (Fig. 1A), spontaneous behavioural seizures (Fig. 1B) were occasionally observed throughout the 6-month survival period, most often when animals were handled. Also, abnormal spontaneous spiking activity was recorded (Fig. 1C), as monitored for 3 min every week from a hippocampal electrode, in both SE profiles (mean frequency during whole survival period: partial SE 0.104 ± 0.023 Hz, generalized SE 0.146 ± 0.064 and control 0.0 ± 0.0 Hz). During the continuous 2-h recording immediately preceding perfusion, abnormal spontaneous spiking activity was observed in six out of 18 partial and one out of six generalized SE animals. Spontaneous behavioural seizures and abnormal spiking activity were not seen in nonstimulated, electrode-implanted control animals (Fig. 1D).

Hippocampal damage in terms of neuronal loss was evaluated using NeuN and Cresyl Violet staining (Fig. 1E). Both partial and generalized SE animals showed substantial loss of NeuN-positive cells in the CA1 region and cell dispersion in the CA3 region. However, the neuronal loss in the dentate hilus was more pronounced after generalized SE. Fluoro-Jade staining detecting degenerating neurons and their processes (Schmued *et al.*, 1997) showed no significant ongoing hippocampal degeneration in either partial or generalized SE animals (data not shown). The body weights of the partial and generalized SE animals increased with time, with no differences between the two SE profiles or compared to control animals at any time point (weight at the time of perfusion: partial SE 572.0 ± 12.5 g, generalized SE 577.3 ± 26.2 g and control 595.7 ± 14.8 g).

SE caused chronic inflammation in dentate gyrus

Neuroinflammation was evaluated by immunohistochemical stainings for Iba1 (demonstrating active and quiescent forms of microglia; Imai & Kohsaka, 2002), Iba1–ED1 double labelling (microglia in phagocytotic phase; Damoiseaux *et al.*, 1994), Iba1–CD45 double labelling (microglia with blood origin; Sieh *et al.*, 1993) and Iba1–Ki67 (microglia undergoing cell division; Fig. 2).

Five weeks after SE, Iba1-positive cells with few and short processes and large cell bodies were observed throughout the SGZ–GCL in an irregular pattern (Fig. 3B and C). In contrast, control rats had a homogenous distribution of cells with long and fine processes extending from small cell bodies (Fig. 3A). The number of Iba1-positive cells in the SGZ–GCL was significantly increased after both partial and generalized SE (Fig. 4A). The majority of the Iba1-positive cells were double-labelled with ED1. These cells had generally larger cell bodies than the Iba1-positive cells not expressing ED1. The intensity of ED1 expression differed, being strongest after generalized SE, lower after partial SE and weakest in the control animals (Fig. 3A–C). Both partial and generalized SE rats showed significantly more Iba1–ED1 double-labelled cells than controls, with the highest numbers after generalized SE (Fig. 4C).

Iba1-positive cells were also abundant in the hilus, with a homogenous pattern in controls (Fig. 3A) and cluster formations comprising 3–5 cells in SE animals (Fig. 3B and C), with sometimes up to 10 cells after generalized SE. Significantly more hilar Iba1- and
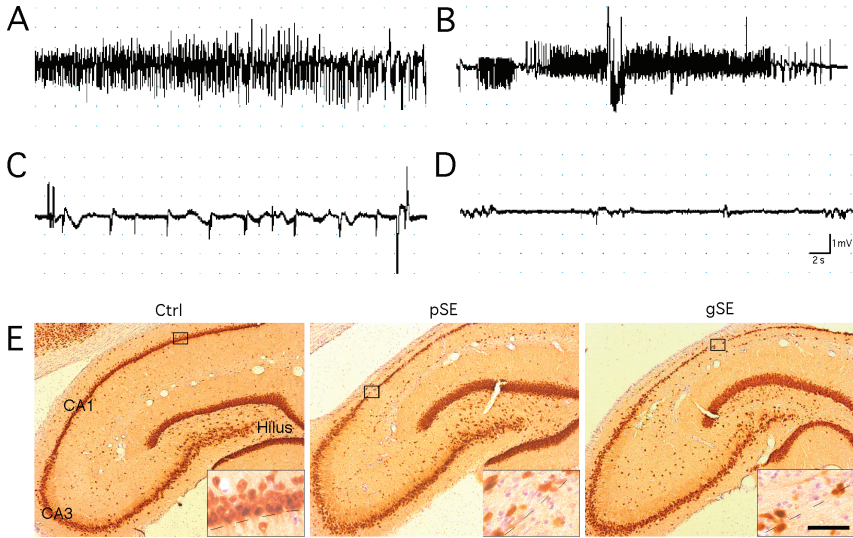
FIG. 1. EEG characteristics and description of hippocampal degeneration in rats subjected to electrically induced SE. (A–D) Examples of EEG recordings from rats (A) during self-sustained SE, (B) during a spontaneous, generalized seizure, (C) during abnormal spiking activity at 4 months post-SE, and (D) from a nonstimulated control animal. (E) Six months after both partial and generalized SE (pSE and gSE, respectively), NeuN (brown)–Cresyl Violet (lilac) staining shows loss of NeuN-positive cells in CA1 and cell dispersion in CA3. Generalized SE is also associated with fewer NeuN-positive cells in the dentate hilus than in control (ctrl) animals. The insets are higher magnifications of the areas marked by rectangles in E, illustrating the presence of Cresyl Violet- and loss of NeuN-positive cells in CA1. Scale bar, 500 μm (E), 50 μm (insets).
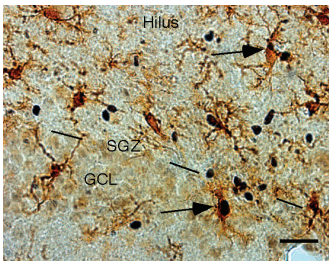
FIG. 2. Ongoing microglia proliferation in subgranular zone and granule cell layer (SGZ–GCL) and dentate hilus 6 months after SE. Examples of Iba1 (brown) and Ki67 (black) double-labelled cells are marked by arrows. Scale bar, 25 μm.

Iba1–ED1-positive cells were found in partial and generalized SE animals than in controls, with more than double the number of cells in generalized as in partial SE (Fig. 4B and D). Some Iba1-positive cells in the SGZ–GCL and hilus were double-labelled with Ki67 (Fig. 2), but the percentage of Iba1–Ki67-positive cells did not differ between the groups (SGZ–GCL: controls 9.5 ± 3.4%, partial SE 5.9 ± 0.5%, generalized SE 9.8 ± 2.3%; hilus: controls 8.3 ± 1.9%, partial SE 6.5 ± 1.3%, generalized SE 14.2 ± 2.8%). None of the Iba1-positive cells in SGZ–GCL or hilus coexpressed CD45.

The morphology of the Iba1-positive cells in SGZ–GCL and hilus at 6 months after SE closely resembled that observed at 5 weeks, but the clusters of cells were fewer (Fig. 3E and F). Also, in control animals the Iba1-positive cell morphology and distribution were similar at these time points (Fig. 3A and D). We found that, at 6 months after SE, the number of Iba1-positive cells in SGZ–GCL was significantly increased in partial SE but not in generalized SE animals (Fig. 4A). The number of Iba1–ED1 double-labelled cells in SGZ–GCL was increased in both SE profiles compared to controls (Fig. 4C). In the hilus, both the number of Iba1- and Iba1–ED1-positive cells were increased in partial and generalized SE animals compared to control rats (Fig. 4B and D). Between 5 weeks and 6 months, the number of Iba1–ED1-positive cells in the SGZ–GCL and hilus decreased by ∼40 and 66%, respectively, in the generalized SE animals, but was stable in the partial SE rats (Fig. 4C and D). There were no differences between the groups in the percentage of Iba1-positive cells double-labelled with Ki67 (SGZ–GCL: control 7.2 ± 1.4%, partial SE 8.9 ± 0.5%, generalized 9.7 ± 0.1%; hilus: control 13.0 ± 0.2%, partial SE 11.6 ± 0.1%, generalized 11.2 ± 0.1%) and virtually no Iba1-positive cells were double-labelled with CD45 (data not shown).

SE produced new neurons that survived for 6 months in dentate gyrus without affecting total number of granule cells

Six months after both partial and generalized SE, increased numbers of BrdU-positive cells were found in the SGZ and inner third of the GCL (Fig. 5). The number of BrdU-positive cells in SGZ–GCL was six- to seven-fold higher in the partial and generalized SE animals than
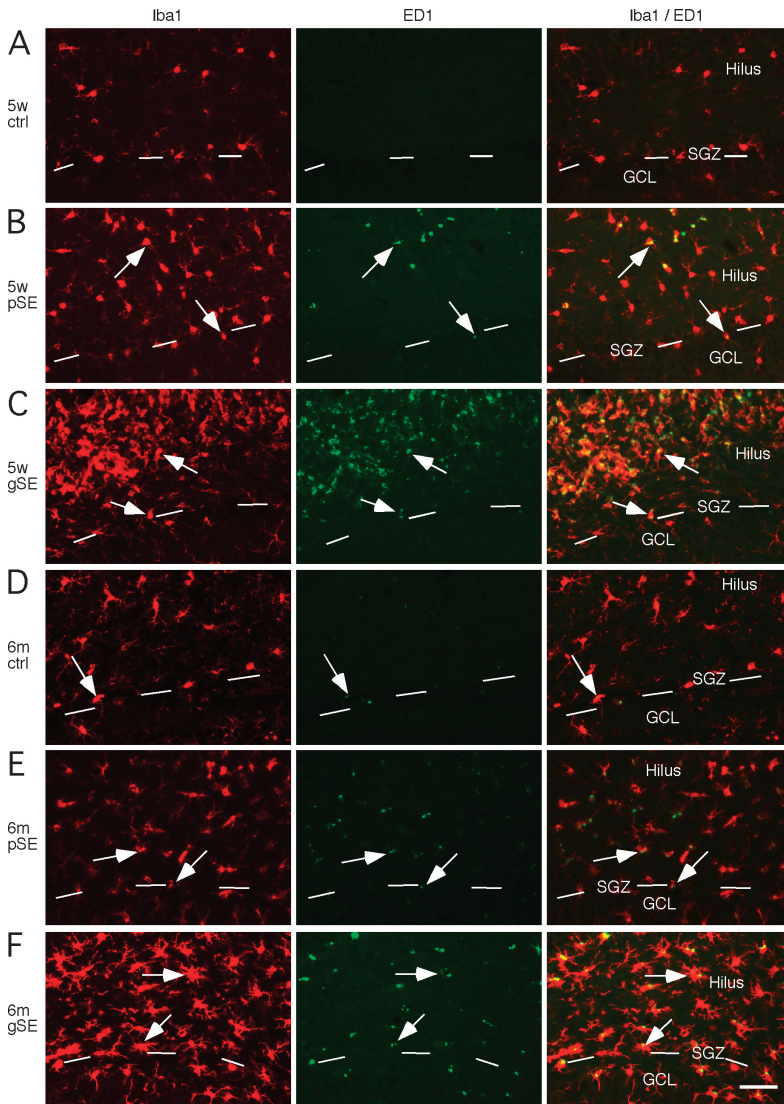
Fig. 3. Continuous microglia activation in dentate gyrus up to 6 months after partial and generalized status epilepticus (pSE and gSE). Iba1 (red)- and ED1 (green)-positive cells in the subgranular zone and granule cell layer (SGZ–GCL) and dentate hilus (A–C) 5 weeks and (D–F) 6 months after (B and E) pSE and (C and F) gSE and in (A and D) nonstimulated, electrode-implanted controls. Examples of microglia cells in a phagocytic state (Iba1–ED1 double-labelled) are marked with arrows. Scale bar, 50 μm.

in nonstimulated, electrode-implanted controls and virtually all BrdU-positive cells were double-labelled with the mature neuronal marker NeuN (Fig. 5A and B). Consequently, also the number of BrdU–NeuN-positive cells was much higher in the SE animals (Fig. 5C), but with no significant differences in cell numbers between partial and generalized SE (Fig. 5C). The total number of mature, NeuN-positive
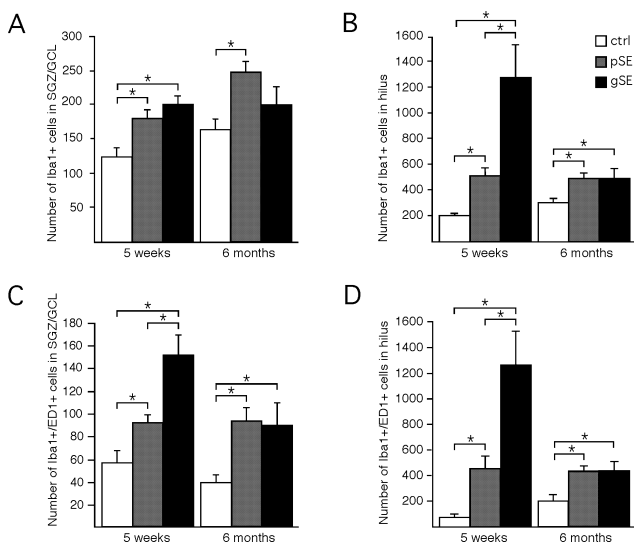
FIG. 4. Increased total number of microglia (Iba1-positive) as well as number of phagocytotic microglia (Iba1–ED1-positive) in dentate gyrus up to 6 months after partial and generalized status epilepticus (pSE and gSE). Number of cells at 5 weeks and 6 months after SE is presented for (A and C) the subgranular zone and granule cell layer (SGZ–GCL) and (B and D) dentate hilus. Bars represent average number of cells per section + SEM. *$P < 0.05$. Numbers of animals: at 5 weeks, ctrl $n = 4$, pSE $n = 4$, gSE $n = 5$; at 6 months, ctrl $n = 6$, pSE $n = 18$, gSE $n = 6$.

neurons in the SGZ–GCL did not differ between SE and control animals (Fig. 5D) and was not correlated with the number of BrdU–NeuN-positive new neurons (data not shown).

In the dentate hilus of SE animals, BrdU-positive cells were found scattered without a clear pattern (Fig. 5A), some in clusters of two or three cells. Such cells were never observed in controls (controls 0.0 ± 0.0, partial SE 4.5 ± 1.4, generalized SE 11.2 ± 5.2 cells). Almost all BrdU-positive cells coexpressed NeuN, and we found no significant differences in number of BrdU–NeuN-positive cells between partial and generalized SE (controls 0.0 ± 0.0, partial SE 4.3 ± 1.4, generalized SE 11.1 ± 5.2 cells). Also, there was no significant correlation between the number of BrdU–NeuN-positive cells in the SGZ–GCL or hilus and the number of Iba1-, Iba1–ED1-, Iba1–CD45- or Iba1–Ki67-positive cells, or the mean spontaneous spiking activity recorded throughout the 6-month survival period (data not shown).

SE induced long-lasting increase in neuroblast formation in dentate hilus but no change in granule cell layer

Six months after SE, uniformly stained DCX-positive cells with processes and large cell bodies were often found in clusters of two to seven cells, primarily in the inner third of the GCL (Fig. 6B and C). At this point, both DCX cell morphology and localization in SE animals closely resembled what was observed in the nonstimulated, electrode-implanted rats (Fig. 6A). Furthermore, the number of DCX-positive cells in the SGZ–GCL did not differ between partial SE, generalized SE and control animals (Fig. 6D and E). However, in the dentate hilus, single DCX-positive cells with similar morphology as seen in the SGZ–GCL were found in both partial and generalized SE

animals but never in control rats (Fig. 6F). The number of DCX-positive hilar cells was not significantly different between the two SE profiles (Fig. 6G). The degree of abnormal spontaneous spiking activity, recorded during the 2-h period immediately prior to perfusion, did not correlate with the number of DCX-positive cells found in the hilus (data not shown).

Discussion

The present study shows that electrically evoked partial and generalized SE is accompanied by inflammation in the DG with a duration of at least 6 months. In the early phase after SE, inflammation is detrimental to the survival of the newborn neuroblasts generated in the SGZ in response to the insult (Ekdahl *et al.*, 2003a). Here we demonstrate that, despite the long-term inflammatory changes in the neurogenic area, a significant number of SE-induced neuroblasts in the SGZ–GCL matured and survived for 6 months. We also provide evidence that, at 6 months after SE, the formation of SGZ–GCL neuroblasts was normal whereas aberrant hilar neurons were still being generated.

SE evoked by electrical stimulation in the hippocampus has previously been shown to induce activated ED1-positive microglia in the SGZ–GCL and hilus, with maximum numbers at 7 days, thereafter declining but still present at 5 weeks after the insult (Ekdahl *et al.*, 2003a). More pronounced inflammatory changes were observed after generalized than partial SE at both time-points. Hattiangady *et al.* (2004) recently reported that the density of activated microglia in the entire hippocampus decreased dramatically between 16 days and 5 months following KA-induced SE, i.e. a severe form of generalized SE. We show here that although the inflammatory changes in the
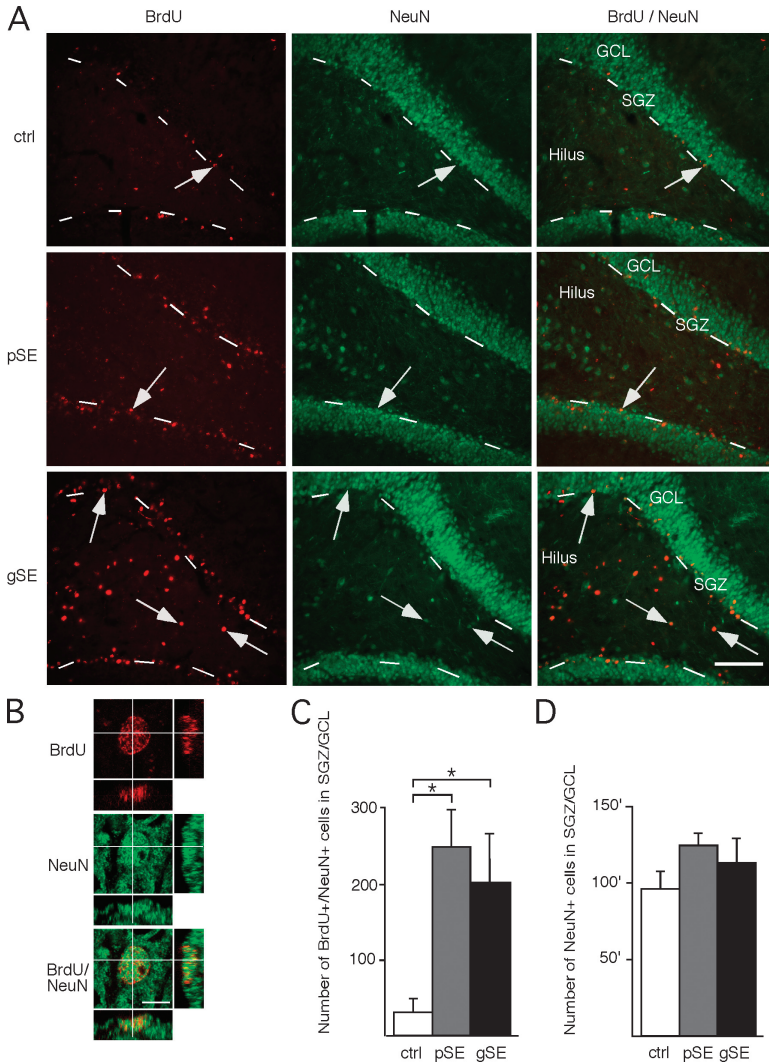
FIG. 5. New hippocampal neurons generated during the initial 2 weeks after SE survived for 6 months without an increase in the total number of dentate granule cells. (A) BrdU (red)- and NeuN (green)-positive cells in the subgranular zone and granule cell layer (SGZ–GCL) and dentate hilus 6 months after partial and generalized SE (pSE and gSE) and in nonstimulated electrode-implanted controls. Arrows mark examples of BrdU–NeuN double-labelled cells. (B) Confocal image with orthogonal projection of a BrdU (red)-NeuN (green) double-labelled cell in the SGZ–GCL 6 months after SE. (C) Increased number of BrdU–NeuN-positive cells in SGZ–GCL in pSE and gSE compared to controls. (D) No increase in total number of NeuN-positive cells in the SGZ–GCL after pSE or gSE. Bars represent average number of cells per section + SEM. *$P < 0.05$; ′ (vertical axis in D), ×1000. Numbers of animals: ctrl $n = 6$, pSE $n = 18$, gSE $n = 6$. Scale bars, 100 µm (A), 6 µm (B).
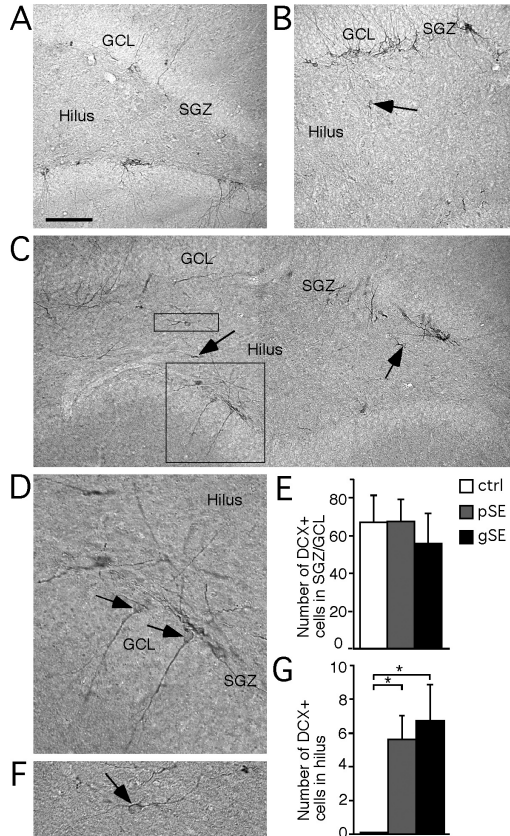
FIG. 6. Continuous aberrant neuroblast formation in dentate hilus, but no long-term alteration in neuroblast formation in subgranular zone and granule cell layer (SGZ–GCL), 6 months after SE. DCX-positive cells are observed in the SGZ–GCL of (A) nonstimulated electrode-implanted controls, and in (B) partial and (C) generalized SE (pSE and gSE). Only SE animals also show DCX-stained cells in the dentate hilus (arrows in B and C). (D and F) Higher magnifications of DCX-positive cells marked by boxes in C and localized in (D) SGZ–GCL and (F) dentate hilus. (E) No differences in number of DCX-positive cells in the SGZ–GCL between controls and SE animals at 6 months. (G) Increased number of DCX-positive cells in the dentate hilus 6 months after pSE and gSE. Bars represent average number of cells per section + SEM; *$P < 0.05$. Numbers of animals: ctrl $n = 6$, pSE $n = 18$, gSE $n = 6$. Scale bars, 60 μm (A–C), 20 μm (D), 25 μm (F).

SGZ–GCL and dentate hilus continued to decrease after 5 weeks in electrically induced generalized SE animals, elevated numbers of activated microglia were still present 6 months after both partial and generalized SE. The initial differences in magnitude of microglial activation at 5 weeks between the milder partial and the more severe generalized SE were no longer observed at 6 months. The persistent increase in the number of microglia could not be explained by enhanced proliferation in the DG, as the percentage of Iba1-positive cells expressing Ki67 was not altered. This finding suggests that microglial cells are recruited to the SGZ–GCL and hilus from other brain areas, but most probably not from the blood because very few Iba1-positive cells coexpressed CD45. It cannot be excluded, though, that the CD45 antigen had been down-regulated in some Iba1-positive cells which had left the bloodstream and entered the epileptic brain

tissue. A few CD45-positive cells not expressing Iba1 were sometimes found in association with vascular structures.

In the intact adult brain, neurons formed in the DG can survive for at least 1 year (Dayer *et al.*, 2003). After ischemic insults leading to neuronal death, new neurons in the striatum and CA1 region, generated from neural stem cells in the subventricular zone and posterior periventricle, respectively, have been reported to survive for at least 4 and 6 months (Nakatomi *et al.*, 2002; Thored *et al.*, 2005). Previous studies have shown that SE-generated neurons can survive for at least 4 weeks (Ekdahl *et al.*, 2003b). In this study, we demonstrate that mature BrdU–NeuN-positive neurons born during the first 2 weeks after SE are able to survive for 6 months in the SGZ–GCL following the insult. Despite their exposure to both acute and chronic inflammatory changes in the tissue environment, the number

of these insult-generated mature neurons was, at 6 months, almost seven-fold higher than the number of cells formed through basal neurogenesis during the same 2-week time period in controls. We have previously shown (Mohapel *et al.*, 2004) that rats exhibiting partial and generalized SE show similar levels of cell proliferation in the SGZ at 1 week after the insult, and that most new neurons survive the subsequent 4 weeks in partial SE animals whereas about two-thirds of them die following generalized SE. Interestingly, the differences between animals with partial and generalized SE in the number of BrdU–NeuN-positive cells in the SGZ–GCL at 5 weeks (Mohapel *et al.*, 2004) were no longer observed at 6 months after SE. One explanation to this finding is that neurons born into an environment with a lower degree of inflammation, such as after partial SE, are less susceptible to immediate death but cannot avoid cell loss caused by the chronic post-SE environment. Another possibility is that only a proportion of the new neurons generated after partial SE survive because the other neurons are surplus and fail to establish synaptic connections.

Although a substantial number of the new neurons generated during the first 2 weeks after SE were still present 6 months after the insult, stereological counting did not reveal any significant differences in the total number of NeuN-positive neurons in the SGZ–GCL between rats exhibiting the two SE profiles and control animals. We estimate that, at 6 months after SE, the new neurons formed during the first 2 weeks constitute $\sim 9\%$ of the total number of neurons in the SGZ–GCL as compared to $\sim 2\%$ generated during the same time period in controls. If a cell addition of this magnitude had occurred in the SGZ–GCL following SE, it would have been detected with the stereological method used here. This finding, along with previous studies showing that electrically induced SE is associated with necrotic and apoptotic death of mature DG neurons (Sloviter *et al.*, 1996; Ekdahl *et al.*, 2003b), suggest that the new SE-generated neurons which survive long-term replace rather than add to the existing population of granule cells.

In the study of Parent *et al.* (1997), the number of BrdU-positive cells in the SGZ was no longer elevated when BrdU was given at 4 weeks after pilocarpine-induced SE. However, two recent articles have reported changes in the generation of new DG neurons at later time-points after SE (Cha *et al.*, 2004; Hattiangady *et al.*, 2004). In the lithium–pilocarpine model of SE, which also gives rise to recurrent seizures, rats which exhibited spontaneous motor seizures and had slightly more hippocampal damage 2 months after the insult showed a modest increase in dentate neurogenesis (Cha *et al.*, 2004). In animals with less damage and no spontaneous seizures, there was decreased number of new, mature neurons (BrdU–NeuN double-labelled) as compared to controls. In contrast, a dramatic reduction in the number of DCX-positive neuroblasts in the entire DG was observed 5 months after intracerebroventricular (64% decrease) and intraperitoneal (81% decrease) administration of kainic acid (Hattiangady *et al.*, 2004). The overall reduction in neuroblast formation was greater in rats showing spontaneous recurrent motor seizures. Our data demonstrate that, at 6 months following electrically evoked SE, the formation of DCX-positive neuroblasts in the SGZ–GCL had returned to baseline levels with no differences compared to nonstimulated controls. We have also previously found that additional seizures do not compromise the survival of the newly generated neurons after electrically induced SE (Ekdahl *et al.*, 2003b). Taken together, available data indicate that the characteristics of the SE model used, e.g. with respect to the extent of hippocampal damage and inflammation, and frequency and severity of spontaneous seizures, determine the long-term effects on neurogenesis in the SGZ–GCL. A recent study on tissue from epileptic patients further supports the idea that the level of neurogenesis at later time points after SE is influenced by the degree of hippocampal damage.

Patients with hippocampal sclerosis had decreased numbers of polysiylated neural cell adhesion molecule (PSA–NCAM)-positive neuroblasts in the GCL and SGZ, while there were no differences compared to nonepileptic specimens if granule cell dispersion was missing (Pirttila *et al.*, 2005).

It is well established that aberrant 'granule-like' neurons, which migrate into the dentate hilus, are formed in the SGZ acutely after SE and survive up to 5 weeks thereafter (Parent *et al.*, 1997; Scharfman *et al.*, 2000). Scharfman *et al.* (2000) have reported that these new hilar neurons, identified by their expression of calbindin, become synchronized with host hippocampal neurons and are activated by spontaneous seizures. These findings suggest that the new hilar neurons are functionally integrated into limbic circuits involved in recurrent seizure generation (Scharfman *et al.*, 2002). Our data show that the SE-generated hilar neurons can survive much longer than previously reported, at least for 6 months despite chronic inflammation, which supports the idea that they become functionally integrated and receive appropriate trophic support. Interestingly, we also demonstrate a persistent, albeit low, production of hilar DCX-positive neuroblasts, which is still ongoing 6 months after SE. This finding is strengthened by a recent human study where a few DCX-positive cells were observed in adult epileptic tissue obtained after hippocampectomy (Crespel *et al.*, 2005). Whether these neuroblasts differentiate into mature neurons is not known. Also, an increase in aberrant PSA–NCAM-positive neuroblasts has been shown in the molecular layer of human epileptic and sclerotic hippocampal specimens (Pirttila *et al.*, 2005). Six months after SE, there was a trend for a higher number of aberrant BrdU–NeuN-positive cells in the dentate hilus of animals which had exhibited generalized SE as compared to those with partial SE. Such a difference could be related to the more pronounced hilar cell death after generalized SE (Mohapel *et al.*, 2004) because newly formed neurons are attracted to damaged brain areas (Arvidsson *et al.*, 2002). However, we found no difference between the two SE profiles in number of hilar DCX-positive cells formed at 6 months, and no ongoing neurodegeneration. Also, it was recently described that aberrant hilar neurons are generated in the intact brain after intrahippocampal infusion of brain-derived neurotrophic factor (Scharfman *et al.*, 2005). Thus, hilar damage is probably only one factor of importance for triggering the ectopic migration of the seizure-generated cells.

In conclusion, we show here that neurons generated in DG after SE can survive long-term despite chronic inflammation. Our data raise the possibility that inflammation is initially detrimental to the new neurons, as demonstrated previously, but its occurrence may be chronically beneficial for their survival and differentiation. We also demonstrate that the neurons formed in response to the SE insult constitute a substantial proportion of the total number of dentate granule cells at 6 months, and that aberrant hilar neurons are continuously produced in the SGZ at least up to this time point. Despite their significant numbers, the functional role of the new neurons in the epileptic brain is as yet unclear. The present data are in accordance with the hypothesis that the new neurons participate in the neural circuits which underlie the pathological excitability in chronic epilepsy or contribute to the cognitive disturbances after SE (Scharfman, 2004).

Abbreviations

AD, afterdischarge; BrdU, 5-bromo-2′-deoxyuridine; DCX, doublecortin; DG, dentate gyrus; EEG, electroencephalogram; GCL, granule cell layer; KPBS, potassium phosphate-buffered saline; SE, status epilepticus; SGZ, subgranular zone; SGZ–GCL, GCL and within two cell diameters below this region in the SGZ.

References

Arvidsson, A., Collin, T., Kirik, D., Kokaia, Z. & Lindvall, O. (2002) Neuronal replacement from endogenous precursors in the adult brain after stroke. *Nat. Med.*, **8**, 963–970.

Arvidsson, A., Kokaia, Z. & Lindvall, O. (2001) N-methyl-D-aspartate receptor-mediated increase of neurogenesis in adult rat dentate gyrus following stroke. *Eur. J. Neurosci.*, **14**, 10–18.

Bengzon, J., Kokaia, Z., Elmer, E., Nanobashvili, A., Kokaia, M. & Lindvall, O. (1997) Apoptosis and proliferation of dentate gyrus neurons after single and intermittent limbic seizures. *Proc. Natl Acad. Sci. USA*, **94**, 10432–10437.

Borges, K., Gearing, M., McDermott, D.L., Smith, A.B., Almonte, A.G., Wainer, B.H. & Dingledine, R. (2003) Neuronal and glial pathological changes during epileptogenesis in the mouse pilocarpine model. *Exp. Neurol.*, **182**, 21–34.

Brown, J.P., Couillard-Despres, S., Cooper-Kuhn, C.M., Winkler, J., Aigner, L. & Kuhn, H.G. (2003) Transient expression of doublecortin during adult neurogenesis. *J. Comp. Neurol.*, **467**, 1–10.

Cha, B.H., Akman, C., Silveira, D.C., Liu, X. & Holmes, G.L. (2004) Spontaneous recurrent seizure following status epilepticus enhances dentate gyrus neurogenesis. *Brain Dev.*, **26**, 394–397.

Collin, T., Arvidsson, A., Kokaia, Z. & Lindvall, O. (2005) Quantitative analysis of the generation of different striatal neuronal subtypes in the adult brain following excitotoxic injury. *Exp. Neurol.*, **195**, 71–80.

Couillard-Despres, S., Winner, B., Schaubeck, S., Aigner, R., Vroemen, M., Weidner, N., Bogdahn, U., Winkler, J., Kuhn, H.G. & Aigner, L. (2005) Doublecortin expression levels in adult brain reflect neurogenesis. *Eur. J. Neurosci.*, **21**, 1–14.

Crespel, A., Rigau, V., Coubes, P., Rousset, M.C., de Bock, F., Okano, H., Baldy-Moulinier, M., Bockaert, J. & Lerner-Natoli, M. (2005) Increased number of neural progenitors in human temporal lobe epilepsy. *Neurobiol. Dis.*, **19**, 436–450.

Damoiseaux, J.G., Dopp, E.A., Calame, W., Chao, D., MacPherson, G.G. & Dijkstra, C.D. (1994) Rat macrophage lysosomal membrane antigen recognized by monoclonal antibody ED1. *Immunology*, **83**, 140–147.

Dayer, A.G., Ford, A.A., Cleaver, K.M., Yassaee, M. & Cameron, H.A. (2003) Short-term and long-term survival of new neurons in the rat dentate gyrus. *J. Comp. Neurol.*, **460**, 563–572.

De Simoni, M.G., Perego, C., Ravizza, T., Moneta, D., Conti, M., Marchesi, F., De Luigi, A., Garattini, S. & Vezzani, A. (2000) Inflammatory cytokines and related genes are induced in the rat hippocampus by limbic status epilepticus. *Eur. J. Neurosci.*, **12**, 2623–2633.

Dolbeare, F. (1995) Bromodeoxyuridine: a diagnostic tool in biology and medicine, Part I: Historical perspectives, histochemical methods and cell kinetics. *Histochem. J.*, **27**, 339–369.

Ekdahl, C.T., Claasen, J.H., Bonde, S., Kokaia, Z. & Lindvall, O. (2003a) Inflammation is detrimental for neurogenesis in adult brain. *Proc. Natl Acad. Sci. USA*, **100**, 13632–13637.

Ekdahl, C.T., Zhu, C., Bonde, S., Bahr, B.A., Blomgren, K. & Lindvall, O. (2003b) Death mechanisms in status epilepticus-generated neurons and effects of additional seizures on their survival. *Neurobiol. Dis.*, **14**, 513–523.

Gage, F.H., Kempermann, G., Palmer, T.D., Peterson, D.A. & Ray, J. (1998) Multipotent progenitor cells in the adult dentate gyrus. *J. Neurobiol.*, **36**, 249–266.

Hattiangady, B., Rao, M.S. & Shetty, A.K. (2004) Chronic temporal lobe epilepsy is associated with severely declined dentate neurogenesis in the adult hippocampus. *Neurobiol. Dis.*, **17**, 473–490.

Imai, Y. & Kohsaka, S. (2002) Intracellular signaling in M-CSF-induced microglia activation: role of Iba1. *Glia*, **40**, 164–174.

Jin, K., Minami, M., Lan, J.Q., Mao, X.O., Batteur, S., Simon, R.P. & Greenberg, D.A. (2001) Neurogenesis in dentate subgranular zone and

rostral subventricular zone after focal cerebral ischemia in the rat. *Proc. Natl Acad. Sci. USA*, **98**, 4710–4715.

Lie, D.C., Song, H., Colamarino, S.A., Ming, G.L. & Gage, F.H. (2004) Neurogenesis in the adult brain: new strategies for central nervous system diseases. *Annu. Rev. Pharmacol. Toxicol.*, **44**, 399–421.

Liu, S., Wang, J., Zhu, D., Fu, Y., Lukowiak, K. & Lu, Y.M. (2003) Generation of functional inhibitory neurons in the adult rat hippocampus. *J. Neurosci.*, **23**, 732–736.

Lothman, E.W., Bertram, E.H., Bekenstein, J.W. & Perlin, J.B. (1989) Self-sustaining limbic status epilepticus induced by 'continuous' hippocampal stimulation: electrographic and behavioral characteristics. *Epilepsy Res.*, **3**, 107–119.

Mohapel, P., Ekdahl, C.T. & Lindvall, O. (2004) Status epilepticus severity influences the long-term outcome of neurogenesis in the adult dentate gyrus. *Neurobiol. Dis.*, **15**, 196–205.

Nakatomi, H., Kuriu, T., Okabe, S., Yamamoto, S., Hatano, O., Kawahara, N., Tamura, A., Kirino, T. & Nakafuku, M. (2002) Regeneration of hippocampal pyramidal neurons after ischemic brain injury by recruitment of endogenous neural progenitors. *Cell*, **110**, 429–441.

Parent, J.M., Yu, T.W., Leibowitz, R.T., Geschwind, D.H., Sloviter, R.S. & Lowenstein, D.H. (1997) Dentate granule cell neurogenesis is increased by seizures and contributes to aberrant network reorganization in the adult rat hippocampus. *J. Neurosci.*, **17**, 3727–3738.

Paxinos, G. & Watson, C. (1997) *The Rat Brain in Stereotaxic Coordinates*. Academic Press, New York.

Pirttila, T.J., Manninen, A., Jutila, L., Nissinen, J., Kalviainen, R., Vapalahti, M., Immonen, A., Paljarvi, L., Karkola, K., Alafuzoff, I., Mervaala, E. & Pitkanen, A. (2005) Cystatin C expression is associated with granule cell dispersion in epilepsy. *Ann. Neurol.*, **58**, 211–223.

van Praag, H., Schinder, A.F., Christie, B.R., Toni, N., Palmer, T.D. & Gage, F.H. (2002) Functional neurogenesis in the adult hippocampus. *Nature*, **415**, 1030–1034.

Racine, R.J. (1972) Modification of seizure activity by electrical stimulation. II. Motor seizure. *Electroencephalogr. Clin. Neurophysiol.*, **32**, 281–294.

Rizzi, M., Perego, C., Aliprandi, M., Richichi, C., Ravizza, T., Colella, D., Veliskova, J., Moshe, S.L., De Simoni, M.G. & Vezzani, A. (2003) Glia activation and cytokine increase in rat hippocampus by kainic acid-induced status epilepticus during postnatal development. *Neurobiol. Dis.*, **14**, 494–503.

Rosell, D.R., Nacher, J., Akama, K.T. & McEwen, B.S. (2003) Spatiotemporal distribution of gp130 cytokines and their receptors after status epilepticus: comparison with neuronal degeneration and microglial activation. *Neuroscience*, **122**, 329–348.

Scharfman, H.E. (2004) Functional implications of seizure-induced neurogenesis. *Adv. Exp. Med. Biol.*, **548**, 192–212.

Scharfman, H., Goodman, J., Macleod, A., Phani, S., Antonelli, C. & Croll, S. (2005) Increased neurogenesis and the ectopic granule cells after intrahippocampal BDNF infusion in adult rats. *Exp. Neurol.*, **192**, 348–356.

Scharfman, H.E., Goodman, J.H. & Sollas, A.L. (2000) Granule-like neurons at the hilar/CA3 border after status epilepticus and their synchrony with area CA3 pyramidal cells: functional implications of seizure-induced neurogenesis. *J. Neurosci.*, **20**, 6144–6158.

Scharfman, H.E., Sollas, A.L. & Goodman, J.H. (2002) Spontaneous recurrent seizures after pilocarpine-induced status epilepticus activate calbindin-immunoreactive hilar cells of the rat dentate gyrus. *Neuroscience*, **111**, 71–81.

Schmued, L.C., Albertson, C. & Slikker, W. Jr (1997) Fluoro-Jade: a novel fluorochrome for the sensitive and reliable histochemical localization of neuronal degeneration. *Brain Res.*, **751**, 37–46.

Sieh, M., Bolen, J.B. & Weiss, A. (1993) CD45 specifically modulates binding of Lck to a phosphopeptide encompassing the negative regulatory tyrosine of Lck. *EMBO J.*, **12**, 315–321.

Sloviter, R.S., Dean, E., Sollas, A.L. & Goodman, J.H. (1996) Apoptosis and necrosis induced in different hippocampal neuron populations by repetitive perforant path stimulation in the rat. *J. Comp. Neurol.*, **366**, 516–533.

Thored, P., Arvidsson, A., Cacci, E., Ahlenius, H., Kallur, T., Darsalia, V., Ekdahl, C.T., Kokaia, Z. & Lindvall, O. (2005) Persistent production of neurons from adult brain stem cells during recovery after stroke. *Stem Cells*, in press.

C

Environment Matters: Synaptic Properties of Neurons Born in the Epileptic Adult Brain Develop to Reduce Excitability

Katherine Jakubs,[1,4] Avtandil Nanobashvili,[1,4]
Sara Bonde,[1,4] Christine T. Ekdahl,[1,4] Zaal Kokaia,[3,4]
Merab Kokaia,[1,2,4,5] and Olle Lindvall[1,4,5,*]
[1] Laboratory of Neurogenesis and Cell Therapy
[2] Experimental Epilepsy Group
Section of Restorative Neurology
Wallenberg Neuroscience Center
University Hospital
SE-221 84 Lund
Sweden
[3] Laboratory of Neural Stem Cell Biology
Section of Restorative Neurology
Stem Cell Institute
University Hospital
SE-221 84 Lund
Sweden
[4] Lund Strategic Research Center for
    Stem Cell Biology and Cell Therapy
Biomedical Center
SE-221 84 Lund
Sweden

Summary

Neural progenitors in the adult dentate gyrus continuously produce new functional granule cells. Here we used whole-cell patch-clamp recordings to explore whether a pathological environment influences synaptic properties of new granule cells labeled with a GFP-retroviral vector. Rats were exposed to a physiological stimulus, i.e., running, or a brain insult, i.e., status epilepticus, which gave rise to neuronal death, inflammation, and chronic seizures. Granule cells formed after these stimuli exhibited similar intrinsic membrane properties. However, the new neurons born into the pathological environment differed with respect to synaptic drive and short-term plasticity of both excitatory and inhibitory afferents. The new granule cells formed in the epileptic brain exhibited functional connectivity consistent with reduced excitability. We demonstrate a high degree of plasticity in synaptic inputs to adult-born new neurons, which could act to mitigate pathological brain function.

Introduction

In the adult mammalian brain, neurogenesis occurs continuously from neural stem/progenitor cells located in the dentate gyrus subgranular zone (SGZ) and the subventricular zone (SVZ) lining the lateral ventricles. The formation of new granule cells in the SGZ and olfactory bulb neurons in the SVZ is modulated by a large number of physiological stimuli. Circumstantial evidence indicates a role for hippocampal neurogenesis in learning and memory and mood regulation, and a role for olfac-

*Correspondence: olle.lindvall@med.lu.se
[5] These authors contributed equally to this work.

tory bulb neurogenesis in olfactory discrimination and memory (for references, see Abrous et al., 2005).

Pathological conditions influence several steps of adult neurogenesis. Following stroke, progenitor proliferation increases in the SVZ and newly formed neuroblasts migrate into the damaged striatum, where they adopt the phenotype of medium spiny neurons (Arvidsson et al., 2002; Parent et al., 2002). Status epilepticus (SE) triggers increased SGZ cell proliferation (Parent et al., 1997), and seizure-generated mature neurons can survive for at least 6 months (Bonde et al., 2006). Inflammation and microglia activation in the SGZ are detrimental to the survival of new hippocampal neurons during the early phase after their formation (Ekdahl et al., 2003; Monje et al., 2003), but activated microglia can probably also promote neurogenesis (Battista et al., 2006).

Several approaches for identification of new neurons have been used in combination with patch-clamp recordings to determine their functional properties in the intact brain. The new neurons have been visualized after intracerebral injection of a retroviral vector carrying the GFP gene (RV-GFP) (van Praag et al., 2002) or in transgenic mice expressing GFP in immature neurons (Overstreet et al., 2004), or they have been identified based on their electrophysiological characteristics by determining input resistance (Schmidt-Hieber et al., 2004). In the intact brain, new granule cells develop membrane properties, action potentials (APs), and synaptic inputs very similar to the rest of the granule cell population (van Praag et al., 2002). In excitatory synapses on newly generated, young dentate neurons, long-term potentiation can be elicited more readily than in old neurons (Schmidt-Hieber et al., 2004). New olfactory bulb neurons also exhibit mature electrophysiological properties and receive afferent synaptic inputs (Belluzzi et al., 2003; Carleton et al., 2003).

Whether the properties of new neurons are altered if they undergo differentiation in a pathological environment is unknown. This information is needed to assess their suitability for cell replacement strategies, i.e., to asses if the new neurons compromise or contribute to functional recovery in the diseased brain. Following SE, new granule cells migrate into the granule cell layer (GCL) or ectopically into the dentate hilus and molecular layer (Crespel et al., 2005; Parent et al., 1997, 2005). Intracellular recordings from aberrant hilar neurons in epileptic rats indicate that they retain the intrinsic properties of granule cells. They also exhibit abnormal burst firing (Scharfman et al., 2000), suggesting involvement in the epileptic condition. There is recent evidence that seizures can accelerate the development of excitatory input to immature dentate granule cells during the first 2 weeks after their formation (Overstreet-Wadiche et al., 2006). However, the functional characteristics of the epilepsy-generated, new but mature granule cells in the GCL have not been investigated.

Here we used whole-cell patch-clamp recordings to determine how a pathological environment influences the electrophysiological properties and functional
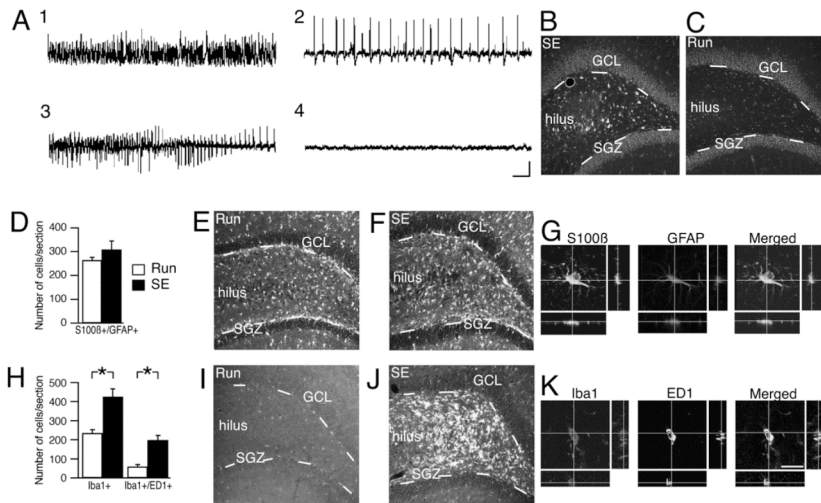
73

Figure 1. Hippocampal Tissue Environment Differs after Status Epilepticus and Running

(A1) High-frequency ictal EEG activity during SE. (A2) Abnormal interictal spiking activity in absence of behavioral seizures at 1 week after SE. (A3) High-frequency EEG activity during a spontaneous behavioral seizure at 4 weeks after SE. (A4) Lack of abnormal EEG activity at 1 week after running. Scale bar in (A) = 2 s, 1 mV. Distribution of Fluoro-Jade-stained, degenerating neurons in dentate gyrus at 1 week after SE (B) or running (C). Number and distribution of astrocytes (D–F) (S100β+ = green, GFAP+ = red) and microglia (H–J) (Iba1+ = red, depicts all microglia; ED1+ = green, shows activated, phagocytic microglia) in SGZ/GCL at 1 week after SE or running. *p < 0.05, Student's unpaired t test. Data in bar graphs depict mean ± standard error of the mean (SEM). Confocal images of S100β+/GFAP+ (G) and Iba1+/ED1+ (K) cells. Orthogonal reconstructions from confocal z-series as viewed in x-z (bottom) and y-z (right) plane. Scale bar = 110 μm (B–C, E–F, I–J), 19 μm (G and K).

integration of new cells aged 5 to 6 weeks in the GCL. New neurons were labeled via intrahippocampal injection of RV-GFP, and we compared those generated following voluntary running, i.e., a physiological stimulus, with cells formed after SE, i.e., a brain insult.

Results

Hippocampal Damage, Inflammation, and Chronic Seizures Characterize the Pathological Environment Caused by Status Epilepticus

Microscopical analysis was performed at 1 week (when RV-GFP was injected to label newborn neurons) and at 5 weeks (just prior to patch-clamp recordings) after SE or running. Virtually all animals exhibited partial SE; fewer than 5% of rats showed generalized SE (Mohapel et al., 2004). Electroencephalographic (EEG) recordings revealed high-frequency activity during SE (Figure 1A1), abnormal, interictal spiking activity throughout the observation period (Figure 1A2), and spontaneous behavioral seizures (Figure 1A3). Runners did not exhibit seizures or abnormal EEG activity (Figure 1A4).

We observed neuronal degeneration in dentate hilus, CA1, and CA3 using Fluoro-Jade staining at 1 (Figure 1B) and 5 weeks after SE (Mohapel et al., 2004; Schmued et al., 1997) but not after running (Figure 1C). There were no differences in the numbers of S100β+/ GFAP+

cells in SGZ/GCL between runners and SE animals (Figures 1D–1G). Microglia were present in the SGZ/GCL of SE animals and runners (Figures 1H–1K). Both the total number of microglia (Iba1+) and the number of activated, phagocytic microglia (Iba1+/ED1+), which gives a measure of degree of inflammation, were higher at 1 week after SE than following running (Figures 1H–1K). At 5 weeks, activated microglia in SE animals were much fewer, their number being similar to that in runners (Ekdahl et al., 2003).

Morphological and Membrane Properties of New Cells Born into a Physiological or an Epileptic Environment Are Characteristic of Dentate Granule Cells

Whole-cell patch-clamp recordings were performed at corresponding time points (between 4.5 and 6.2 weeks) after intrahippocampal injection of RV-GFP in SE animals and runners. Recordings were made in the GCL from GFP+ cells formed at the time of virus injection (referred to as "new cells"), and from GFP− cells most likely born prior to SE and running (called "mature cells"). Retroviral GFP-labeling was similar in both groups; we observed GFP+ cells with morphology typical of dentate granule cells (small soma, dendritic tree extending into molecular layer) throughout the GCL (Figure 2A). There were no differences between runners
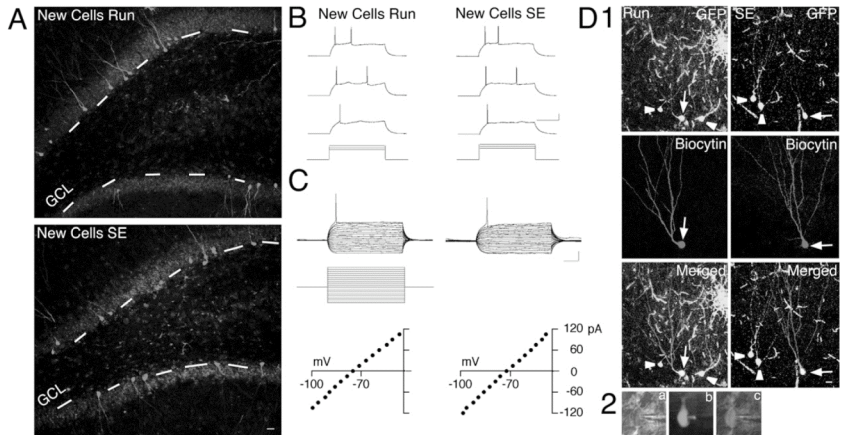
Figure 2. New Cells Born into a Physiological or an Epileptic Environment Exhibit Similar Intrinsic Membrane Properties

(A) Distribution of GFP+ cells in runners and SE animals at 4 weeks after RV-GFP injection. Broken line depicts GCL. Scale bar = 50 μm. (B) Action potentials elicited in new cells in runners and SE animals. Scale bar = 200 ms, 10 mV. (C) Voltage responses in new cells born after running or SE recorded in current-clamp mode at resting membrane potential (−77.1 ± 1.4 mV, n = 10, and −79.0 ± 1.8 mV, n = 8). Scale bar = 100 ms, 20 mV. Recordings were performed 4.5–5 weeks after RV-GFP injection; 500 ms duration current steps with 15 pA increments in (B) and (C). (D1) Confocal images of cells in runners and SE animals. Scale bar = 10 μm. Cells expressing only GFP (not recorded) are indicated with arrowheads, and GFP-expressing, recorded cells filled with biocytin are depicted by arrows. Merged images show coexpression of GFP and biocytin in recorded cells. (D2) Granule cell visualized in a live hippocampal slice; (a) and (b) are overlaid in (c). Note GFP diffusion into recording pipette in (b) and (c).

and SE animals in the numbers of GFP+ cells in the hippocampal formation (257 ± 53 versus 249 ± 30). We found hilar basal dendrites on 2 out of 37 new and 2 out of 23 mature granule cells in SE animals, but on no cells in runners (n = 48).

Newly formed granule cells are functionally mature at 4 weeks, but continue maturation for up to 4 months, which is reflected by lower membrane rise time constant (τ_m) (van Praag et al., 2002). In order to support that GFP− cells were older than GFP+ ones, we analyzed τ_m and found that GFP+ cells had lower τ_m than GFP− cells (37.8 ± 2.6 and 52.5 ± 3.0 ms, respectively; p < 0.05, Student's unpaired t test; τ_m values did not differ between runners and SE animals). Adult-born granule cells extend their dendrites well into the outer molecular layer by 4 weeks of age, but the complexity of dendritic branching continues to increase for several months thereafter (van Praag et al., 2002). Higher numbers of proximal branches of apical dendrites arised from

GFP− cells compared with GFP+ cells after both SE and running (SE: 0.78 ± 0.16 versus 1.7 ± 0.2; running: 0.72 ± 0.18 versus 1.5 ± 0.3, respectively; p < 0.05, Student's unpaired t test), but the number of apical dendrites arising from the soma did not differ between GFP+ and GFP− cells after SE or running (SE: 1.4 ± 0.1 versus 1.3 ± 0.1; running: 1.2 ± 0.1 versus 1.5 ± 0.1, respectively). Our data therefore indicate that the GFP+ cells were born later than the GFP− cells.

We explored if the intrinsic membrane properties of new neurons differed depending on whether they had been formed in response to a physiological or pathological stimulus. Recordings from GFP+ and GFP− cells revealed no differences in any parameters between either new or mature cells generated after running or SE (Table 1 and Figures 2B and 2C). The intrinsic membrane properties were similar in old and new cells (Table 1), and resembled those of mature dentate granule cells (Table 1, Figures 2B and 2C) (Scharfman, 1992). We found no

Table 1. Intrinsic Membrane Properties of New and Mature Cells in the Dentate Granule Cell Layer

	Group	n	Resting membrane potential (mV)	Input resistance (MΩ)	Action potential threshold (mV)	Action potential half-width (ms)
New cells	Runners	10(5)	−77.1 ± 1.4	411 ± 36.7	−35.4 ± 2.2	1.67 ± 0.13
	SE	8(4)	−79.0 ± 1.8	347 ± 46.0	−35.6 ± 1.5	1.72 ± 0.08
Mature cells	Runners	10(6)	−82.2 ± 1.6	320 ± 42.6	−34.6 ± 2.7	1.53 ± 0.10
	SE	7(7)	−83.4 ± 0.4	302 ± 36.7	−37.2 ± 3.1	1.37 ± 0.11

Recordings were made from new (GFP+) and mature (GFP−) cells in animals subjected to SE or running at 4.5–5 weeks after RV-GFP injection. n = number of recorded cells; number of animals is in parentheses. Values are means ± SEM. Comparisons between new cells and mature cells revealed no significant differences; p > 0.05, Student's unpaired t test.

differences between new or mature cells in the number of spikes generated at action potential threshold (GFP+: 1.1 ± 0.1 versus 1.1 ± 0.1 and GFP−: 2.1 ± 0.5 versus 1.2 ± 0.2 in SE animals and runners, respectively; p > 0.05, Student's unpaired t test).

Microscopical analysis confirmed colocalization of GFP and biocytin in recorded new cells (Figures 2D1 and 2D2), whereas mature cells contained biocytin only. Our data indicate that new cells developed intrinsic membrane properties characteristic of dentate granule cells, and that these properties were not influenced by a pathological environment.

Cells Born into an Epileptic Environment Receive Less Excitatory Synaptic Drive

Excitatory synaptic currents in new cells were recorded while blocking GABA$_A$ receptors with picrotoxin (PTX). Mean frequency of spontaneous excitatory postsynaptic currents (sEPSCs) in new cells born after SE was about 66% lower as compared with that in new cells in runners; in contrast, we detected no differences between mature cells in runners and SE animals (Figure 3A). Cumulative fraction analysis confirmed that sEPSCs occurred at longer interevent intervals (IEIs) at synapses on SE new cells compared with running-generated new cells (Figures 3B and 3C). This difference was maintained after blocking APs with tetrodotoxin (TTX). The IEIs of sEPSCs at synapses on mature cells were not different between runners and SE animals. Mean amplitudes of sEPSCs did not differ either between new or mature cells (Figure 3D). However, sEPSCs in mature granule cells from SE rats occurred at shorter IEIs and with higher amplitude than in those from untreated animals (Figures 3E and 3F). In summary, our data indicate that excitatory synaptic drive was attenuated on new cells born in an epileptic environment.

Cells Born into an Epileptic Environment Exhibit Increased Paired-Pulse Facilitation of Excitatory Postsynaptic Currents

We analyzed whether excitatory synapses on new cells in runners and SE animals differed with respect to short-term plasticity. Delivering paired stimulations to the lateral perforant path (LPP) induces paired-pulse facilitation (PPF) of excitatory postsynaptic responses (Colino and Malenka, 1993; McNaughton, 1980). PPF is a presynaptic form of plasticity with an inverse relationship to overall release probability (P$_r$) of glutamate (Debanne et al., 1996; Murthy et al., 1997; Zucker and Stockbridge, 1983). We stimulated LPP and recorded EPSCs while blocking GABA$_A$ receptors. PPF at synapses on new cells was several-fold higher in SE animals than in runners at both a 25 ms and 50 ms interstimulus interval (ISI) (Figures 4A and 4D). Furthermore, overall PPF (combined ISIs) was 3-fold higher in the new cells in SE animals as compared with runners (Figure 4A). In contrast, the response at LPP synapses on mature cells did not differ between SE animals and runners (Figure 4B). We detected paired-pulse depression (PPD) in both groups, whereas PPF of EPSCs was recorded from granule cells in intact animals (Figures 4B and 4C). Taken together, our data show that new cells in SE animals and runners received functional excitatory inputs through LPP, but
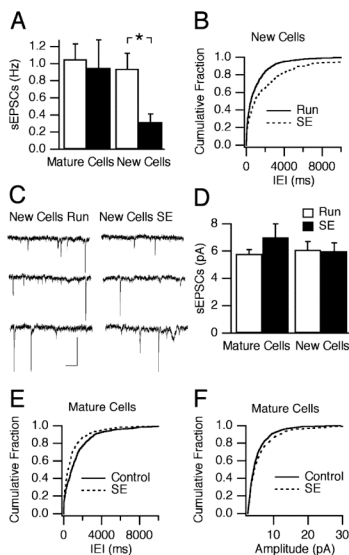

Figure 3. New Cells Born into an Epileptic Environment Receive Less Excitatory Synaptic Drive

(A) Average frequency of sEPSCs in new and mature cells from runners and SE animals. Frequency of sEPSCs was lower in new cells born after SE than in those born after running (*p < 0.05, Student's unpaired t test, n = 7 and 6 cells, respectively), but similar in mature cells in runners and SE animals (p > 0.05, n = 10 and 6 cells, respectively). (B) Cumulative fraction curves of interevent intervals (IEIs) for sEPSCs in new cells showing longer IEIs in cells born after SE compared with those born after running (p < 0.05, K-S test). (C) Examples of sEPSCs in cells born after running and SE. Note fewer sEPSCs in traces from SE animals. Scale bar = 200 ms, 10 pA. (D) Average amplitude of sEPSCs in new and mature cells did not differ between runners and SE animals (p > 0.05, Student's unpaired t test). sEPSCs in mature cells occurred with shorter IEIs (E) and higher amplitudes (F) in SE animals than in untreated control rats (p < 0.05, K-S test; n = 6 and 7 cells, respectively). Recordings were performed 4.5–5 weeks after RV-GFP injection. Data in bar graphs depict mean ± SEM.

short-term plasticity at these synapses was markedly influenced by the epileptic environment.

Higher PPF of EPSCs in LPP synapses on new cells in SE animals indicated lower overall P$_r$ of glutamate (Debanne et al., 1996; Murthy et al., 1997). To support this hypothesis, we estimated the coefficient of variation (CV) of first stimulation-evoked EPSC peak amplitudes in the new cells (Berninger et al., 1999; Min et al., 1998). A larger CV of EPSC amplitude is associated with lower P$_r$ and vice versa (Berninger et al., 1999). We found a higher CV value for EPSCs in new cells formed following SE as compared with ones formed after running, but no difference in mature cells (Figure 4E). We then used MK-801, an open-channel blocker for NMDA receptors; the rate at which successive NMDA receptor-mediated EPSCs are attenuated by MK-801 reflects the rate at which released glutamate activates NMDA receptors
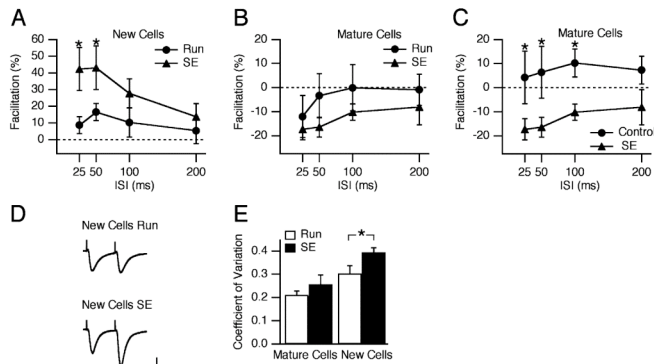
Figure 4. Excitatory Synapses on New Cells Born into an Epileptic Environment Show Increased Paired-Pulse Facilitation of Excitatory Postsynaptic Currents

Average PPF of evoked EPSCs in LPP synapses on new (A) and mature (B and C) cells in SE animals or runners, or in untreated animals (C), expressed as percent change of second EPSC compared with the first one. Recordings were made at 4.5–5.1 weeks after RV-GFP injection. (A) Overall PPF (all ISIs combined), as well as PPF with 25 and 50 ms ISIs (*), was higher in cells born after SE than those born after running ($p < 0.05$, one-way factorial ANOVA and Student's unpaired t test, respectively; $n = 6$ and 9 cells, respectively). In contrast, PPF of EPSCs in mature cells (B) was similar at all ISIs ($p > 0.05$, $n = 8$ and 7 cells, respectively). (C) PPF was reduced in mature granule cells of SE animals compared with untreated animals (*$p < 0.05$, Student's unpaired t test, $n = 8$ cells and 9 cells, respectively). (D) Traces of paired EPSCs in cells born after running and SE at 50 ms ISI. Scale bar = 20 ms, 20 pA. (E) The coefficient of variation (CV) (S.D./mean) of EPSC amplitudes (first response of the pair) at LPP synapses on new and mature cells. The coefficient was higher for EPSCs recorded in new cells from SE animals as compared with those from runners (*$p < 0.05$, Student's unpaired t test, $n = 6$ and 7 cells, respectively), but did not differ between mature cells of either group ($p > 0.05$, $n = 6$ cells for each group). Data represent mean ± SEM.

(Hessler et al., 1993; Min et al., 1998; Rosenmund et al., 1993). Therefore, MK-801's blocking rate of NMDA EPSCs is a measure of overall P_r of glutamate. Stimulations to LPP in presence of MK-801 revealed slower reduction in amplitude of NMDA receptor-mediated EPSCs in new cells from SE animals (Figure 5A). Mean, normalized EPSC amplitudes in SE animals plotted against those in runners were all above the 45° line, indicating that each successive stimulation caused larger attenuation of NMDA-receptor-mediated EPSCs in runners (Figure 5B). EPSCs elicited in presence of MK-801 had faster decay time than NMDA receptor-mediated responses before MK-801 addition (Figures 5C and 5D), and identical kinetics were evident in all subsequent responses, indicating stable, saturated concentration of MK-801 during experiments. Our findings support that LPP synapses on new cells in the epileptic environment exhibit lower overall P_r of glutamate.

Cells Born into an Epileptic Environment Receive More Inhibitory Synaptic Drive
We next recorded sIPSCs while blocking glutamate receptors with NBQX and D-AP5. Mean sIPSC frequency (Figure 6A) and amplitude (Figure 6B) in new cells did not differ between those of runners and SE animals. However, cumulative fraction analysis showed that sIPSCs at synapses on new cells born into an epileptic environment occurred at significantly shorter IEIs (Figures 6C–6E). In contrast, IEIs of sIPSCs in mature cells were longer in SE animals (Figure 6F). Mean sIPSC amplitude in mature cells was higher after SE (Figure 6B), and cumulative fraction analysis revealed such a differ-

ence also at synapses on new cells (Figures 6G and 6H). IEIs of IPSCs in mature cells from SE rats were longer, and amplitudes were larger when compared with granule cells in untreated animals (Figures 6I and 6J).

Cumulative fraction analysis showed that TTX induced a more pronounced shift toward longer IEIs of IPSCs in new cells born after SE than those born after running (Figures 7A and 7B). Thus, a larger proportion of the inhibitory input to new cells in SE animals was due to action potential activity in afferent GABAergic neurons. Following TTX, there was a shift in the kinetics of sIPSCs toward slower rise and decay times in cells born after SE but not after running (Figures 7C and 7D); the amplitude of IPSCs recorded in the presence of TTX was also smaller ($p < 0.05$, Kolmogorov-Smirnov [K-S] test). Slower kinetics and lower amplitude of IPSCs usually indicate activation of axo-dendritic synapses distal to the recording pipette (in the cell soma), while faster kinetics and higher amplitude are associated with axo-somatic synapses located proximal to the pipette (see, e.g., Wierenga and Wadman, 1999; Kobayashi and Buckmaster, 2003). Our data suggest that most of the action potential-dependent sIPSCs in new cells of SE animals were generated at axo-somatic synapses.

Cells Born into an Epileptic Environment Exhibit Decreased Paired-Pulse Depression of Inhibitory Postsynaptic Currents
We determined whether short-term plasticity at inhibitory synapses on new cells differed between SE animals and runners. We induced PPD of monosynaptic IPSCs in
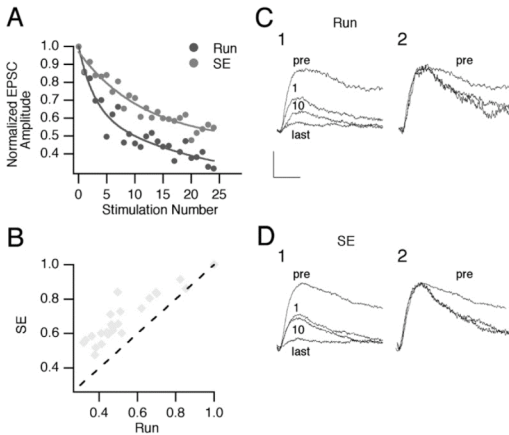
77

Figure 5. Lateral Perforant Path Synapses on Cells Born into an Epileptic Environment Exhibit Reduced Overall Release Probability of Glutamate

(A) Amplitude decay and corresponding exponential fits (solid lines) of stimulation-induced EPSCs in LPP synapses on GFP+ cells in SE animals and runners after addition of MK-801 (80 μM). Slower reduction in amplitude of consecutive NMDA receptor-mediated EPSCs was recorded in new cells in SE animals as compared with those in runners (p < 0.05, Student's unpaired t test for decay coefficients of individual exponential fits, n = 8 and 5, respectively). (B) Same cells as in (A), with EPSC amplitudes of cells from SE animals plotted against those from runners during MK-801 application. Virtually all points fall above the 45° line, indicating that the amplitude of consecutive EPSCs in cells in SE animals decayed with a slower rate compared with those in runners. Traces demonstrate examples of the progressive decay of amplitudes of EPSCs recorded in a GFP+ cell from a runner (C1) or SE animal (D1) after MK-801 addition. The scaled responses (C2, D2; same traces as in C1 and D1) demonstrate the faster decay time of individual EPSCs in the presence of, compared with before the application of, MK-801. Note that traces after MK-801 application have identical decay time kinetics, indicating that the concentration of MK-801 was saturating and stable over time. Scale bar = 20 ms, 20 pA. Presented are averages of two consecutive traces.

granule cells by delivering paired stimulations to the dentate molecular layer. The inhibitory synapses on new cells in SE animals expressed reduced PPD of IPSCs compared with synapses on new cells in runners, as assessed with all ISIs combined and at 100 ms ISI (Figures 8A and 8D). In contrast, PPD of IPSCs at inhibitory synapses on mature cells did not differ between SE animals and runners or untreated controls (Figures 8B and 8C).

We then assessed the CV of first stimulation-evoked IPSC amplitudes. For cells formed after SE, the CV was lower compared with that in new cells formed after running, while the CV of IPSCs in mature cells did not differ (Figure 8E). Together with increased frequency of sIPSCs, these data suggest higher overall P_r at GABAergic synapses on new cells formed in SE animals.

We studied the possible involvement of presynaptic GABA$_B$ receptors using the agonist baclofen (Gloveli et al., 2003; Wu and Leung, 1997). Baclofen caused marked reduction of PPD of stimulation-evoked IPSCs in cells from runners, but caused no change in SE-generated cells (Figures 8F–8H). These data provide evidence that decreased presynaptic GABA$_B$ receptor expression or sensitivity at afferent synapses on cells born into an epileptic environment causes a reduction of PPD of IPSCs in these cells.

During early stages of postnatal development, activation of GABA$_A$ receptors depolarizes hippocampal neurons (Leinekugel et al., 1999; Rivera et al., 1999). GABA also depolarizes adult-born granule cells during the first 2 weeks of development, but becomes hyperpolarizing around 3 weeks (Ge et al., 2006). Using perforated-patch recordings, we found that GABA$_A$ receptor-mediated IPSCs reversed at −68, −78, and −79 mV, respectively (average −75 mV), in three new cells in SE animals

(see Figure S1 in the Supplemental Data). This finding argues against IPSCs depolarizing new cells at the time point studied here.

Taken together, our data show that short-term plasticity at inhibitory synapses on new cells was clearly dependent on whether the cells had been born into a pathological or physiological environment. New cells formed after SE expressed less PPD of IPSCs, which, together with the observed increased sIPSC frequency, would stabilize elevated GABA release onto these neurons, particularly during repeated activation as in seizures (Buhl et al., 1996).

Discussion

Here we demonstrate that environmental conditions confronting newborn neurons generated from neural progenitors in the adult dentate gyrus affect their functional synaptic connectivity. Neurogenesis was increased by a physiological stimulus or a brain insult, i.e., voluntary running or SE, respectively. New cells in runners and SE animals exhibited many characteristics of dentate granule cells and had similar intrinsic membrane properties. In contrast, new neurons which had developed in the physiological and pathological tissue environments differed with respect to synaptic drive and short-term plasticity of both excitatory and inhibitory afferents.

The excitatory synaptic drive to the new neurons was reduced in SE animals as compared with runners, reflected by reduced mean frequency of sEPSCs. This difference was specific for new cells and was not observed when comparing mature cells. In fact, previous studies in kainate and pilocarpine epilepsy models have shown *increased* frequency of sEPSCs in granule
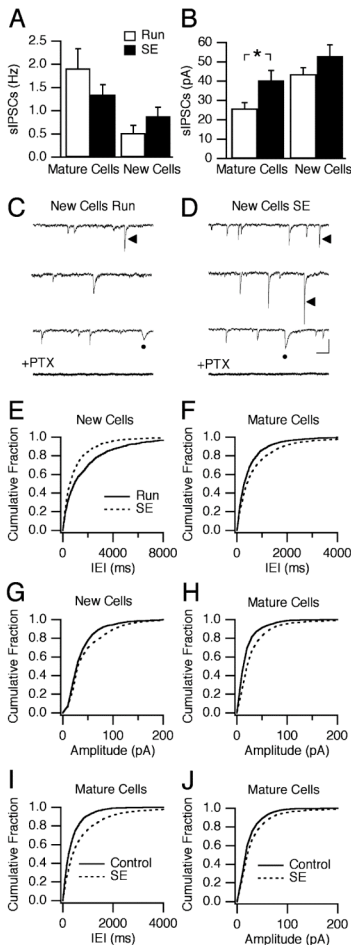
cells (Simmons et al., 1997; Wuarin and Dudek, 2001), which we also observed when comparing SE with untreated rats. Our data indicate that the lower excitatory drive on new cells in SE animals was due to decreased overall P_r of glutamate. First, the fluctuation of the peak amplitude of the EPSC in response to LPP stimulation, assessed using CV, was higher on new cells in the epileptic environment. Second, the SE-generated new neurons showed higher PPF of EPSCs evoked by LPP stimulations. In contrast to the new cells, the LPP synapses onto mature cells in SE animals and runners did not differ with respect to CV or responses to paired stimulations. We observed PPD of EPSCs in mature cells in SE animals, but PPF in intact controls. Our findings are in agreement with the work of Klapstein et al. (1999), and more recently, the work of Scimemi et al. (2006), who showed that LPP simulation elicited reduced or abolished PPF of EPSCs in dentate granule cells after kindling and SE, respectively. Third, the MK-801 experiments showed slower blocking rates of consecutive NMDA receptor-mediated EPSCs in new cells born in the SE environment as compared with those generated after running. Taken together, these data indicate that excitatory synapses on the new cells responded in an opposite way to the epileptic environment as compared with those formed prior to SE, which seemed to exhibit increased overall P_r of glutamate.

The new cells born into the epileptic environment received increased inhibitory input. The frequency of sIPSCs was higher in new cells in SE animals, whereas we found lower frequency in mature cells, which agrees with the reduced frequency of sIPSCs and mIPSCs observed in granule cells in pilocarpine- and kainic acid-induced epileptic rats (Kobayashi and Buckmaster, 2003; Shao and Dudek, 2005). The elevated inhibitory drive on new cells formed after SE was mostly due to increased action potential activity in axo-somatic afferent fibers. Three hypothetical mechanisms may explain why the frequency of action potential-dependent IPSCs was higher in new cells, but not in mature cells, in SE animals. The new and mature cells could be innervated by separate pools of interneurons with different frequencies of action potential generation. Another possibility is that the surrounding interneurons form more synapses on the new cells. Finally, overall P_r could be higher at synapses on new cells. The decreased CV of stimulation-evoked IPSCs in new cells in SE animals suggests that the changes are localized presynaptically, and probably involve an increased overall P_r of GABA (Ivanova et al., 2004). Seemingly in contradiction to this hypothesis, the observed decrease of PPD of IPSCs indicated reduced P_r. The depression of the second IPSC during paired, monosynaptic stimulations is predominantly

Figure 6. New Cells Born into an Epileptic Environment Receive More Inhibitory Synaptic Drive

(A) Average frequency of sIPSCs in new and mature cells from runners and SE animals 5.1–5.5 weeks after RV-GFP injection. (B) Average amplitude of sIPSCs in new and mature cells from runners and SE animals. The amplitude in mature cells was larger in SE animals than in runners (*p < 0.05, n = 10 and 7 cells, respectively), but was similar in new cells born in both environments (p > 0.05, Student's unpaired t test, n = 9 and 8 cells, respectively). Data depict mean ± SEM. (C and D) Examples of sIPSCs in cells born after running and SE. The sIPSCs were blocked by PTX, confirming that they were mediated by GABA$_A$ receptor activation. Note the larger, more frequent sIPSCs in the cells from SE animals. Also note that the sISPCs had two different characteristics: slow kinetics and lower amplitude (dots), and fast kinetics and higher amplitude (arrow-

heads). Scale bar = 200 ms, 50 pA. Cumulative fraction curves of IEIs (E, F, and I) and of amplitude (G, H, and J) for sIPSCs recorded in new (E and G) and mature (F, H, I, and J) cells in SE animals and runners, or in untreated animals (I and J). The IEIs were shorter in new cells from SE animals compared with runners; however, the opposite effect was observed when comparing the mature cells between the two groups (E and F). The amplitude in both new and mature cells was larger in SE animals than it was in runners (G and H). Spontaneous IPSCs in mature granule cells occurred with longer IEIs and higher amplitudes in SE rats compared with untreated rats (I and J) (7 cells in each group). (E–J: p < 0.05, K-S test).
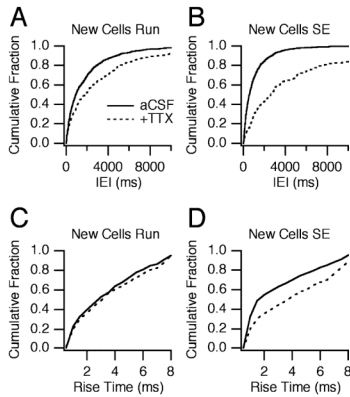
79

Figure 7. New Cells Born into an Epileptic Environment Receive More Axo-Somatic, Action Potential-Dependent Inhibition

Cumulative fraction curves of IEIs (A and B) and rise times (10%–90%; C and D) of IPSCs in cells born after running (A and C) and SE (B and D), before ("aCSF") and after ("+TTX") TTX application. Exposure to TTX caused a significantly larger shift of the curve toward longer IEIs in new cells in SE animals compared to the TTX-induced shift in new cells from runners (p < 0.05, K-S test). Furthermore, TTX addition shifted the curve toward longer rise times in new cells in SE animals, but not in runners (p < 0.05, K-S test). Recordings were performed 5.1–5.5 weeks after RV-GFP injection.

due to activation of presynaptic GABA$_B$ receptors by GABA released by the first pulse (Davies et al., 1990; Otis et al., 1993; Wu and Leung, 1997) (see, however, Wilcox and Dichter, 1994). We hypothesized that the decreased PPD of IPSCs could result from reduced sensitivity or expression of presynaptic GABA$_B$ receptors at synapses on new cells in SE animals. Our finding of marked suppression of PPD of IPSCs induced by baclofen in new cells in runners, but not in SE animals, provides strong support for this hypothesis.

The amplitude of sIPSCs was higher in both new and mature cells in SE animals as compared with runners or intact animals, which could be explained by altered GABA$_A$ receptor subunit composition and increased sensitivity or upregulation of postsynaptic GABA$_A$ receptors. In support, GABA$_A$ receptors exhibit enhanced efficacy following SE (Brooks-Kayal et al., 1998; Cohen et al., 2003; Gibbs et al., 1997), and the number of postsynaptic GABA$_A$ receptors is increased at the soma and initial axon segment, resulting in larger IPSC amplitude after kindling (Nusser et al., 1998).

The efficiency of GFP labeling with the retroviral vector used here is low, and labeling of a sufficient number of cells for whole-cell patch-clamp recordings necessitates stimulation of neurogenesis, e.g., by running (Esposito et al., 2005; van Praag et al., 2002). Therefore, it was not feasible to obtain recordings from new cells in naive animals and compare those with our findings in runners and SE animals. As an internal control, we compared recordings from mature GFP− granule cells in SE animals with those from cells in intact animals. The re-

sults regarding both excitatory and inhibitory synaptic inputs were in agreement with previous reports (see, e.g., Klapstein et al., 1999; Kobayashi and Buckmaster, 2003; Scimemi et al., 2006; Simmons et al., 1997; Wuarin and Dudek, 2001). Because the emphasis of our study was on the comparison between new granule cells born under physiological versus pathological conditions, running and SE provided appropriate models. In the future, it will be important to also record from new cells in naive animals, which will require more efficient vectors similar to the one used by Zhao et al. (2006) for morphological analysis.

The maturation of new dentate granule cells in the intact adult brain occurs in distinct morphological (Zhao et al., 2006) and electrophysiological (Ambrogini et al., 2004; Esposito et al., 2005) stages. Recent evidence from adult mice (Zhao et al., 2006) shows prolonged morphological plasticity in dendritic spines of new neurons, and shows that physiological stimulation of neurogenesis through running can lead to structural modifications. These data are consistent with our findings revealing a marked influence of environmental conditions on functional properties of afferent synapses on new cells born in the adult brain. Seizure activity, which persisted long-term after the SE insult, can remodel synapses (Wong, 2005; Zha et al., 2005) and induce production of molecules which may change their functional properties (Scharfman, 2005). However, the SE insult also altered the environment encountering the new cells with respect to the number of activated microglia and the occurence of neuronal damage. These characteristics will conceivably create a milieu which promotes plastic changes. For example, activated microglia secrete cytokines and growth factors, such as TNF-α and BDNF, which can modulate excitatory (Pickering et al., 2005) and inhibitory (Henneberger et al., 2005) synaptic transmission and alter dendritic spine morphology (Schratt et al., 2006; von Bohlen und Halbach et al., 2005). Both TNF-α receptor subtypes are expressed on hippocampal progenitor cells (Iosif et al., 2006), and TNF-α mediates synaptic scaling in the hippocampus (Stellwagen and Malenka, 2006).

Do the observed characteristics of new neurons formed in the epileptic environment provide any evidence as to whether neurogenesis restores or impairs brain function after insults? The dentate gyrus acts as a gate for seizure propagation from the entorhinal cortex via the perforant path to the hippocampus, and changes in granule cell excitability contribute to epilepsy development (Behr et al., 1998; Sutula et al., 1986). New neurons which migrate to the dentate hilus after SE may be involved in recurrent seizure generation (Scharfman et al., 2002). In contrast, the present data raise the possibility that the absolute majority of SE-generated new neurons, which are located in the GCL, receive afferent excitatory and inhibitory synaptic input favoring reduced overall excitability of the dentate gyrus. A substantial proportion of the mature cells in dentate GCL 6 months after SE are formed during the first two weeks after the insult (Bonde et al., 2006). If the new neurons generated after SE establish efferent connections with the CA3 region, as has been shown for new neurons formed in intact brains (Hastings and Gould, 1999; Markakis and Gage, 1999), and continue to exhibit reduced
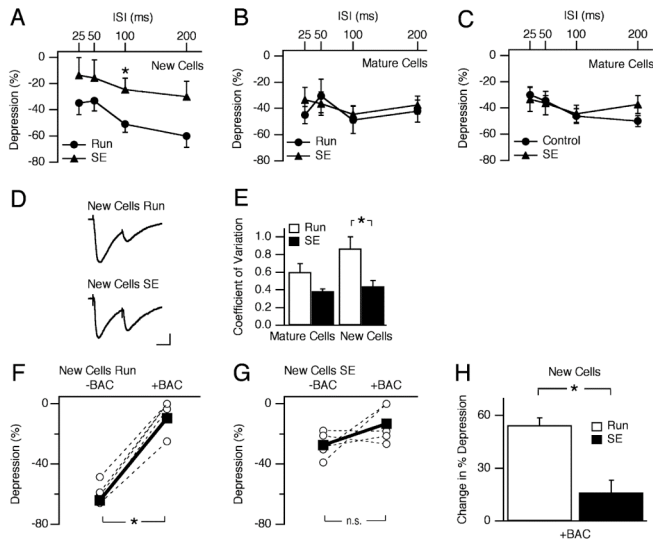
Figure 8. Paired-Pulse Depression of Inhibitory Postsynaptic Currents in New Cells Born into an Epileptic Environment Is Decreased and Insensitive to GABA$_B$ Agonist Application

Average PPD of evoked monosynaptic IPSCs at GABAergic synapses on new (A) and mature (B and C) cells in SE animals (B and C) or runners (A and B), or in untreated controls (C), expressed as percent change in the second IPSC compared with the first one. (A) Overall PPD of IPSCs (all ISIs combined) and PPD at 100 ms ISI (*) were lower in cells born after SE than those following running (p < 0.05, one-way factorial ANOVA and Student's unpaired t test, respectively; n = 5 and 6 cells, respectively). (B) In contrast, PPD of IPSCs in mature cells did not differ between SE animals and runners (p > 0.05, Student's unpaired t test). (C) PPD of IPSCs was unchanged in mature granule cells of SE animals as compared with cells in untreated rats (p > 0.05, n = 6 and 8 cells, respectively). (D) Traces of paired IPSCs in cells born after running and SE at 100 ms ISI. Scale bar = 50 ms, 50 pA. (E) CV of the amplitudes of the first IPSC of each paired stimulation-induced response in new and mature cells. The coefficient was lower in new cells born after SE compared with those born after running (*p < 0.05, Student's unpaired t test, n = 5 and 6 cells, respectively), but was similar in mature cells in SE animals and runners (p = 0.065, n = 6 and 7 cells, respectively). Recordings were performed at 5.6–6.2 weeks after RV-GFP injection. Application of GABA$_B$ receptor agonist baclofen (10 μM) caused a marked decrease in PPD (100 ms ISI) of IPSCs at synapses on new cells in runners (F) (*p < 0.05), but caused no change in SE animals (G) (not significant, p > 0.05). Percent depression of IPSCs in individual cells before (−BAC) and after (+BAC) addition of baclofen is represented by the connected points in the graph; mean values are shown in bold (Student's paired t test, n = 5 cells in both groups). (H) The change in PPD of IPSCs due to baclofen application (the absolute change in percent depression was measured for each cell) was larger in runners compared with SE animals (*p < 0.05, Student's unpaired t test). Plots represent mean ± SEM (A–C, E, and H).

excitatory and increased inhibitory synaptic input, they could have significant beneficial effects on the epileptic syndrome by increasing the threshold for seizure propagation through limbic circuitry. Suppression of neurogenesis, which has been reported in a severe form of limbic epilepsy (Hattiangady et al., 2004), may aggravate the condition.

Our study demonstrates that both a physiological stimulus and an insult to the adult brain trigger the formation of new dentate granule cells, which are functionally integrated into hippocampal neural circuitry. The new neurons exhibit a high degree of plasticity in their afferent synaptic inputs. Following insult, the functional connectivity of new neurons seems to develop in order to mitigate the dysfunction in the epileptic brain. These data provide further evidence for a therapeutic potential of endogenous neurogenesis.

Experimental Procedures

Animal Groups, Status Epilepticus, and Running

Two hundred and twenty male Sprague-Dawley rats were subjected to SE (n = 113) or voluntary wheel running (n = 95), or served as untreated controls (n = 12). Experimental procedures were approved by the Malmö-Lund Ethical Committee. Animals subjected to SE were anesthetized with halothane (1%–2%) or ketamine/xylazine (90/16.9 mg/kg) and implanted unilaterally with a bipolar stainless steel stimulating/recording electrode (Plastics One, Roanoke, VA) in ventral hippocampal CA1-CA3 region (coordinates: 4.8 mm caudal and 5.2 mm lateral to bregma, 6.3 mm ventral from dura, toothbar at −3.3 mm) (Paxinos and Watson, 1997). Seven days later, two-hour SE was induced by electrical stimulation as described previously (Lothman et al., 1989; Mohapel et al., 2004). Animals subjected to voluntary running were placed in cages with one running wheel (ScanBur, BK, Denmark) during 9–10 days (Naylor et al., 2005). Separate animals were used for electrophysiology and morphological analysis or EEG monitoring (during 3 min every week for 5 weeks).

Labeling of New Neurons

At 1 week after SE or running, rats were anesthetized and injected unilaterally at two dorsal hippocampal sites (coordinates: 3.6 mm caudal and 2.0 mm lateral to bregma, 2.8 ventral to dura; 4.4 mm caudal and 3.0 mm lateral to bregma, 3.0 mm ventral to dura, tooth-bar at −3.3 mm) with 1.5 μl of retroviral pLNIT/GFP vector (van Praag et al., 2002).

Slice Preparation

At 4.5 to 6.2 weeks after virus injection, animals were anesthetized and decapitated. Brains were placed in ice-cold artificial cerebrospinal fluid (aCSF; pH 7.2–7.4, 295–300 mOsm), containing sucrose (225 mM), KCl (2.5 mM), CaCl$_2$ (0.5 mM), MgCl$_2$ (7.0 mM), NaHCO$_3$ (28 mM), NaH$_2$PO$_4$ (1.25 mM), glucose (7.0 mM), ascorbate (1.0 mM), and pyruvate (3.0 mM). Transverse hippocampal slices (225 μm), cut on a Vibratome (3000 Deluxe, Ted Pella, Inc, CA), were placed in an incubation chamber with gassed (95% O$_2$/5% CO$_2$) aCSF containing NaCl (119 mM), KCl (2.5 mM), MgSO$_4$ (1.3 mM), CaCl$_2$ (2.5 mM), NaHCO$_3$ (26.2 mM), NaH$_2$PO$_4$ (1 mM), and glucose (11 mM), and were allowed to rest for at least 1 hr.

Electrophysiological Recordings

Individual slices were placed in a submerged recording chamber and constantly perfused with gassed aCSF at +32°C–34°C during recordings of spontaneous and miniature postsynaptic currents (to optimize event frequency for analysis) and APs, or with gassed aCSF at room temperature during paired-pulse stimulation experiments. GFP+ cells were visualized with fluorescence microscopy, and infrared light in combination with differential interference contrast microscopy was used for visual approach and whole-cell patch-clamp recordings. Recording pipettes (3–7 MΩ resistance, 295–300 mOsm, pH 7.2–7.4) contained K-gluconate (122.5 mM), KCl (12.5 mM), KOH-HEPES (10.0 mM), KOH-EGTA (0.2 mM), MgATP (2.0 mM), Na$_3$GTP (0.3 mM), and NaCl (8.0 mM) (current-clamp recordings of intrinsic properties, and voltage-clamp recordings of sEPSCs and miniature excitatory postsynaptic currents [mEPSCs]); Cs-gluconate (117.5 mM), CsCl (17.5 mM), NaCl (8.0 mM), CsOH-HEPES (10.0 mM), CsOH-EGTA (0.2 mM), MgATP (2.0 mM), Na$_3$GTP (0.3 mM), and QX-314 (5.0 mM) (voltage-clamp recordings of stimulation-evoked EPSCs); or CsCl (135.0 mM), CsOH (10.0 mM), CsOH-EGTA (0.2 mM), Mg-ATP (2.0 mM), Na$_3$-GTP (0.3 mM), NaCl (8.0 mM), and QX-314 (5.0 mM) (voltage-clamp recordings of spontaneous, miniature, and paired stimulation-evoked inhibitory postsynaptic currents [sIPSCs, mIPSCs, and IPSCs, respectively]). EPSCs were recorded with 100 μM PTX (Tocris) in aCSF to block GABA$_A$ receptor activation. Evoked EPSCs were standardized to a current between 70 and 120 pA, which was estimated to be a submaximal response amplitude. For recordings of IPSCs, 50 μM D-AP5 and 5 μM NBQX (Tocris) were added to the aCSF to block NMDA and non-NMDA receptors, respectively. One micromolar TTX was used to block APs. One hundred micromolar PTX was used to block IPSCs at the end of experiments. Biocytin was dissolved in the pipette solutions (0.5%) for identification of recorded cells. Electrical stimulations were performed with bipolar, stainless steel electrodes placed in LPP for EPSCs, dentate molecular layer for PPD of IPSCs, and GCL for perforated-patch recordings. The LPP was identified as described (Kokaia et al., 1998; Min et al., 1998). The stimulating electrode was placed in the outer third of the molecular layer while recording field EPSPs (fEPSPs) in response to paired stimulations of 50 ms ISI, which elicited PPF of fEPSPs, a characteristic feature of LPP (Colino and Malenka, 1993; McNaughton, 1980). Moving recording pipette to the middle third of the molecular layer elicited PPF, but with reversed polarity of fEPSPs (Hanse and Gustafsson, 1992; McNaughton, 1980).

For MK-801 experiments, five to ten stimulations were delivered to LPP to evoke non-NMDA receptor-mediated EPSCs of approximately 100 pA amplitude at a holding potential of −70 mV. Thereafter, non-NMDA receptor-mediated EPSCs were blocked by 10 μM NBQX. Ten NMDA receptor-mediated EPSCs were then recorded at a holding potential of +40 mV before stimulation was interrupted for 8–10 min to wash in 80 μM MK-801 (Sigma) at a holding potential of −70 mV. Stimulations were then resumed and EPSCs were recorded at +40 mV until response was completely blocked.

For GABA$_B$ experiments, 20 paired stimulations were delivered to molecular layer at 100 ms ISI and IPSCs were recorded at a holding potential of −70 mV. Eight minutes wash-in of ten micromolar baclofen (Tocris) was followed by twenty paired stimulations. IPSCs were blocked with PTX.

For perforated-patch recordings, the pipette solution consisted of K-gluconate (154 mM), NaCl (9 mM), MgCl$_2$ (1 mM), HEPES (10 mM), and EGTA (0.2 mM), with gramicidin A (Sigma) freshly dissolved in DMSO and diluted to 35 μg/ml. Series resistance of 50–80 MΩ was accepted for perforated-patch whole-cell configuration. Stimulations were delivered to GCL and IPSC reversal potential was assessed by varying holding potentials between −100 and 0 mV.

Data were filtered at 2.9 kHz and sampled at 10 kHz with patch-clamp amplifier EPC9 (HEKA Electronik, Lambrecht, Germany) and stored on a G4 Macintosh computer.

Analysis of Electrophysiological Data

Off-line analysis was carried out using IgorPro (version 5.02, Wave-Metrics, Lake Oswego, OR), MiniAnalysis software (Synaptosoft Inc., Decatur, GA), and FitMaster (version 2.05, HEKA Electronik, Lambrecht, Germany). Recordings during which the whole-cell access resistance varied more than 20% were excluded from analysis. Input resistance was determined by the voltage response of the cell to a constant 0.5 s current injection of 15 or 30 pA amplitude. Action potential threshold was defined as the point where the fastest rising phase of the AP started. Amplitude of the AP was defined as the difference between threshold and peak, and half-duration (half-width) was defined as the width of the AP measured at half-maximal amplitude. The CV was measured for amplitudes of first stimulation-evoked EPSCs or IPSCs in all paired-pulse responses in each cell. Stimulation-induced NMDA receptor-mediated decay rate was estimated by a single exponential curve fit to all EPSCs recorded in each cell in presence of MK-801. For GABA$_B$ experiments, percent depression after drug addition was subtracted from initial percent depression. For IPSC reversal potential experiments, current-voltage relationship was plotted and reversal potential was the value at which the potential curve crossed zero current.

Group differences in resting membrane potential, input resistance, AP threshold, AP half-width, AP amplitude, paired-pulse responses, and CV were assessed with Student's unpaired t test or one-way factorial ANOVA using StatView software (version 5.0.1, Abacus Concepts, Berkeley, CA). Frequency, amplitude, 10%–90% rise times, and decay times of spontaneous and miniature postsynaptic currents were analyzed using MiniAnalysis software and compared between the groups with Student's unpaired t test (n = number of cells) and with cumulative probability curves combined with K-S test (n = number of events). Events were automatically accepted for analysis in MiniAnalysis program if their magnitude was at least 4.5 times higher than the average root-mean-square noise level measured by the software. Values are means ± SEM. Significant difference is set at p < 0.05.

Microscopical Analysis and Cell Counting

Sections from electrophysiology experiments were fixed for 2–24 hr in 4% paraformaldehyde immediately after recording and stored in antifreeze medium at −20°C. For double-staining of biocytin and GFP, free-floating sections were preincubated for 1 hr in 5% serum in 0.25% Triton X-100 KPBS (T-KPBS) (blocking solution) and exposed to rabbit-anti-GFP primary antibody (1:10,000, Abcam) overnight at room temperature. FITC-donkey-anti-rabbit secondary antibody and Cy3-streptavidin (1:200, Jackson Immunoresearch) were added for 2 hr in the dark at room temperature. Sections were mounted on glass slides and cover-slipped. The number of apical and basal dendrites arising from soma, and proximal apical dendritic branches within one cell diameter from soma, were quantified in biocytin-labeled cells. Colocalization of GFP and biocytin was validated with confocal microscopy. GFP+ cells were counted in every seventh section throughout the hippocampal formation. Data are presented as the sum of all counted cells per animal.

To characterize the tissue environments, rats received an overdose of pentobarbital (250 mg/kg i.p.) and were transcardially perfused with 100 ml ice-cold saline and 250 ml ice-cold paraformaldehyde (4% in 0.1 M PBS, pH = 7.4) at 1 or 5 weeks following running and SE. Brains were postfixed for 24 hr and then dehydrated for

24 hr in 20% sucrose/0.1 M phosphate buffer. The brains were cut in 30 μm sections. Three sections from each anterior hippocampus (located at −3.3 mm to −4.1 mm, according to Paxinos and Watson, 1997) were processed. For Iba1/ED1 and S100β/GFAP double-staining, sections were preincubated for 1 hr in blocking solution and incubated at +4°C overnight in either rabbit-anti-GFAP (1:1000, DAKO, Glostrup, Denmark) and mouse-anti-S100β (1:10,000, Sigma, Saint Louis, MO) or mouse-anti-ED1 (1:200, Serotec Ltd., Oxford, UK) and rabbit-anti-Iba1 (1:1000, Wako Chemicals, Neuss, Germany). Sections were incubated for 2 hr in Cy3-conjugated donkey-anti-rabbit and biotinylated horse-anti-mouse secondary antibodies (1:200, Jackson ImmunoResearch, West Grove, PA), then incubated for 2 hr in streptavidin-conjugated Alexa Fluor 488 (1:200, Molecular Probes, The Netherlands), mounted, and cover-slipped. Sections were rinsed in KPBS or T-KPBS between incubations. For Fluoro-Jade (Histochem Inc., Jefferson, AR) staining, sections were mounted with KPBS and allowed to dry overnight. Following 15 min pretreatment with 0.06% potassium permanganate, sections were agitated for 30 min in 0.001% Fluoro-Jade in 0.1% acetic acid. Sections were rinsed, dehydrated in ethanol, and immersed in xylene before cover-slipping.

Cell counts and qualitative analysis of Fluoro-Jade staining were performed using epifluorescence/light microscopy. Cells were counted within the GCL and two cell diameters below in the SGZ. Iba1/ED1 and S100β/GFAP double-labeling was validated with confocal microscopy. An observer blind to treatment conditions performed all analyses. Comparisons were made using one-way ANOVA with subsequent Bonferroni-Dunn post-hoc test. Results are means ± SEM. Differences are considered significant at p < 0.05. Statistical analyses were conducted using StatView software.

Supplemental Data

The Supplemental Data for this article can be found online at http://www.neuron.org/cgi/content/full/52/6/1047/DC1/.

References

Abrous, D.N., Koehl, M., and Le Moal, M. (2005). Adult neurogenesis: from precursors to network and physiology. Physiol. Rev. 85, 523–569.

Ambrogini, P., Lattanzi, D., Ciuffoli, S., Agostini, D., Bertini, L., Stocchi, V., Santi, S., and Cuppini, R. (2004). Morpho-functional characterization of neuronal cells at different stages of maturation in granule cell layer of adult rat dentate gyrus. Brain Res. 1017, 21–31.

Arvidsson, A., Collin, T., Kirik, D., Kokaia, Z., and Lindvall, O. (2002). Neuronal replacement from endogenous precursors in the adult brain after stroke. Nat. Med. 8, 963–970.

Battista, D., Ferrari, C.C., Gage, F.H., and Pitossi, F.J. (2006). Neurogenic niche modulation by activated microglia: transforming growth factor beta increases neurogenesis in the adult dentate gyrus. Eur. J. Neurosci. 23, 83–93.

Behr, J., Lyson, K.J., and Mody, I. (1998). Enhanced propagation of epileptiform activity through the kindled dentate gyrus. J. Neurophysiol. 79, 1726–1732.

Belluzzi, O., Benedusi, M., Ackman, J., and LoTurco, J.J. (2003). Electrophysiological differentiation of new neurons in the olfactory bulb. J. Neurosci. 23, 10411–10418.

Berninger, B., Schinder, A.F., and Poo, M.M. (1999). Synaptic reliability correlates with reduced susceptibility to synaptic potentiation by brain-derived neurotrophic factor. Learn. Mem. 6, 232–242.

Bonde, S., Ekdahl, C.T., and Lindvall, O. (2006). Long-term neuronal replacement in adult rat hippocampus after status epilepticus despite chronic inflammation. Eur. J. Neurosci. 23, 965–974.

Brooks-Kayal, A.R., Shumate, M.D., Jin, H., Rikhter, T.Y., and Coulter, D.A. (1998). Selective changes in single cell GABA(A) receptor subunit expression and function in temporal lobe epilepsy. Nat. Med. 4, 1166–1172.

Buhl, E.H., Otis, T.S., and Mody, I. (1996). Zinc-induced collapse of augmented inhibition by GABA in a temporal lobe epilepsy model. Science 271, 369–373.

Carleton, A., Petreanu, L.T., Lansford, R., Alvarez-Buylla, A., and Lledo, P.M. (2003). Becoming a new neuron in the adult olfactory bulb. Nat. Neurosci. 6, 507–518.

Cohen, A.S., Lin, D.D., Quirk, G.L., and Coulter, D.A. (2003). Dentate granule cell GABA(A) receptors in epileptic hippocampus: enhanced synaptic efficacy and altered pharmacology. Eur. J. Neurosci. 17, 1607–1616.

Colino, A., and Malenka, R.C. (1993). Mechanisms underlying induction of long-term potentiation in rat medial and lateral perforant paths in vitro. J. Neurophysiol. 69, 1150–1159.

Crespel, A., Rigau, V., Coubes, P., Rousset, M.C., de Bock, F., Okano, H., Baldy-Moulinier, M., Bockaert, J., and Lerner-Natoli, M. (2005). Increased number of neural progenitors in human temporal lobe epilepsy. Neurobiol. Dis. 19, 436–450.

Davies, C.H., Davies, S.N., and Collingridge, G.L. (1990). Paired-pulse depression of monosynaptic GABA-mediated inhibitory postsynaptic responses in rat hippocampus. J. Physiol. 424, 513–531.

Debanne, D., Guerineau, N.C., Gahwiler, B.H., and Thompson, S.M. (1996). Paired-pulse facilitation and depression at unitary synapses in rat hippocampus: quantal fluctuation affects subsequent release. J. Physiol. 491, 163–176.

Ekdahl, C.T., Claasen, J.H., Bonde, S., Kokaia, Z., and Lindvall, O. (2003). Inflammation is detrimental for neurogenesis in adult brain. Proc. Natl. Acad. Sci. USA 100, 13632–13637.

Esposito, M.S., Piatti, V.C., Laplagne, D.A., Morgenstern, N.A., Ferrari, C.C., Pitossi, F.J., and Schinder, A.F. (2005). Neuronal differentiation in the adult hippocampus recapitulates embryonic development. J. Neurosci. 25, 10074–10086.

Ge, S., Goh, E.L., Sailor, K.A., Kitabatake, Y., Ming, G.L., and Song, H. (2006). GABA regulates synaptic integration of newly generated neurons in the adult brain. Nature 439, 589–593.

Gibbs, J.W., 3rd, Shumate, M.D., and Coulter, D.A. (1997). Differential epilepsy-associated alterations in postsynaptic GABA(A) receptor function in dentate granule and CA1 neurons. J. Neurophysiol. 77, 1924–1938.

Gloveli, T., Behr, J., Dugladze, T., Kokaia, Z., Kokaia, M., and Heinemann, U. (2003). Kindling alters entorhinal cortex-hippocampal interaction by increased efficacy of presynaptic GABA(B) autoreceptors in layer III of the entorhinal cortex. Neurobiol. Dis. 13, 203–212.

Hanse, E., and Gustafsson, B. (1992). Long-term potentiation and field EPSPs in the lateral and medial perforant paths in the dentate gyrus in vitro: a comparison. Eur. J. Neurosci. 4, 1191–1201.

Hastings, N.B., and Gould, E. (1999). Rapid extension of axons into the CA3 region by adult-generated granule cells. J. Comp. Neurol. 413, 146–154.

Hattiangady, B., Rao, M.S., and Shetty, A.K. (2004). Chronic temporal lobe epilepsy is associated with severely declined dentate neurogenesis in the adult hippocampus. Neurobiol. Dis. 17, 473–490.

Henneberger, C., Kirischuk, S., and Grantyn, R. (2005). Brain-derived neurotrophic factor modulates GABAergic synaptic transmission by enhancing presynaptic glutamic acid decarboxylase 65 levels, promoting asynchronous release and reducing the number of activated postsynaptic receptors. Neuroscience 135, 749–763.

Hessler, N.A., Shirke, A.M., and Malinow, R. (1993). The probability of transmitter release at a mammalian central synapse. Nature 366, 569–572.

Iosif, R.E., Ekdahl, C.T., Ahlenius, H., Pronk, C.J., Bonde, S., Kokaia, Z., Jacobsen, S.E., and Lindvall, O. (2006). Tumor necrosis factor receptor 1 is a negative regulator of progenitor proliferation in adult hippocampal neurogenesis. J. Neurosci. 26, 9703–9712.

Ivanova, S.Y., Lushnikova, I.V., Pivneva, T.A., Belan, P.V., Storozhuk, M.V., and Kostyuk, P.G. (2004). Differential properties of GABAergic synaptic connections in rat hippocampal cell cultures. Synapse 53, 122–130.

Klapstein, G.J., Meldrum, B.S., and Mody, I. (1999). Decreased sensitivity to Group III mGluR agonists in the lateral perforant path following kindling. Neuropharmacology 38, 927–933.

Kobayashi, M., and Buckmaster, P.S. (2003). Reduced inhibition of dentate granule cells in a model of temporal lobe epilepsy. J. Neurosci. 23, 2440–2452.

Kokaia, M., Asztely, F., Olofsdotter, K., Sindreu, C.B., Kullmann, D.M., and Lindvall, O. (1998). Endogenous neurotrophin-3 regulates short-term plasticity at lateral perforant path-granule cell synapses. J. Neurosci. 18, 8730–8739.

Leinekugel, X., Khalilov, I., McLean, H., Caillard, O., Gaiarsa, J.L., Ben-Ari, Y., and Khazipov, R. (1999). GABA is the principal fast-acting excitatory transmitter in the neonatal brain. Adv. Neurol. 79, 189–201.

Lothman, E.W., Bertram, E.H., Bekenstein, J.W., and Perlin, J.B. (1989). Self-sustaining limbic status epilepticus induced by 'continuous' hippocampal stimulation: electrographic and behavioral characteristics. Epilepsy Res. 3, 107–119.

Markakis, E.A., and Gage, F.H. (1999). Adult-generated neurons in the dentate gyrus send axonal projections to field CA3 and are surrounded by synaptic vesicles. J. Comp. Neurol. 406, 449–460.

McNaughton, B.L. (1980). Evidence for two physiologically distinct perforant pathways to the fascia dentata. Brain Res. 199, 1–19.

Min, M.Y., Asztely, F., Kokaia, M., and Kullmann, D.M. (1998). Long-term potentiation and dual-component quantal signaling in the dentate gyrus. Proc. Natl. Acad. Sci. USA 95, 4702–4707.

Mohapel, P., Ekdahl, C.T., and Lindvall, O. (2004). Status epilepticus severity influences the long-term outcome of neurogenesis in the adult dentate gyrus. Neurobiol. Dis. 15, 196–205.

Monje, M.L., Toda, H., and Palmer, T.D. (2003). Inflammatory blockade restores adult hippocampal neurogenesis. Science 302, 1760–1765.

Murthy, V.N., Sejnowski, T.J., and Stevens, C.F. (1997). Heterogeneous release properties of visualized individual hippocampal synapses. Neuron 18, 599–612.

Naylor, A.S., Persson, A.I., Eriksson, P.S., Jonsdottir, I.H., and Thorlin, T. (2005). Extended voluntary running inhibits exercise-induced adult hippocampal progenitor proliferation in the spontaneously hypertensive rat. J. Neurophysiol. 93, 2406–2414.

Nusser, Z., Hajos, N., Somogyi, P., and Mody, I. (1998). Increased number of synaptic GABA(A) receptors underlies potentiation at hippocampal inhibitory synapses. Nature 395, 172–177.

Otis, T.S., De Koninck, Y., and Mody, I. (1993). Characterization of synaptically elicited GABAB responses using patch-clamp recordings in rat hippocampal slices. J. Physiol. 463, 391–407.

Overstreet, L.S., Hentges, S.T., Bumaschny, V.F., de Souza, F.S., Smart, J.L., Santangelo, A.M., Low, M.J., Westbrook, G.L., and Rubinstein, M. (2004). A transgenic marker for newly born granule cells in dentate gyrus. J. Neurosci. 24, 3251–3259.

Overstreet-Wadiche, L.S., Bromberg, D.A., Bensen, A.L., and Westbrook, G.L. (2006). Seizures accelerate functional integration of adult-generated granule cells. J. Neurosci. 26, 4095–4103.

Parent, J.M., Yu, T.W., Leibowitz, R.T., Geschwind, D.H., Sloviter, R.S., and Lowenstein, D.H. (1997). Dentate granule cell neurogenesis is increased by seizures and contributes to aberrant network reorganization in the adult rat hippocampus. J. Neurosci. 17, 3727–3738.

Parent, J.M., Vexler, Z.S., Gong, C., Derugin, N., and Ferriero, D.M. (2002). Rat forebrain neurogenesis and striatal neuron replacement after focal stroke. Ann. Neurol. 52, 802–813.

Parent, J.M., Elliott, R.C., Pleasure, S.J., Barbaro, N.M., and Lowenstein, D.H. (2005). Aberrant seizure-induced neurogenesis in experimental temporal lobe epilepsy. Ann. Neurol. 59, 81–91.

Paxinos, G., and Watson, C. (1997). The Rat Brain in Stereotaxic Coordinates (San Diego, CA: Academic).

Pickering, M., Cumiskey, D., and O'Connor, J.J. (2005). Actions of TNF-alpha on glutamatergic synaptic transmission in the central nervous system. Exp. Physiol. 90, 663–670.

Rivera, C., Voipio, J., Payne, J.A., Ruusuvuori, E., Lahtinen, H., Lamsa, K., Pirvola, U., Saarma, M., and Kaila, K. (1999). The K+/Cl-co-transporter KCC2 renders GABA hyperpolarizing during neuronal maturation. Nature 397, 251–255.

Rosenmund, C., Clements, J.D., and Westbrook, G.L. (1993). Nonuniform probability of glutamate release at a hippocampal synapse. Science 262, 754–757.

Scharfman, H. (2005). Seizure-Induced Neurogenesis in the Dentate Gyrus and its Dependence on Growth Factors and Cytokines. In Growth Factors and Epilepsy, D.K. Binder and H.E. Scharfman, eds. (New York: Nova Science Publishers, Inc.), pp. 1–40.

Scharfman, H.E. (1992). Differentiation of rat dentate neurons by morphology and electrophysiology in hippocampal slices: granule cells, spiny hilar cells and aspiny 'fast-spiking' cells. Epilepsy Res. Suppl. 7, 93–109.

Scharfman, H.E., Goodman, J.H., and Sollas, A.L. (2000). Granule-like neurons at the hilar/CA3 border after status epilepticus and their synchrony with area CA3 pyramidal cells: functional implications of seizure-induced neurogenesis. J. Neurosci. 20, 6144–6158.

Scharfman, H.E., Sollas, A.L., and Goodman, J.H. (2002). Spontaneous recurrent seizures after pilocarpine-induced status epilepticus activate calbindin-immunoreactive hilar cells of the rat dentate gyrus. Neuroscience 111, 71–81.

Schmidt-Hieber, C., Jonas, P., and Bischofberger, J. (2004). Enhanced synaptic plasticity in newly generated granule cells of the adult hippocampus. Nature 429, 184–187.

Schmued, L.C., Albertson, C., and Slikker, W., Jr. (1997). Fluoro-Jade: a novel fluorochrome for the sensitive and reliable histochemical localization of neuronal degeneration. Brain Res. 751, 37–46.

Schratt, G.M., Tuebing, F., Nigh, E.A., Kane, C.G., Sabatini, M.E., Kiebler, M., and Greenberg, M.E. (2006). A brain-specific microRNA regulates dendritic spine development. Nature 439, 283–289.

Scimemi, A., Schorge, S., Kullmann, D.M., and Walker, M.C. (2006). Epileptogenesis is associated with enhanced glutamatergic transmission in the perforant path. J. Neurophysiol. 95, 1213–1220.

Shao, L.R., and Dudek, F.E. (2005). Changes in mIPSCs and sIPSCs after kainate treatment: evidence for loss of inhibitory input to dentate granule cells and possible compensatory responses. J. Neurophysiol. 94, 952–960.

Simmons, M.L., Terman, G.W., and Chavkin, C. (1997). Spontaneous excitatory currents and kappa-opioid receptor inhibition in dentate gyrus are increased in the rat pilocarpine model of temporal lobe epilepsy. J. Neurophysiol. 78, 1860–1868.

Stellwagen, D., and Malenka, R.C. (2006). Synaptic scaling mediated by glial TNF-alpha. Nature 440, 1054–1059.

Sutula, T., Harrison, C., and Steward, O. (1986). Chronic epileptogenesis induced by kindling of the entorhinal cortex: the role of the dentate gyrus. Brain Res. 385, 291–299.

van Praag, H., Schinder, A.F., Christie, B.R., Toni, N., Palmer, T.D., and Gage, F.H. (2002). Functional neurogenesis in the adult hippocampus. Nature 415, 1030–1034.

von Bohlen und Halbach, O., Krause, S., Medina, D., Sciarretta, C., Minichiello, L., and Unsicker, K. (2005). Regional- and Age-Dependent Reduction in trkB Receptor Expression in the Hippocampus Is Associated with Altered Spine Morphologies. Biol. Psychiatry, in press.

Wierenga, C.J., and Wadman, W.J. (1999). Miniature inhibitory postsynaptic currents in CA1 pyramidal neurons after kindling epileptogenesis. J. Neurophysiol. 82, 1352–1362.

Wilcox, K.S., and Dichter, M.A. (1994). Paired pulse depression in cultured hippocampal neurons is due to a presynaptic mechanism

independent of GABAB autoreceptor activation. J. Neurosci. *14*, 1775–1788.

Wong, M. (2005). Modulation of dendritic spines in epilepsy: cellular mechanisms and functional implications. Epilepsy Behav. *7*, 569–577.

Wu, C., and Leung, L.S. (1997). Partial hippocampal kindling decreases efficacy of presynaptic GABAB autoreceptors in CA1. J. Neurosci. *17*, 9261–9269.

Wuarin, J.P., and Dudek, F.E. (2001). Excitatory synaptic input to granule cells increases with time after kainate treatment. J. Neurophysiol. *85*, 1067–1077.

Zha, X.M., Green, S.H., and Dailey, M.E. (2005). Regulation of hippocampal synapse remodeling by epileptiform activity. Mol. Cell. Neurosci. *29*, 494–506.

Zhao, C., Teng, E.M., Summers, R.G., Jr., Ming, G.L., and Gage, F.H. (2006). Distinct morphological stages of dentate granule neuron maturation in the adult mouse hippocampus. J. Neurosci. *26*, 3–11.

Zucker, R.S., and Stockbridge, N. (1983). Presynaptic calcium diffusion and the time courses of transmitter release and synaptic facilitation at the squid giant synapse. J. Neurosci. *3*, 1263–1269.

D

Development/Plasticity/Repair

Inflammation Regulates Functional Integration of Neurons Born in Adult Brain

Katherine Jakubs,[1,4]* **Sara Bonde,**[1,4]* **Robert E. Iosif,**[1,4] **Christine T. Ekdahl,**[1,4,5] **Zaal Kokaia,**[3,4] **Merab Kokaia,**[2,4] **and Olle Lindvall**[1,4]

[1]Laboratory of Neurogenesis and Cell Therapy and [2]Experimental Epilepsy Group, Section of Restorative Neurology, Wallenberg Neuroscience Center, University Hospital, [3]Laboratory of Neural Stem Cell Biology, Section of Restorative Neurology, University Hospital, and [4]Lund Strategic Research Center for Stem Cell Biology and Cell Therapy, SE-221 84 Lund, Sweden, and [5]Division of Clinical Neurophysiology, University Hospital, SE-221 85 Lund, Sweden

Inflammation influences several steps of adult neurogenesis, but whether it regulates the functional integration of the new neurons is unknown. Here, we explored, using confocal microscopy and whole-cell patch-clamp recordings, whether a chronic inflammatory environment affects the morphological and electrophysiological properties of new dentate gyrus granule cells, labeled with a retroviral vector encoding green fluorescent protein. Rats were exposed to intrahippocampal injection of lipopolysaccharide, which gave rise to long-lasting microglia activation. Inflammation caused no changes in intrinsic membrane properties, location, dendritic arborization, or spine density and morphology of the new cells. Excitatory synaptic drive increased to the same extent in new and mature cells in the inflammatory environment, suggesting increased network activity in hippocampal neural circuitries of lipopolysaccharide-treated animals. In contrast, inhibitory synaptic drive was more enhanced by inflammation in the new cells. Also, larger clusters of the postsynaptic GABA$_A$ receptor scaffolding protein gephyrin were found on dendrites of new cells born in the inflammatory environment. We demonstrate for the first time that inflammation influences the functional integration of adult-born hippocampal neurons. Our data indicate a high degree of synaptic plasticity of the new neurons in the inflammatory environment, which enables them to respond to the increase in excitatory input with a compensatory upregulation of activity and efficacy at their afferent inhibitory synapses.

Key words: adult neurogenesis; inflammation; synaptic plasticity; gephyrin; electrophysiology; hippocampus

Introduction

In the adult brain, neural stem cells in the subgranular zone (SGZ) and the subventricular zone (SVZ) form new dentate granule cells and olfactory bulb interneurons, respectively. Available evidence points to a role for hippocampal neurogenesis in mood regulation, learning, and memory, and for olfactory bulb neurogenesis in olfactory discrimination and memory (Zhao et al., 2008). Neurogenesis is influenced by pathological conditions [e.g., status epilepticus (SE) and stroke], which stimulate the formation of new neurons in SVZ and SGZ (Bengzon et al., 1997; Parent et al., 1997, 2002; Arvidsson et al., 2001, 2002).

Brain inflammation is involved in the pathogenesis of neurological disorders such as stroke (Danton and Dietrich, 2003) and epilepsy (Gorter et al., 2006) and can be both detrimental and beneficial for neurogenesis. Autoimmune T-cells promote SGZ and SVZ progenitor proliferation by interacting with microglia (Ziv et al., 2006). Tumor necrosis factor-α, released by activated microglia, suppresses SGZ and SVZ progenitor proliferation through tumor necrosis factor receptor 1 after SE and stroke (Iosif et al., 2006, 2008). Microglia activated early after stroke or SE, or by administration of the bacterial endotoxin lipopolysaccharide (LPS), compromises survival and differentiation of newly formed hippocampal and striatal neurons (Ekdahl et al., 2003; Monje et al., 2003; Hoehn et al., 2005). However, the newly formed granule cells, which do not die during the first month after SE, survive for 5 months thereafter despite chronic inflammation (Bonde et al., 2006).

Whether brain inflammation alters the functional integration of new neurons into existing neural circuitries is unknown. In the intact brain, the maturation of new granule cells follows distinct morphological stages (Zhao et al., 2006), and they develop synaptic inputs closely resembling those of mature granule cells (van Praag et al., 2002). The functional synaptic connectivity of adult-born granule cells is remarkably similar to that of cells generated during development (Laplagne et al., 2006, 2007). Recent experimental evidence suggests that developing in an inflammatory environment may influence the synaptic connectivity of the new neurons. Activated microglia secrete cytokines and growth factors, which can modulate synaptic transmission (Henneberger et

89

al., 2005; Pickering et al., 2005) and alter dendritic spine morphology (Schratt et al., 2006; von Bohlen und Halbach et al., 2006). Moreover, after SE, new hippocampal neurons exhibit increased inhibitory and decreased excitatory drive at their afferent synapses (Jakubs et al., 2006), which may mitigate abnormal excitability. The epileptic insult causes seizures, neuronal death, and inflammation, and each of these pathologies could underlie the altered synaptic properties (Jakubs et al., 2006).

Here, we created a chronic inflammatory environment by LPS injection into rat hippocampal formation and labeled new granule cells through injection of a retroviral (RV) vector encoding green fluorescent protein (GFP) 1 week thereafter. After 6–8 weeks, we performed detailed microscopical analysis of the new neurons and whole-cell patch-clamp recordings to assess their intrinsic membrane properties and excitatory and inhibitory synaptic inputs. We demonstrate for the first time that inflammation regulates the functional synaptic connectivity of new neurons generated in the adult brain.

Materials and Methods

Animal groups and lipopolysaccharide administration. One hundred fourteen male Sprague Dawley rats were used, weighing 200–250 g at the beginning of experiments. Experimental procedures were approved by the Malmö-Lund Ethical Committee. Animals were anesthetized with isoflurane (2%) or ketamine/xylazine (90/16.9 mg/kg), and LPS from *Salmonella enterica*, serotype *abortus equi* [Sigma-Aldrich; 15 μg in 1.5 μl of artificial CSF (aCSF)] or vehicle (1.5 μl of aCSF) was stereotaxically injected into the left dorsal dentate gyrus (DG) (coordinates: 4.0 mm caudal and 2.5 mm lateral to bregma, 2.9 mm ventral from dura, toothbar at −3.3 mm) (Paxinos and Watson, 1997) using a glass microcapillary. Fifty-three rats were used for electrophysiological recordings (LPS, n = 28; vehicle, n = 25), and 61 animals for morphological analysis (LPS, n = 31; vehicle, n = 30). To explore whether the LPS-induced inflammation had caused epileptic activity, a recording electrode was implanted into the right ventral hippocampus (coordinates: 4.8 mm caudal and 5.2 mm lateral to bregma, 6.3 mm ventral from dura, toothbar at −3.3 mm) in five rats before LPS (n = 3) or vehicle (n = 2) injection for subsequent electroencephalogram (EEG) recording. EEG activity was monitored for 5 min at 1 and 8 weeks after LPS injection.

Labeling of new neurons. One week after vehicle or LPS injection, rats were anesthetized with isoflurane or ketamine/xylazine and injected with 1.5 μl of retrovirus, containing the GFP gene under the CAG promoter (1.2–1.3 × 10^8 transducing U/ml) [for details, see Zhao et al. (2006)], ipsilaterally at two dorsal hippocampal sites (coordinates: 3.6 mm caudal and 2.0 mm lateral to bregma, and 2.8 ventral to dura; 4.4 mm caudal and 3.0 mm lateral to bregma, and 3.0 mm ventral to dura; toothbar at −3.3 mm).

Electrophysiological analysis and tissue preparation. Seven to 9 weeks after LPS or vehicle injection, animals were deeply anesthetized with isoflurane and decapitated. Brains were immediately removed, and ipsilateral hippocampi were dissected and placed in ice-cold modified aCSF containing the following (in mM): 225 sucrose, 2.5 KCl, 0.5 CaCl$_2$, 7.0 MgCl$_2$, 28 NaHCO$_3$, 1.25 NaH$_2$PO$_4$, 7.0 glucose, 1.0 ascorbate, and 3.0 pyruvate, pH 7.2–7.4, 295–300 mOsm. Transverse 225-μm-thick hippocampal slices were cut using a vibratome, transferred to gassed aCSF (95% O$_2$, 5% CO$_2$) containing the following (in mM): 119 NaCl, 2.5 KCl, 1.3 MgSO$_4$, 2.5 CaCl$_2$, 26.2 NaHCO$_3$, 1 NaH$_2$PO$_4$, and 11 glucose, and then allowed to rest for at least 1 h.

Whole-cell patch-clamp recordings were performed at room temperature (RT) in all cases except for spontaneous EPSCs (sEPSCs), which were recorded at 32–34°C. Individual slices were placed in a submerged recording chamber constantly perfused with gassed aCSF. Cells for recording were visualized with Olympus upright microscope and a digital camera using infrared light with differential interference contrast and UV light for identifying GFP-expressing cells in the granule cell layer (GCL). Recording pipettes with a tip resistance of 3–6 MΩ were filled with pipette solution, pH 7.2–7.4 and 295–300 mOsm, containing the

following (in mM): 135.0 CsCl, 10.0 CsOH, 0.2 CsOH-EGTA, 2.0 Mg-ATP, 0.3 Na$_3$-GTP, 8.0 NaCl, and 5.0 lidocaine *N*-ethyl bromide (QX-314) for voltage-clamp recordings of IPSCs, or 117.5 Cs-gluconate, 17.5 CsCl, 8.0 NaCl, 10.0 CsOH-HEPES, 0.2 CsOH-EGTA, 2.0 Mg-ATP, 0.3 Na$_3$GTP, and 5.0 QX-314, for voltage-clamp recordings of EPSCs. For current-clamp recordings, the pipette solution contained the following (in mM): 122.5 K-gluconate, 12.5 KCl, 10.0 KOH-HEPES, 0.2 KOH-EGTA, 2.0 MgATP, 0.3 Na$_3$GTP, and 8.0 NaCl. Biocytin (0.5%; Sigma-Aldrich) was freshly dissolved in the pipette solution before recordings. Spontaneous and miniature IPSCs (sIPSCs and mIPSCs, respectively) were recorded continuously for 3 min while holding the cell membrane potential at −80 mV and blocking NMDA and non-NMDA glutamate receptors with D-AP5 (50 μM) and 1,2,3,4-tetrahydro-6-nitro-2,3-dioxobenzo[*f*]quinoxaline-7-sulfonamide (NBQX) (10 μM), respectively, in the aCSF perfusion solution. Tetrodotoxin (TTX) (1 μM)-containing perfusion solution was applied to the slices during 8 min and mIPSCs were then recorded for a 3 min period. Spontaneous EPSCs were recorded for 3 min while blocking GABA$_A$ receptors with 100 μM picrotoxin (PTX) in the perfusion solution. Whole-cell access resistance was continuously monitored by a test pulse applied through the patch pipette, and recordings were discarded if access resistance changed >20%. For paired-pulse experiments, a bipolar stimulation electrode was placed in the middle part of the molecular layer (ML) for monosynaptic IPSC induction, or lateral perforant path (outer one-third of ML) for EPSCs induction [for more details, see Jakubs et al. (2006)], and a series of 20 paired stimulations was delivered with 25, 50, 100, or 200 ms interstimulus intervals. For inhibitory experiments, the GABA$_B$ receptor agonist baclofen (10 μM) (Wu and Leung, 1997; Gloveli et al., 2003) was added to the aCSF, and the slices were perfused with this solution for 8 min after which another series of 20 paired stimulations was applied. IPSCs were then blocked with 100 μM PTX, confirming that they were mediated by GABA$_A$ receptors. For recordings of intrinsic membrane properties, resting membrane potential was estimated in current-clamp mode immediately after breaking the membrane and establishing whole-cell configuration. For measuring current–voltage relationship, 500 ms hyperpolarizing and depolarizing current pulses were delivered in 15 pA increments through the whole-cell pipette. The GFP expression of all recorded new cells was confirmed either by visualization of GFP that had diffused into the pipette during the recording, or with *post hoc* immunocytochemical detection of GFP colocalization with biocytin. All drugs were from Tocris unless otherwise stated.

Spontaneous and miniature postsynaptic currents were detected and analyzed using MiniAnalysis software (Synaptosoft). The last 100 sIPSCs and first 50 mIPSCs or 50 sEPSCs were analyzed from each cell. Minimum amplitude for detection was set at 5 times root-mean-square noise level as determined by the software for s/mIPSCs, or 5 pA for sEPSCs. Recordings with root-mean-square level of >5 pA were discarded. All detected events were visually controlled. Group interevent intervals (IEIs) and amplitudes were compared using Kolmogorov–Smirnov's statistical test. Approximately 20 stimulation-evoked IPSCs or EPSCs were averaged for each cell (both before and after baclofen application for IPSCs), and peak amplitudes were measured to calculate paired-pulse depression (PPD) or facilitation (PPF) in percentage. Average PPD or PPF values were compared between groups using Student's unpaired *t* test or ANOVA. Current–voltage relationship was plotted as steady-state potential 100 ms after onset of the test current pulses. Input resistance was calculated from the steady-state membrane potential response to a 15 pA hyperpolarizing current injection. Membrane time constant was calculated by fitting a single exponential curve to the membrane voltage response (5–90 ms from onset) to a 15 pA hyperpolarizing current injection. Action potential threshold was determined at the beginning of the steepest rising phase of the membrane potential. Amplitude of the action potential was estimated as absolute difference between threshold and peak, and duration (half-width) was measured as the time between rising and falling phase at half-amplitude. Level of significance for the statistical tests was set at $p < 0.05$.

Sections from electrophysiology experiments were fixed for 2–24 h in 4% paraformaldehyde (PFA) immediately after recordings and stored in antifreeze medium at −20°C. For double staining of biocytin and GFP,
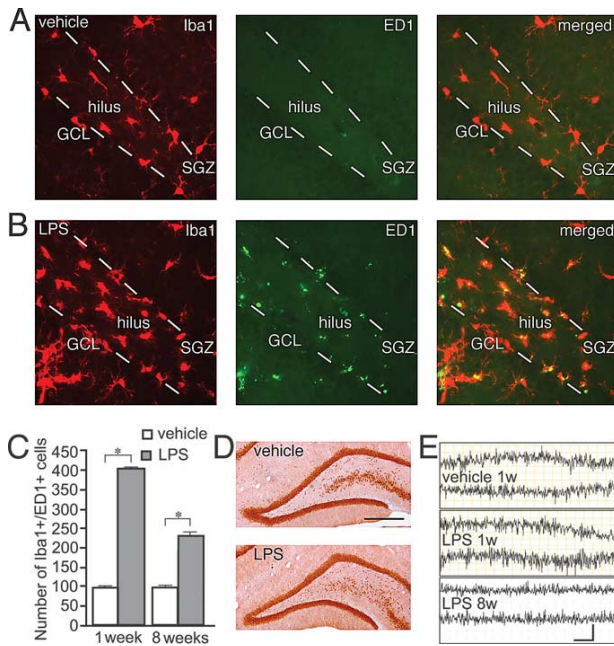
Figure 1. Lipopolysaccharide injection induces a long-lasting inflammatory response in dentate gyrus without neuronal death or seizure activity. Distribution of Iba1$^+$ (red), ED1$^+$ (green), and Iba1$^+$/ED1$^+$ (yellow) microglia in the dentate gyrus 1 week after intrahippocampal vehicle (*A*) or LPS (*B*) injection. *C*, Increased numbers of Iba1$^+$/ED1$^+$, activated microglia in the SGZ/GCL in LPS-treated animals at 1 and 8 weeks after injection. Student's unpaired *t* test, *$p < 0.05$ (LPS and vehicle at 1 week, $n = 4$ and 3, and 8 weeks, $n = 6$ and 6, respectively). Error bars indicate SEM. *D*, NeuN expression showing intact cytoarchitecture in the dentate gyrus at 1 week after LPS or vehicle injection. *E*, EEG recordings after vehicle injection, or at 1 and 8 weeks (1w and 8w) after LPS injection without pathological manifestations. Scale bar (in *D*): *A*, *B*, 50 μm; *D*, 400 μm. Calibration: *E*, 4 s, 0.2 mV.

free-floating sections were preincubated for 1 h in 5% serum in 0.25% Triton X-100 in potassium PBS, and exposed to rabbit anti-GFP primary antibody (1:10,000; Abcam) overnight at RT. FITC-conjugated donkey anti-rabbit secondary antibody and Cy3-streptavidin (1:200; Jackson ImmunoResearch) were then added for 2 h in the dark at RT. Sections were mounted on glass slides and coverslipped.

Tissue preparation and morphological analysis. At 10, 17, 23 d, and 8 weeks after LPS ($n = 6$, 6, 6, and 6 animals) or vehicle injection ($n = 6$, 6, 6, and 4 animals), rats received an overdose of pentobarbital (250 mg/kg, i.p.) and were transcardially perfused with 100 ml of saline followed by 250 ml of 4% ice-cold PFA. Brains were postfixed overnight, dehydrated in 20% sucrose in 0.1 M PBS overnight, cut in 30 μm sections, and stored in cryoprotective solution. For analysis of gephyrin distribution (Schneider Gasser et al., 2006), 10 rats (LPS, $n = 6$; vehicle, $n = 4$) were anesthetized and decapitated. Brains were dissected and placed in ice-cold aCSF, cut in transverse 300-μm-thick sections, placed in gassed aCSF for 20 min and in PFA for 10 min, rinsed in PBS, dehydrated in 30% sucrose in 0.1 M PBS, cut in 14 μm sections, and stored at −20°C for at least 1 h.

For immunohistochemistry, incubation with appropriate primary antibodies was performed for 1 h at RT. Primary antibodies were: rabbit anti-Iba1 (1:1000; Wako Chemicals) for active and quiescent microglia (Imai and Kohsaka, 2002), mouse-anti-ED1 (1:200; Serotec) for phagocytic microglia (Damoiseaux et al., 1994), rabbit anti-GFP, mouse anti-NeuN (1:100; Millipore Bioscience Research Reagents), and mouse anti-gephyrin (1:10,000; Synaptic Systems). Free-floating sections were

incubated overnight at 4°C. Secondary antibodies were as follows: Cy3-conjugated donkey anti-rabbit, biotinylated horse anti-mouse (both 1:200; Vector Laboratories), Cy3-conjugated donkey anti-mouse (1:300; Jackson ImmunoResearch), and FITC-conjugated donkey anti-rabbit with incubation for 2 h at RT (1 h for gephyrin). Rinsing in potassium PBS with or without 0.25% Triton X-100 was performed between each incubation. For double stainings, biotinylated antibodies were detected with streptavidin-conjugated Alexa Fluor 488 (1:200; Invitrogen) for 2 h at RT, whereas in single stainings, avidin–biotin–peroxidase complex (Elite ABC kit; Vector Laboratories), 3,3′-diaminobenzidine, and hydrogen peroxide were used. Chromogenic visualization included pretreatment with blocking of endogenous peroxidase activity with 3% H_2O_2 and 10% methanol. Sections were mounted on microscope slides and immersed in xylene and coverslipped with Pertex mounting medium (HistoLab). For terminal deoxynucleotidyl transferase-mediated biotinylated UTP nick end labeling (TUNEL)/Hoechst staining of DNA fragmentation in cells with apoptotic morphology, sections were immersed in 99% ethanol for 30 min, proteinase K (10 μg/ml) for 6 min, PFA for 5 min, and in 0.1% Triton X-100 in 0.1% sodium citrate for 2 min on ice, before being incubated for 1 h with terminal deoxynucleotidyl transferase buffer (TdT) containing TdT enzyme (5 μl/section) and TUNEL label solution with fluorescein-conjugated dUTP (45 μl/section; all Roche Diagnostics) and finally labeled with the nuclear marker Hoechst 33342 (1:1000; Invitrogen) for 10 min in the dark followed by mounting and coverslipping with glycerol-based mounting medium. For Fluoro-Jade staining of dying cells (Schmued et al., 1997), mounted sections were pretreated with 0.06% potassium permanganate before being agitated for 30 min in 0.001% Fluoro-Jade (Histochem) in 0.1% acetic acid, immersed in xylene, and coverslipped with Pertex mounting medium.

Cell counts and morphological analyses were performed ipsilaterally to LPS injections in six hippocampal sections per animal located 3.3–5.1 mm posterior to bregma (Paxinos and Watson, 1997) by an observer blind to treatment conditions. Numbers of Iba1$^+$/ED1$^+$, Fluoro-Jade$^+$, and TUNEL$^+$ cells with apoptotic morphology were counted with an Olympus BX61 epifluorescence and light microscope in SGZ/GCL, which for GFP$^+$ cell counts was further subdivided into inner, middle, and outer GCL. GFP$^+$ cell counts also included dentate hilus and ML. The volume of SGZ/GCL was measured in NeuN-stained sections using stereological equipment [Olympus BH-2; 40× objective; CC-IRIS color video camera; CAST-GRID software (Olympus)]. The polarization axis was classified for all GFP$^+$ cells (LPS, $n = 130$ cells; vehicle, $n = 332$ cells) into either of three categories: 0–22, 22.5–67, and 67.5–90°, where 90° is perpendicular to the GCL. Numbers of apical dendrites, and percentage of GFP$^+$ cells with apical, basal, and recurrent basal dendrites, and basal, medial, and apical axons were analyzed for all GFP$^+$ cells. Dendritic branching of GFP$^+$ cells was analyzed by assessing the cumulative number of branching points when following each dendrite (LPS, $n = 60$; vehicle, $n = 173$) from the cell soma in 12.5 μm increments until reaching 75 μm.

Spine density (numbers per micrometer) and morphology (divided into four categories: thin, stubby, filopodia, and mushroom) (Zhao et al., 2006) and gephyrin cluster density (numbers per micrometer) and size (area in square micrometers) were analyzed in a confocal laser scanning
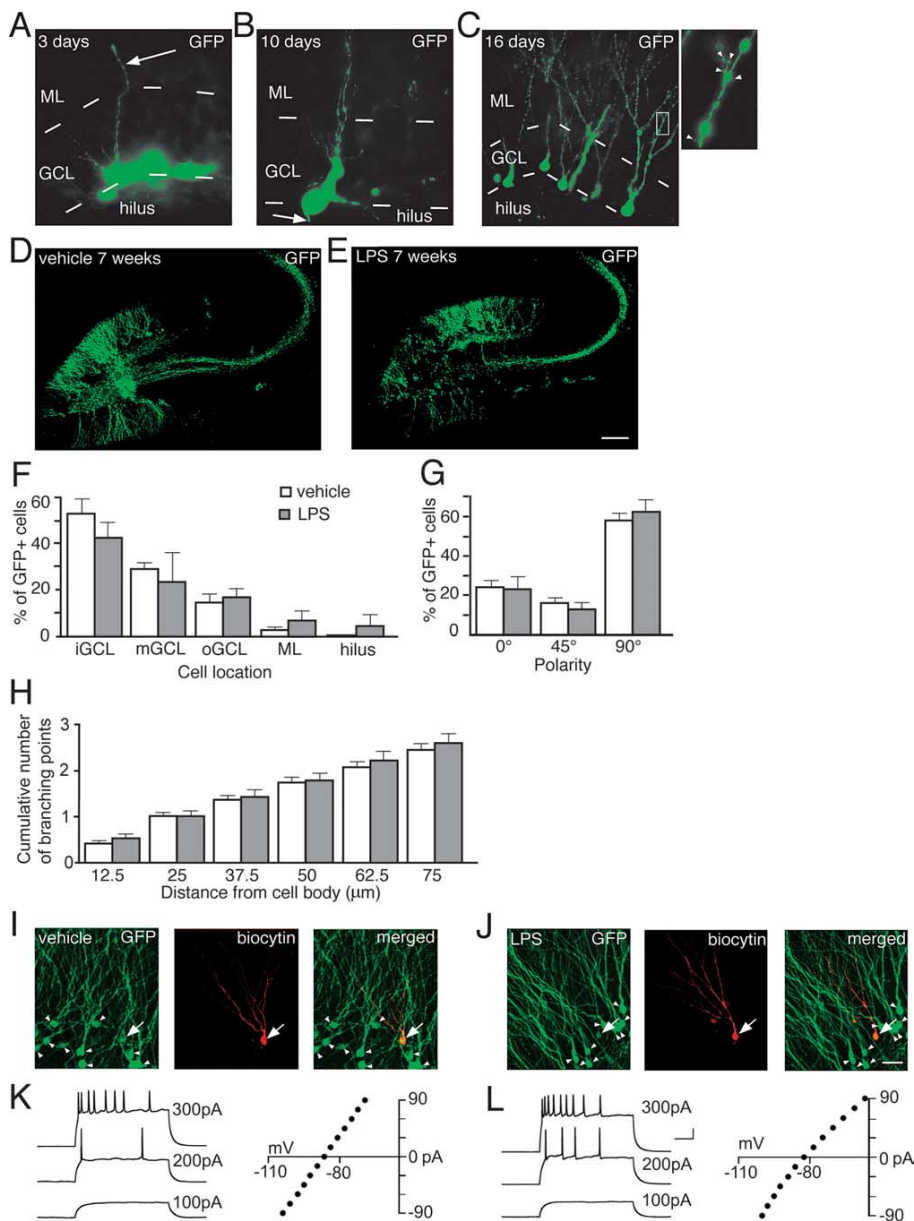
91

Figure 2. New neurons born into a chronic inflammatory environment differentiate into mature dentate granule cells. **A**, GFP$^+$ cell located in the GCL with dendrite (arrow) reaching well into the ML 3 d after RV-GFP labeling. **B**, GFP$^+$ cell with branched dendrites and an axon (arrow) in the hilus 10 d after RV-GFP labeling. Highly branched dendritic trees (**C**) with spines (inset, arrowheads) on GFP$^+$ cells 16 d after RV-GFP labeling. Distribution of new GFP$^+$ neurons in the GCL of vehicle- (**D**) or LPS-injected (**E**) animals 7 weeks after RV-GFP labeling. **F**, Relative location of GFP$^+$ cells in inner, middle, or outer GCL (iGCL, mGCL, and oGCL, respectively), ML, or hilus. **G**, Polarity of the GFP$^+$ cell soma, where 90° is perpendicular to GCL direction. (*Figure legend continues.*)

microscope (Bio-Rad MRC1021UV) with Kr–Ar 488 and 568 nm excitation filters, 100× objective and 16× digital zoom in six squares (9.38 × 9.38 μm) per animal, on proximal and distal dendrites in the inner and outer ML, respectively. The area of each gephyrin cluster was measured in the z-focal plane.

Data were compared using Student's unpaired nonparametric t test. Results are presented as means ± SEM. Differences are considered significant at $p < 0.05$.

Results

Lipopolysaccharide induces chronic inflammation in dentate gyrus without neuronal death or seizure activity

Lipopolysaccharide has previously been used to study the effect of inflammation on hippocampal neurogenesis (Ekdahl et al., 2003; Monje et al., 2003). We found here that the single LPS injection into the dorsal DG induced a long-lasting inflammatory response (Fig. 1A–C). At 1 week after LPS injection, the time point at which the newborn neurons were labeled with RV-GFP, both the total number of microglia (Iba1^{+} cells; LPS, 831.5 ± 8.0; vehicle, 555.7 ± 5.8) and the number of microglia with a phagocytic phenotype (Iba1^{+}/ED1^{+} cells) were elevated in the SGZ/GCL (Fig. 1A–C) to similar magnitude as we have previously observed 1 week after SE (Ekdahl et al., 2003; Jakubs et al., 2006). The numbers of Iba1^{+} (LPS, 683.8 ± 7.8; vehicle, 456.3 ± 9.5) and Iba1^{+}/ED1^{+} cells were still elevated 7 weeks later (approximate time point of electrophysiological recordings) (Fig. 1C). Despite the marked increase in numbers of microglia, NeuN staining revealed that the general cytoarchitecture remained intact (Fig. 1D) and the volume of the SGZ/GCL did not differ between LPS- and vehicle-treated animals at 1 week (LPS, 7.6 ± 0.3 mm[3]; vehicle, 8.2 ± 0.5 mm[3]) or 8 weeks (LPS, 8.3 ± 0.4 mm[3]; vehicle, 7.9 ± 0.4 mm[3]) after injections. We did not detect any neurodegeneration using Fluoro-Jade staining (data not shown). Also, we found only occasional apoptotic TUNEL^{+} cells in the SGZ/GCL, with no differences between LPS and vehicle groups at either 1 week (2.5 ± 0.7 and 2.3 ± 0.8 cells, respectively) or 8 weeks (0.5 ± 0.3 and 0.7 ± 0.3 cells, respectively). Abnormal EEG activity (seizure activity or presence of interictal spikes) was not observed at any time point after vehicle or LPS treatment (Fig. 1E).

Inflammatory environment does not alter location, dendritic tree, or intrinsic membrane properties of new granule cells

The RV-GFP vector induced stable GFP expression in new neurons in the DG when injected into both vehicle- and LPS-treated animals (Fig. 2A–E). The spatiotemporal maturation of the newborn GFP^{+} cells in the inflammatory and control environment closely resembled that previously reported for dentate granule cells in intact brain (Zhao et al., 2006; Shapiro et al., 2007). The

←

(*Figure legend continued.*) 0, 45, and 90° comprise 0 –22, 22.5– 67, and 67.5–90°, respectively. **H**, Cumulative number of dendritic branching points at increasing distances from the GFP[+] cell body. Microscopical analyses in **F–H** were performed 8 weeks after LPS or vehicle injection. No differences between LPS- and vehicle-treated animals were observed. Error bars indicate SEM. Student's unpaired t test, $p > 0.05$. GFP^{+} neurons visualized for patch-clamp analysis after vehicle (**I**) and LPS (**J**) injection. Coexpression of GFP (green) and biocytin (red) that diffused from the patch pipette into the recorded cell (yellow; arrow) with neighboring, nonrecorded GFP[+]/biocytin^{−} cells (arrowheads). Cells in **I** and **J** are from same animals as in **D** and **E**. Action potentials and current–voltage relationship plots of new and mature neurons from vehicle-treated (**K**) and LPS-treated (**L**) animals (recordings at 7– 8 weeks after RV-GFP injection). Current injections of 500 ms were delivered in 15 pA increments. Traces are shown with 100, 200, and 300 pA injection. LPS, n = 130 cells; vehicle, n = 332 cells (**F–H**). Scale bars: (in **E**) **A**, **B**, 10 μm; (in **E**) **C**, 25 μm; (in **E**) **C**, inset, 5 μm; (in **E**) **D**, **E**, 215 μm; (in **J**) **I**, **J**, 30 μm. Calibration: **K**, **L**, 100 ms, 20 mV.

apical dendrites of GFP^{+} cells reached into the molecular layer at 3 d (Fig. 2A), and axonal projections toward CA3 were clearly visible in the hilus at 10 d after GFP labeling (Fig. 2B), with no differences between groups. Large dendritic trees (Fig. 2C) with spines (inset) had developed at 16 d. Despite the detrimental effect of inflammation on hippocampal neurogenesis, causing death of many newly formed neurons (Ekdahl et al., 2003), we observed that a substantial number of GFP^{+} cells had differentiated into mature granule cells 7 weeks later (LPS, 32.5 ± 13.0 cells; vehicle, 55.3 ± 15.4 cells; $p > 0.05$), with highly arborized dendritic tree throughout the ML, and axons reaching CA3 at 7 weeks after GFP labeling in vehicle-treated (Fig. 2D) and LPS-treated animals (Fig. 2E).

The distributional pattern of GFP^{+} cells in the DG was similar in LPS- and vehicle-treated animals (Fig. 2F). The absolute majority of the new cells were located in the GCL, preferentially in its inner part, but a few GFP^{+} cells were found in the hilus and the ML. We observed no differences between LPS- and vehicle-treated animals in the polarity of the GFP[+] cell soma (Fig. 2G). For most of the cells, the somata were aligned vertically, at a 90° angle to the direction of the GCL. The numbers of apical dendrites per GFP[+] cell (LPS, 1.6 ± 0.2; vehicle, 1.4 ± 0.1), dendritic branching points at increasing distances from the soma (Fig. 2H), recurrent basal dendrites (which were very rare), as well as exit points for the axons on the soma did not differ between GFP^{+} cells in LPS- and vehicle-treated animals. Most axons originated from the basal side, some from the medial side, and very few from the apical side of the GFP[+] cell soma (LPS, 68.7 ± 12.4, 29.8 ± 11.3, and 1.5 ± 1.5%; vehicle, 79.8 ± 6.4, 20.0 ± 6.3, and 0.4 ± 0.4%, respectively).

We performed whole-cell patch-clamp recordings from both GFP^{+} cells (new cells, born at the time of RV-GFP injection) and GFP^{−} cells (mature cells, most likely born before LPS and vehicle injection) (Jakubs et al., 2006) in the GCL at 6–8 weeks after RV-GFP injection. Whole-cell current-clamp recordings revealed that the intrinsic membrane properties (resting membrane potential, membrane time constant, input resistance, and action potential threshold, amplitude, and duration) of the new and mature cells in LPS-treated animals were similar to those of new and mature cells in vehicle-treated animals, and closely resembled those characteristic of dentate granule cells (Fig. 2I–L; supplemental Fig. 1, available at www.jneurosci.org as supplemental material).

Inflammatory environment causes similar increase in excitatory synaptic drive on new and mature granule cells

We first analyzed whether the LPS-induced chronic inflammation influenced the excitatory synaptic input to the new and mature neurons in the GCL. Whole-cell voltage-clamp recordings of EPSCs were performed while blocking GABA$_A$ receptors with PTX. Both the new and mature cells in the LPS-treated animals exhibited increased frequency but no change in amplitude of sEPSCs compared with the new and mature cells in the vehicle-treated animals (Fig. 3A–E). Cumulative fraction analysis showed that this effect of LPS-induced inflammation was of the same magnitude in new and mature cells (Fig. 3F,G). We then explored whether short-term plasticity at excitatory synapses on new and mature cells was affected by the chronic inflammatory environment. When we delivered paired stimulations to the lateral perforant path, we observed the same level of PPF of EPSCs in the new and mature granule cells in vehicle- and LPS-treated animals at all interstimulus intervals (Fig. 4). In summary, our findings revealed increased overall excitatory synaptic activity

because of the LPS-induced chronic inflammation but no specific effect at synapses on the new compared with the mature cells.

Inflammatory environment leads to more inhibitory synaptic drive on new compared with mature granule cells

We next determined whether the new neurons exhibited altered inhibitory synaptic input if they had been born into a chronic inflammatory environment. Whole-cell voltage-clamp recordings of sIPSCs were performed while blocking glutamate receptors with NBQX and D-AP5. In animals treated with LPS, the IEIs of sIPSCs recorded in new cells were reduced compared with those in new cells from vehicle-treated animals (Fig. 5A,C). Also, the sIPSCs recorded in the mature cells after LPS treatment occurred with shorter IEIs compared with mature cells in vehicle-injected animals (Fig. 5B,D). The amplitude of sIPSCs in new cells was higher in LPS- than in vehicle-injected animals (Fig. 5E), whereas no such difference was observed in mature cells (data not shown).

When comparing the cells within each treatment group, cumulative fraction analysis revealed that the sIPSCs occurred with similar IEIs (Fig. 6A) and amplitude (data not shown) in new and mature cells in vehicle-treated animals. In contrast, the IEIs of sIPSCs were shorter and their amplitude was larger in new cells compared with mature cells from LPS-treated animals (Fig. 6B,C). When action potential-dependent IPSCs were blocked with TTX (thereby isolating mIPSCs) (Fig. 6D–F), IEIs of mIPSCs did not differ between new and old cells in vehicle-injected animals (Fig. 6D). Moreover, the decreased IEIs and increased amplitude of sIPSCs observed in LPS-treated animals were no longer observed in new cells after TTX application (Fig. 6E,F). Together, these data indicate that LPS-induced inflammation causes a more marked action potential-dependent inhibitory drive at afferent synapses on the new compared with the mature dentate granule cells.

We then analyzed the effect of LPS-induced chronic inflammation on short-term plasticity at inhibitory synapses on the new cells by delivering paired stimulations to the ML of the DG with an interstimulus interval of 100 ms while blocking glutamatergic neurotransmission with NBQX and D-AP5. The first stimulation-induced release of GABA during paired stimulation-induced, monosynaptic IPSCs activates, apart from postsynaptic GABA_A receptors, presynaptic GABA_B receptors, causing an autoinhibition of the subsequent release of GABA, which results in depress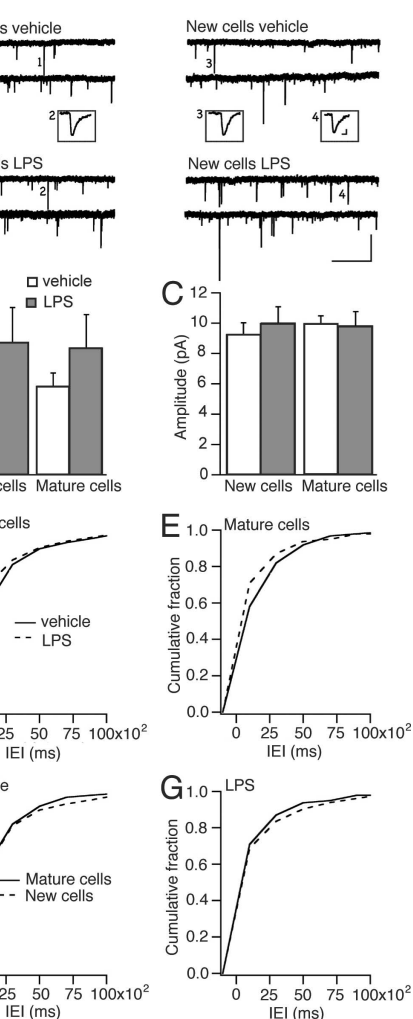ion of the second IPSC (Davies et al., 1990; Otis et al., 1993). In our experiment, the PPD of the stimulation-evoked IPSCs recorded in the new cells born into an inflammatory environment closely resembled that of the new cells in vehicle-treated animals
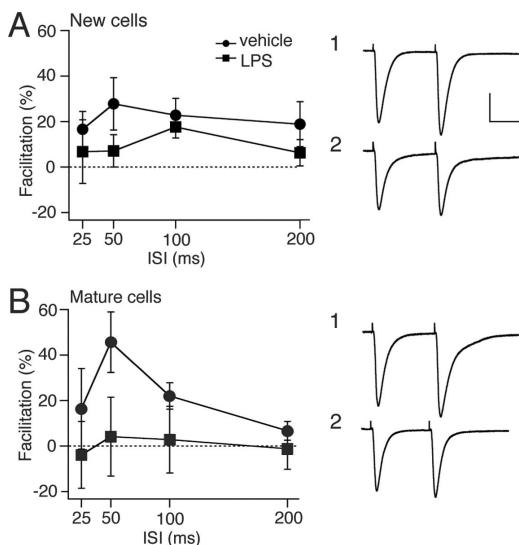

Figure 3. Chronic inflammatory environment causes increased frequency of spontaneous EPSCs in new and mature neurons. *A*, Continuous whole-cell voltage-clamp recordings of sEPSCs in mature or new cells in hippocampal slices, perfused with aCSF containing PTX, from either vehicle- or LPS-injected rats at 7.5–8 weeks after RV-GFP injection. Mean frequency (*B*) and amplitude (*C*) of sEPSCs in new and mature granule cells from LPS- and vehicle-treated animals. Error bars indicate SEM. Cumulative fraction curves of IEIs showing shorter intervals (i.e., higher frequency) in both new (*D*) ($p < 0.001$) and mature (*E*) ($p < 0.001$) cells in LPS-treated compared with vehicle-treated animals but no differences between new and mature cells in vehicle-treated (*F*) ($p > 0.05$) or LPS-treated (*G*) ($p > 0.05$) animals (Kolmogorov–Smirnov test). Numbers of cells recorded were as follows: in vehicle, six GFP $^+$, seven GFP $^-$; in LPS, seven GFP $^+$, five GFP $^-$.

Figure 4. Chronic inflammatory environment does not influence short-term plasticity at excitatory synapses on new and mature neurons. Whole-cell voltage-clamp recordings of paired stimulation-induced EPSCs in new and mature granule cells in hippocampal slices, perfused with aCSF containing PTX, from vehicle- or LPS-treated animals 6.5–7.5 weeks after RV-GFP labeling. Paired stimulations were delivered to lateral perforant path in the outer one-third of the molecular layer with interstimulus intervals (ISIs) of 25, 50, 100, and 200 ms. Average paired-pulse facilitation plotted at each ISI for new (**A**) and mature cells (**B**) in slices from vehicle- or LPS-treated animals. Representative EPSCs elicited with 100 ms ISI are shown in insets from vehicle-treated (**A1**, **B1**) or LPS-treated (**A2**, **B2**) animals. Twenty responses were averaged for each cell at each ISI. Comparisons using one-way ANOVA, or Student's unpaired *t* test at each ISI, revealed no differences between new cells or between mature cells in vehicle- and LPS-treated animals, or between new and mature cells within the same treatment group. Numbers of cells recorded were as follows: in vehicle, four GFP[+], five GFP[−]; in LPS, five GFP[+], five GFP[−]. Error bars indicate SEM. Calibration: **A1**, **A2**, **B1**, **B2**, 50 ms, 50 pA.

(LPS, $-48.0 \pm 4.8\%$; vehicle, $-50.7 \pm 7.2\%$). We then maximally activated $GABA_B$ receptors by exogenous application of the selective agonist baclofen. This treatment strongly suppressed IPSCs and abolished PPD in new cells from vehicle- and LPS-treated animals to the same extent, resulting in similar paired-pulse ratio (Fig. 7A–C). These data indicate that short-term plasticity and presynaptic $GABA_B$ receptor sensitivity or expression at afferent inhibitory synapses on new dentate granule cells are not altered in the chronic inflammatory environment.

Inflammatory environment causes no change of dendritic spines but increased area of gephyrin clusters at inhibitory synapses on new granule cells

We finally wanted to explore whether the chronic inflammation, induced by the LPS treatment, gave rise to structural alterations at excitatory and inhibitory synapses on the new neurons. We first analyzed the dendritic spines, which are the major postsynaptic sites for the excitatory, glutamatergic inputs on dentate granule cells. Using confocal microscopy, we estimated the density and morphology of spines on the GFP[+] new granule cells in the ML of the DG. No difference in spine density was observed between LPS- and vehicle-treated animals in inner and outer ML (Fig. 8A,B). We then compared the density of dendritic spines with specific morphology (mushroom, thin, stubby, and filopodia)

between new cells born in an inflammatory or control environment. Mushroom spines are likely to be associated with stronger excitatory synapses, and accelerated mushroom spine formation on new granule cells has been reported in running animals (Zhao et al., 2006). No differences were found in the density of mushroom spines (Fig. 8C) or any of the other morphological subtypes of dendritic spines between new cells in LPS- and vehicle-treated animals (data not shown). Together, our data do not reveal any morphological alterations caused by the inflammatory environment at presumed excitatory synapses on the dendrites of the new cells.

To detect inflammation-induced alterations at inhibitory synapses on the new neurons, we analyzed with confocal microscopy the immunohistochemical staining of the postsynaptic scaffolding protein gephyrin in the dendrites of GFP^{+} cells. Gephyrin is a multifunctional protein involved in the clustering of glycine and $GABA_A$ receptors at inhibitory synapses (Fritschy et al., 2008). We found no differences in the density of gephyrin clusters in the inner and outer ML on new cells in vehicle- and LPS-treated animals (Fig. 8D–F). However, the area of the gephyrin clusters was larger on the distal dendrites (located in the outer ML) of the new cells that had matured in the inflammatory environment (Fig. 8D,E,G). This finding indicates that chronic inflammation leads to structural alterations at inhibitory synapses on new dentate granule cells.

Discussion

Here, we demonstrate that new hippocampal neurons, which have developed in a chronic inflammatory environment, respond with more pronounced enhancement of the afferent inhibitory synaptic drive than mature neurons that were born already before the onset of inflammation. The new neurons show normal location, dendritic morphology, and intrinsic membrane properties, and exhibit increased excitatory synaptic drive of the same magnitude as the mature neurons.

Chronic inflammation, without neuronal damage and abnormal EEG activity, was induced by a single intrahippocampal injection of LPS. This treatment caused increased numbers of microglia with phagocytotic activity (Iba1^{+}/ED1^{+}) in the SGZ/GCL, both at the time when the new cells were born (1 week after LPS injection) and when they had reached the mature state (at the time of recording and morphological analysis, 7 weeks later). Consistent with our findings, Herber et al. (2006) reported that microglia remain activated 4 weeks after a single intrahippocampal injection of LPS in mice. Previous studies have shown that LPS-induced inflammation can alter synaptic transmission between mature neurons as well as influence behaviors regulated in the hippocampal formation. Administration of LPS by systemic injection causes impairment of both hippocampal-dependent learning (Shaw et al., 2001; Hennigan et al., 2007) and long-term
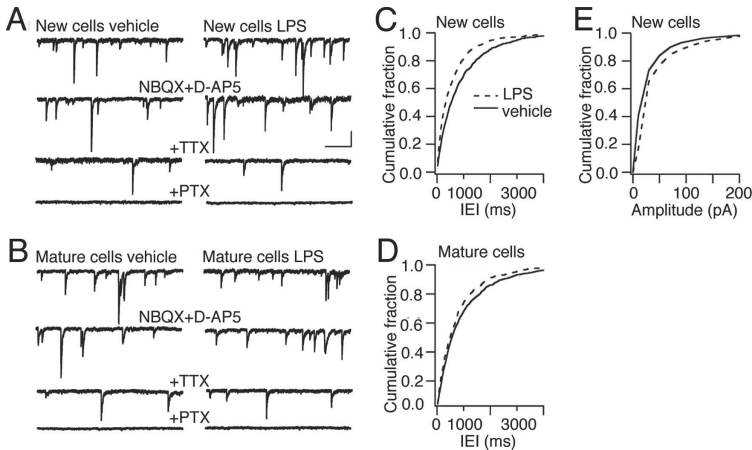
Figure 5. Chronic inflammatory environment causes increased frequency of spontaneous IPSCs in new and mature neurons. Whole-cell voltage-clamp recordings from new (**A**) and mature (**B**) cells in slices from vehicle- and LPS-treated animals at 6 –7.4 weeks after RV-GFP injection in the presence of the glutamate receptor blockers NBQX and D-AP5. The top two traces in each group represent sIPSCs ("NBQX + D-AP5"), the third trace depicts mIPSCs ("+TTX"), and the bottom trace demonstrates blockade of IPSCs by picrotoxin ("+PTX"). **C**, Cumulative fraction analysis showing shorter IEIs of sIPSCs recorded in new cells from LPS-treated animals compared with those in new cells from vehicle-treated rats ($p < 0.001$; 8 cells in each group). **D**, Spontaneous IPSCs at shorter IEIs in mature cells from LPS- than from vehicle-injected animals ($p < 0.05$; 8 and 10 cells in LPS and vehicle groups, respectively). **E**, Higher amplitudes of sIPSCs in new cells from LPS-treated animals than in those from vehicle-treated animals ($p < 0.001$) (Kolmogorov–Smirnov test). Calibration: **A**, **B**, 50 ms, 50 pA.

potentiation (Vereker et al., 2000; Hennigan et al., 2007). Furthermore, injection of LPS in the hippocampal CA1 area of rats gives rise to learning and memory deficits and decreased glutamatergic neurotransmission but no cell death (Tanaka et al., 2006). LPS-evoked inflammation causes increased levels of cyclooxygenase-2, which, via oxidative metabolism of endocannabinoids, induces higher frequency of mEPSCs in hippocampal cultures (Sang et al., 2005, 2007). We find here that the frequency of sEPSCs was increased to the same extent in mature and new cells in the inflammatory environment compared with the control environment. The lack of inflammation-induced changes of spine density and morphology in the new cells argue against the possibility that such alterations would underlie the increased excitatory drive at their afferent excitatory synapses. Moreover, we found no changes of PPF at the excitatory synapses in the new and mature neurons, indicating unaltered overall glutamate release probability (Zucker and Stockbridge, 1983; Debanne et al., 1996; Murthy et al., 1997). Therefore, the increased excitatory drive on new and mature granule cells is most likely attributable to increased network activity in hippocampal neural circuitries caused by the inflammation.

Both the new and the mature granule cells exhibited increased inhibitory synaptic drive in response to LPS-induced inflammation. Exposure to LPS causes increased expression of
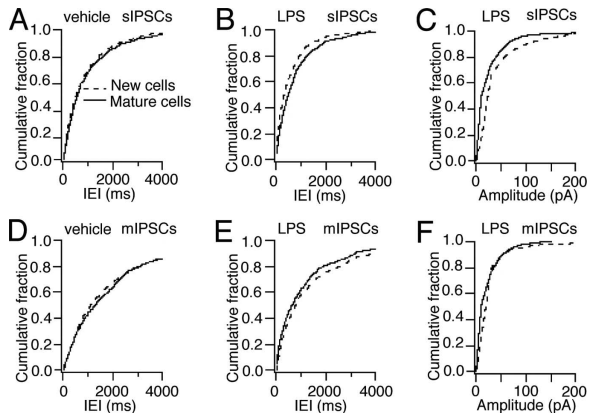

Figure 6. Chronic inflammatory environment leads to more action potential-dependent inhibitory drive in new than in mature neurons. Whole-cell voltage-clamp recordings of sIPSCs (in the presence of NBQX plus D-AP5) and mIPSCs (after addition of TTX) in cells from vehicle-treated (**A**, **D**) and LPS-treated (**B**, **C**, **E**, **F**) animals. Cumulative fraction curves showing sIPSCs at similar IEIs in new and mature cells in vehicle-treated animals (**A**) ($p > 0.05$) but with shorter IEIs (**B**) ($p < 0.001$) in new cells compared with mature cells in LPS-treated animals. **C**, Higher amplitude of sIPSCs in new cells compared with old cells in LPS animals ($p < 0.001$). Similar IEIs of mIPSCs in new and mature cells in vehicle-treated animals (**D**) ($p > 0.05$), and similar IEIs (**E**) ($p > 0.05$) and amplitudes (**F**) ($p > 0.05$) of mIPSCs in new cells compared with mature cells in LPS-treated rats after action potential blockade with TTX (Kolmogorov–Smirnov test). The cells are the same as in Figure 5.

interleukin-1β in microglia (Lund et al., 2006) and elevated levels of this cytokine in hippocampal organotypic cultures (Hellstrom et al., 2005). Similarly, intrahippocampal LPS administration gives rise to a rapid, severalfold increase of interleukin-1β production from microglia (Tanaka et al., 2006). In line with our
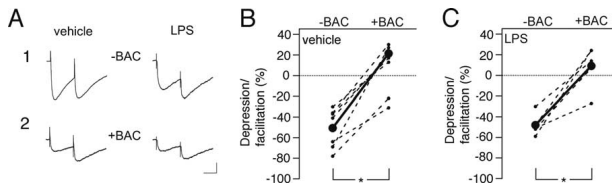
Figure 7. Chronic inflammatory environment does not influence short-term plasticity at inhibitory synapses in new neurons. **A**, Representative recordings (each trace is average of 20 responses from the same cell) from new cells in vehicle- and LPS-treated animals before ("−BAC"; **B1**) and after ("+BAC"; **B2**) addition of the GABAB receptor agonist baclofen. Baclofen eliminated PPD similarly in new cells from vehicle (**B**) and LPS (**C**) animals. **B**, **C**, Depression/facilitation of IPSCs in individual cells; each cell is plotted before and after baclofen addition (connected with dashed lines), and group averages are depicted by the solid line (n = 5 and 7 cells in LPS- and vehicle-treated animals, respectively). *p < 0.05, Student's paired t test. Recordings were performed 6.1–7.7 weeks after RV-GFP injection. Calibration: **A1**, 50 ms, 100 pA; **A2**, 50 ms, 50 pA.

observations, LPS-treated organotypic cultures showed increased inhibitory transmission in CA1 pyramidal neurons (larger amplitude of monosynaptic IPSPs during electrical stimulation of GABAergic afferent fibers), which was prevented by coincubation with an IL-1 receptor antagonist (Hellstrom et al., 2005). Thus, the increased inhibitory drive on the new and mature cells in our experiment could have been induced by microglial release of proinflammatory cytokines such as interleukin-1β.

The enhancement of the inhibitory synaptic drive (i.e., the frequency and amplitude of sIPSCs) in the chronic inflammatory environment was more pronounced on the new compared with the mature cells. Inhibitory synaptic inputs are mostly located close to the soma and can be synchronized (Cobb et al., 1995; Miles et al., 1996). Therefore, even small changes in the mean rate of inhibitory synaptic input are likely to significantly modulate the gain of action potential generation by the cell (Mitchell and Silver, 2003). We obtained no evidence in the PPD paradigm for any changes in short-term synaptic plasticity at inhibitory synapses on the new cells. Because no differences in frequency or amplitude of IPSCs in new compared with mature granule cells remained after TTX administration, the higher inhibitory synaptic drive on the new cells in the inflammatory environment is most likely caused by action potential-dependent, presynaptic changes. Hypothetically, the new cells might interact with the afferent inhibitory neurons through putative retrograde messengers, and the presynaptic alterations could occur according to one of several scenarios. First, the new cells in the inflammatory environment may receive inhibitory input from a population of interneurons with higher frequency of action potential generation compared with the mature cells. Second, the inhibitory synapses could be more numerous or have higher overall release probability of GABA on the new cells born in a chronic inflammatory environment. Arguing against this possibility, the differences in sIPSC frequency between new and mature cells were no longer observed after TTX application. Third, the increase in sIPSC frequency could be attributed to enhanced expression or activation of voltage-dependent calcium channels on the inhibitory afferents at the new cells in LPS-treated animals. Increased release of GABA would then primarily be attributable to more activation of voltage-dependent calcium channels and higher calcium influx triggered by action potential-induced depolarization at the presynapses (Mintz et al., 1995). This interpretation is also consistent with the elevated amplitude of sIPSCs but not of mIPSCs in the new cells in LPS-treated animals.

The increased amplitude of sIPSCs could, alternatively, reflect postsynaptic alterations, which is supported by our finding of larger gephyrin clusters on the dendrites of the new cells, which had developed in the chronic inflammatory environment. Gephyrin is an important postsynaptic scaffolding protein that is required for clustering of glycine and GABAA receptors at inhibitory synapses (Fritschy et al., 2008), and is essential for the stability of GABAergic synapses. Disruption of gephyrin clusters causes reduced presynaptic GABAergic innervation and decreased amplitude and frequency of sIPSCs in cultured hippocampal neurons (Yu et al., 2007). The size of gephyrin clusters in hippocampal slice cultures was found to be inversely regulated by neuronal activity (Marty et al., 2004). It is conceivable that the larger gephyrin clusters on the new cells born in the chronic inflammatory environment indicate a more efficacious inhibitory input. In support, Lim et al. (1999) reported a positive correlation between synaptic strength and the size of postsynaptic gephyrin clusters. Inconsistent with a major role of the postsynaptic changes, the difference in amplitude of sIPSCs between new cells in LPS- and vehicle-treated animals did not remain after blockade of action potentials. It should be pointed out, however, that given the lower overall amplitude of mIPSCs compared with sIPSCs, and that the gephyrin clusters were increased in the axodendritic inhibitory synapses on the distal dendrites (i.e., distal to the patch pipette in the cell soma), subtle changes in mIPSC amplitudes could have escaped detection.

Inflammation did not alter the migration or polarity of the new cells, the timing when apical dendrites had reached the ML and the axons had reached CA3, the arborizations of the dendrites, or the development, density, or shape of the spines. Thus, the morphological maturation of the new cells, which has previously been described in adult mouse hippocampus using the same RV-GFP vector (Zhao et al., 2006), was strictly controlled also in the chronic inflammatory environment. Spines on dendrites of new granule cells are highly motile, transforming from one subtype/form to another in a very dynamic manner, as demonstrated by time-lapse imaging (Zhao et al., 2006). We analyzed spine density and morphology only at one time point (~49 d after RV-GFP injection) and found no differences between LPS-treated and control animals. In agreement, running-induced increased hippocampal activity in mice caused no alterations of spine density on new cells at any time point (Zhao et al., 2006). Mushroom spine density was increased in runners at 56 d but not at earlier and later time points. This transient change of spine morphology occurred in the mice 1 week after our analysis in the rats, which may explain why it was not detected in the present study.

Our findings provide evidence of a high degree of plasticity of the new neurons at their afferent synaptic inputs when exposed to the pathological environment. Recordings were made 6–8 weeks after the new cells had been born (i.e., after the critical period of enhanced synaptic plasticity between 1 and 1.5 months of cell age) (Ge et al., 2007). We find that the new neurons had responded to the increased excitatory synaptic drive, caused by the chronic inflammation, with an additional upregulation of inhibitory activity at their afferent synapses and the development of larger gephyrin clusters. The previously unknown regulation of gephyrin in adult-born neurons reveals another mechanism that can contribute to the plasticity in their functional synaptic con-

nectivity. It remains to be explored whether the observed plastic changes in inhibitory inputs on the new neurons, and to a lesser extent on the mature neurons, are directly induced by the inflammation, or if they are indirect and compensatory, aiming to preserve cellular and/or network homeostasis in a pathological condition with increased excitatory drive on both new and mature granule cells.

The synaptic properties of the new cells in the LPS-induced, chronic inflammatory environment differed from those of cells that had developed after SE (Jakubs et al., 2006). Compared with cells born into a physiological environment, the new cells generated after SE exhibited decreased excitatory drive because of reduced release probability of glutamate, and increased inhibitory drive, most likely because of decreased sensitivity/expression of presynaptic $GABA_B$ receptors and increased postsynaptic $GABA_A$ receptor expression. It is conceivable that these changes in the afferent synapses on the cells born after SE were compensatory and occurred in response to network hyperexcitability. In the LPS-induced chronic inflammatory environment, both the new and the mature cells exhibited increased excitatory and inhibitory afferent drive, primarily because of changes at the network level and not at their afferent synapses. In addition, the new cells that had developed in a chronic inflammatory environment showed synapse-specific enhancement of the afferent inhibitory drive, but this change was not attributable to alterations in presynaptic $GABA_B$ receptors as after SE. Together, our findings provide evidence that the pathological environments induced by SE and LPS lead to different and specific compensatory alterations of the properties of the afferent synapses on the new neurons.

In the present study, inflammation was induced by LPS already before the formation of the new neurons, and there was chronic inflammation in the environment throughout their development/maturation and still at the time of recordings and morphological analysis. Our findings raise several important issues that need to be explored in future experiments: first, to determine when during the development of the new neurons they are particularly sensitive to inflammation and respond with alterations of their functional synaptic connectivity. Ideally, inflammation could be induced by LPS at different time points after the formation of the new neurons. However, a major confounding factor, which would make the findings difficult to compare with the present data, is that the acute effects of LPS, which are unlikely to play a role when cells are born at 1 week after LPS injection, most probably will affect the properties of the new neurons if LPS is delivered when the
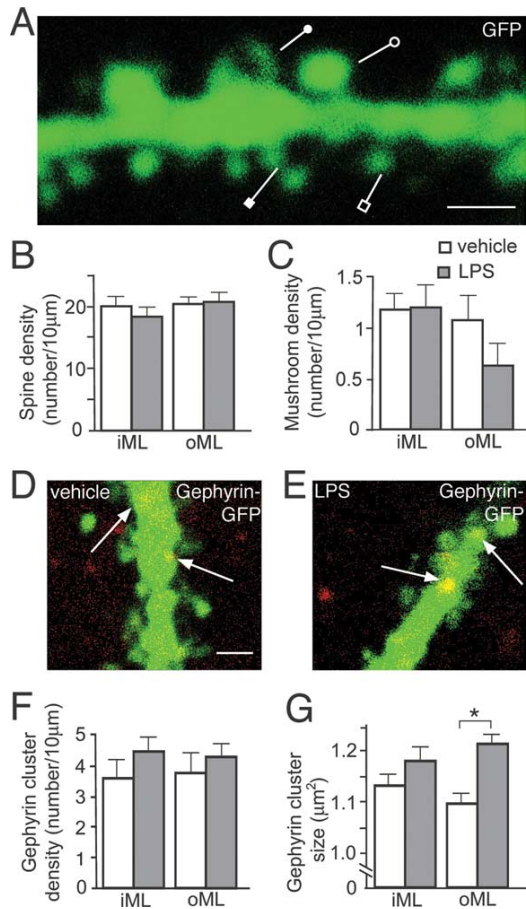

Figure 8. New neurons born into a chronic inflammatory environment develop normal spine density and morphology but increased size of the postsynaptic scaffolding protein gephyrin. New neurons develop dendritic tree with thin (open square), stubby (closed square), filopodia (closed circle), and mushroom spines (open circle) (*A*), and with similar density of dendritic spines (*B*) and mushroom spines (*C*) in vehicle- and LPS-treated animals in inner and outer ML (iML and oML, respectively). New neurons born in vehicle-treated (*D*) or LPS-treated (*E*) animals develop gephyrin clusters on dendrites (arrows), with similar density (*F*) but increased size (*G*) on distal dendrites in outer ML of LPS-treated compared with vehicle-treated animals (**p* < 0.001) (Student's unpaired *t* test) (LPS, *n* = 23–34 dendrites; vehicle, *n* = 21–33 dendrites). Error bars indicate SEM. Scale bars: *A, D* (for *D, E*), 1 μm.

neurons have already been formed. For example, LPS injection *in vivo* induces acute, transient increases (returning to baseline within 24 h) of several inflammatory markers such as IL-6, MCP-1, and TNF-α (tumor necrosis factor-α) (Lund et al., 2006). Second, to analyze whether the alterations of excitatory and, in particular, inhibitory synaptic drive onto the new neurons are permanent. This will require assessment of their properties both if the chronic inflammation has declined and if it is maintained. Our hypothesis postulates that the increased excitatory

drive onto both new and mature neurons is induced by inflammation, which leads to the enhanced increase of inhibitory drive on new neurons. Because there was a substantial reduction of microglia from 1 to 8 weeks, continued inflammation at later time points would probably require additional LPS injections, which could result in cyclic exacerbations of the inflammatory response. Third is to investigate how the characteristics of the inflammatory environment will affect the development of the functional synaptic connectivity. Microglia can have both detrimental and beneficial effects on adult neurogenesis depending on their morphological and molecular phenotype and whether they are acutely or chronically activated [for references, see, for example, Ekdahl et al. (2008)]. Moreover, autoimmune, CNS-specific T-lymphocytes, by interacting with resident microglia, can promote neurogenesis in the SGZ and possibly also influence neuronal differentiation (Ziv et al., 2006). Here, we only assessed the consequences of one type of chronic inflammatory environment. Hypothetically, if the features of the different cellular and molecular players in the inflammation are altered, this could lead to a different development of the functional synaptic connectivity of the new neurons.

The continuous generation of new dentate granule cells probably plays a role in learning and memory, and deterioration of hippocampal neurogenesis may be linked to the cognitive decline in aging and Alzheimer's disease. Brain inflammation and microglia activation are involved in many disorders associated with cognitive impairment. Our data provide the first experimental evidence that inflammation affects the functional integration of the new adult-born neurons in existing neural circuitries. Thus, clarifying the extent of involvement of adult neurogenesis in pathological conditions associated with inflammation (e.g., in mouse Alzheimer models) mandates functional analysis at the cellular level to complement quantitative data on progenitor proliferation and neuron numbers. Whether the changes of functional synaptic connectivity of new neurons, which have developed in an inflammatory environment, act to mitigate or worsen brain dysfunction remains to be investigated.
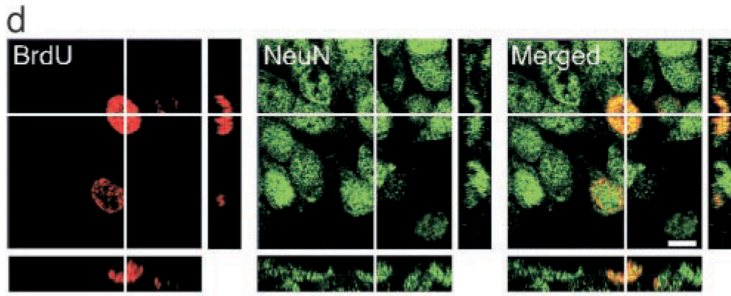
References

Arvidsson A, Kokaia Z, Lindvall O (2001) N-Methyl-D-aspartate receptor-mediated increase of neurogenesis in adult rat dentate gyrus following stroke. Eur J Neurosci 14:10–18.

Arvidsson A, Collin T, Kirik D, Kokaia Z, Lindvall O (2002) Neuronal replacement from endogenous precursors in the adult brain after stroke. Nat Med 8:963–970.

Bengzon J, Kokaia Z, Elmér E, Nanobashvili A, Kokaia M, Lindvall O (1997) Apoptosis and proliferation of dentate gyrus neurons after single and intermittent limbic seizures. Proc Natl Acad Sci U S A 94:10432–10437.

Bonde S, Ekdahl CT, Lindvall O (2006) Long-term neuronal replacement in adult rat hippocampus after status epilepticus despite chronic inflammation. Eur J Neurosci 23:965–974.

Cobb SR, Buhl EH, Halasy K, Paulsen O, Somogyi P (1995) Synchronization of neuronal activity in hippocampus by individual GABAergic interneurons. Nature 378:75–78.

Damoiseaux JG, Döpp EA, Calame W, Chao D, MacPherson GG, Dijkstra CD (1994) Rat macrophage subset heterogeneity in monoclonal antibody ED1. Immunology 83:140–147.

Danton GH, Dietrich WD (2003) Inflammatory mechanisms after ischemia and stroke. J Neuropathol Exp Neurol 62:127–136.

Davies CH, Davies SN, Collingridge GL (1990) Paired-pulse depression of monosynaptic GABA-mediated inhibitory postsynaptic responses in rat hippocampus. J Physiol 424:513–531.

Debanne D, Guerineau NC, Gahwiler BH, Thompson SM (1996) Paired-pulse facilitation and depression at unitary synapses in rat hippocampus: quantal fluctuation affects subsequent release. J Physiol 491:163–176.

Ekdahl CT, Claasen JH, Bonde S, Kokaia Z, Lindvall O (2003) Inflammation

is detrimental for neurogenesis in adult brain. Proc Natl Acad Sci U S A 100:13632–13637.

Ekdahl CT, Kokaia Z, Lindvall O (2008) Brain inflammation and adult neurogenesis: the dual role of microglia. Neuroscience. Advance online publication. Retrieved November 3, 2008. doi:10.1016/j.neuroscience.2008.06.052

Fritschy JM, Harvey RJ, Schwarz G (2008) Gephyrin: where do we stand, where do we go? Trends Neurosci 31:257–264.

Ge S, Yang CH, Hsu KS, Ming GL, Song H (2007) A critical period for enhanced synaptic plasticity in newly generated neurons of the adult brain. Neuron 54:559–566.

Gloveli T, Behr J, Dugladze T, Kokaia Z, Kokaia M, Heinemann U (2003) Kindling alters entorhinal cortex-hippocampal interaction by increased efficacy of presynaptic GABA(B) autoreceptors in layer III of the entorhinal cortex. Neurobiol Dis 13:203–212.

Gorter JA, van Vliet EA, Aronica E, Breit T, Rauwerda H, Lopes da Silva FH, Wadman WJ (2006) Potential new antiepileptogenic targets indicated by microarray analysis in a rat model for temporal lobe epilepsy. J Neurosci 26:11083–11110.

Henneberger C, Kirischuk S, Grantyn R (2005) Brain-derived neurotrophic factor modulates GABAergic synaptic transmission by enhancing presynaptic glutamic acid decarboxylase 65 levels, promoting asynchronous release and reducing the number of activated postsynaptic receptors. Neuroscience 135:749–763.

Hennigan A, Trotter C, Kelly AM (2007) Lipopolysaccharide impairs long-term potentiation and recognition memory and increases p75NTR expression in the rat dentate gyrus. Brain Res 1130:158–166.

Herber DL, Maloney JL, Roth LM, Freeman MJ, Morgan D, Gordon MN (2006) Diverse microglial responses after intrahippocampal administration of lipopolysaccharide. Glia 53:382–391.

Hoehn BD, Palmer TD, Steinberg GK (2005) Neurogenesis in rats after focal cerebral ischemia is enhanced by indomethacin. Stroke 36:2718–2724.

Imai Y, Kohsaka S (2002) Intracellular signaling in M-CSF-induced microglia activation: role of Iba1. Glia 40:164–174.

Iosif RE, Ekdahl CT, Ahlenius H, Pronk CJ, Bonde S, Kokaia Z, Jacobsen SE, Lindvall O (2006) Tumor necrosis factor receptor 1 is a negative regulator of progenitor proliferation in adult hippocampal neurogenesis. J Neurosci 26:9703–9712.

Iosif RE, Ahlenius H, Ekdahl CT, Darsalia V, Thored P, Jovinge S, Kokaia Z, Lindvall O (2008) Suppression of stroke-induced progenitor proliferation in adult subventricular zone by tumor necrosis factor receptor 1. J Cereb Blood Flow Metab 28:1574–1587.

Jakubs K, Nanobashvili A, Bonde S, Ekdahl CT, Kokaia Z, Kokaia M, Lindvall O (2006) Environment matters: synaptic properties of neurons born in the epileptic adult brain develop to reduce excitability. Neuron 52:1047–1059.

Laplagne DA, Espósito MS, Piatti VC, Morgenstern NA, Zhao C, van Praag H, Gage FH, Schinder AF (2006) Functional convergence of neurons generated in the developing and adult hippocampus. PLoS Biol 4:e409.

Laplagne DA, Kamienkowski JE, Espósito MS, Piatti VC, Zhao C, Gage FH, Schinder AF (2007) Similar GABAergic inputs in dentate granule cells born during embryonic and adult neurogenesis. Eur J Neurosci 25:2973–2981.

Lim R, Alvarez FJ, Walmsley B (1999) Quantal size is correlated with receptor cluster area at glycinergic synapses in the rat brainstem. J Physiol 516:505–512.

Lund S, Christensen KV, Hedtjärn M, Mortensen AL, Hagberg H, Falsig J, Hasseldam H, Schrattenholz A, Pörzgen P, Leist M (2006) The dynamics of the LPS triggered inflammatory response of murine microglia under different culture and in vivo conditions. J Neuroimmunol 180:71–87.

Marty S, Wehrlé R, Fritschy JM, Sotelo C (2004) Quantitative effects produced by modifications of neuronal activity on the size of GABAA receptor clusters in hippocampal slice cultures. Eur J Neurosci 20:427–440.

Miles R, Tóth K, Gulyás AI, Hájos N, Freund TF (1996) Differences between somatic and dendritic inhibition in the hippocampus. Neuron 16:815–823.

Mintz IM, Sabatini BL, Regehr WG (1995) Calcium control of transmitter release at a cerebellar synapse. Neuron 15:675–688.

Mitchell SJ, Silver RA (2003) Shunting inhibition modulates neuronal gain during synaptic excitation. Neuron 38:433–445.

Monje ML, Toda H, Palmer TD (2003) Inflammatory blockade restores adult hippocampal neurogenesis. Science 302:1760–1765.

Murthy VN, Sejnowski TJ, Stevens CF (1997) Heterogeneous release properties of visualized individual hippocampal synapses. Neuron 18:599–612.

Otis TS, De Koninck Y, Mody I (1993) Characterization of synaptically elicited GABAB responses using patch-clamp recordings in rat hippocampal slices. J Physiol 463:391–407.

Parent JM, Yu TW, Leibowitz RT, Geschwind DH, Sloviter RS, Lowenstein DH (1997) Dentate granule cell neurogenesis is increased by seizures and contributes to aberrant network reorganization in the adult rat hippocampus. J Neurosci 17:3727–3738.

Parent JM, Vexler ZS, Gong C, Derugin N, Ferriero DM (2002) Rat forebrain neurogenesis and striatal neuron replacement after focal stroke. Ann Neurol 52:802–813.

Paxinos G, Watson C (1997) The rat brain in stereotaxic coordinates. San Diego: Academic.

Pickering M, Cumiskey D, O'Connor JJ (2005) Actions of TNF-alpha on glutamatergic synaptic transmission in the central nervous system. Exp Physiol 90:663–670.

Sang N, Zhang J, Marcheselli V, Bazan NG, Chen C (2005) Postsynaptically synthesized prostaglandin E2 (PGE2) modulates hippocampal synaptic transmission via a presynaptic PGE2 EP2 receptor. J Neurosci 25:9858–9870.

Sang N, Zhang J, Chen C (2007) COX-2 oxidative metabolite of endocannabinoid 2-AG enhances excitatory glutamatergic synaptic transmission and induces neurotoxicity. J Neurochem 102:1966–1977.

Schmued LC, Albertson C, Slikker W Jr (1997) Fluoro-Jade: a novel fluorochrome for the sensitive and reliable histochemical localization of neuronal degeneration. Brain Res 751:37–46.

Schneider Gasser EM, Straub CJ, Panzanelli P, Weinmann O, Sassoè-Pognetto M, Fritschy JM (2006) Immunofluorescence in brain sections: simultaneous detection of presynaptic and postsynaptic proteins in identified neurons. Nat Protoc 1:1887–1897.

Schratt GM, Tuebing F, Nigh EA, Kane CG, Sabatini ME, Kiebler M, Greenberg ME (2006) A brain-specific microRNA regulates dendritic spine development. Nature 439:283–289.

Shapiro LA, Upadhyaya P, Ribak CE (2007) Spatiotemporal profile of dendritic outgrowth from newly born granule cells in the adult rat dentate gyrus. Brain Res 1149:30–37.

Shaw KN, Commins S, O'Mara SM (2001) Lipopolysaccharide causes deficits in spatial learning in the watermaze but not in BDNF expression in the rat dentate gyrus. Behav Brain Res 124:47–54.

Tanaka S, Ide M, Shibutani T, Ohtaki H, Numazawa S, Shioda S, Yoshida T (2006) Lipopolysaccharide-induced microglial activation induces learning and memory deficits without neuronal cell death in rats. J Neurosci Res 83:557–566.

van Praag H, Schinder AF, Christie BR, Toni N, Palmer TD, Gage FH (2002) Functional neurogenesis in the adult hippocampus. Nature 415:1030–1034.

Vereker E, Campbell V, Roche E, McEntee E, Lynch MA (2000) Lipopolysaccharide inhibits long term potentiation in the rat dentate gyrus by activating caspase-1. J Biol Chem 275:26252–26258.

von Bohlen und Halbach O, Krause S, Medina D, Sciarretta C, Minichiello L, Unsicker K (2006) Regional- and age-dependent reduction in trkB receptor expression in the hippocampus is associated with altered spine morphologies. Biol Psychiatry 59:793–800.

Wu C, Leung LS (1997) Partial hippocampal kindling decreases efficacy of presynaptic GABAB autoreceptors in CA1. J Neurosci 17:9261–9269.

Yu W, Jiang M, Miralles CP, Li RW, Chen G, de Blas AL (2007) Gephyrin clustering is required for the stability of GABAergic synapses. Mol Cell Neurosci 36:484–500.

Zhao C, Teng EM, Summers RG Jr, Ming GL, Gage FH (2006) Distinct morphological stages of dentate granule neuron maturation in the adult mouse hippocampus. J Neurosci 26:3–11.

Zhao C, Deng W, Gage FH (2008) Mechanisms and functional implications of adult neurogenesis. Cell 132:645–660.

Ziv Y, Ron N, Butovsky O, Landa G, Sudai E, Greenberg N, Cohen H, Kipnis J, Schwartz M (2006) Immune cells contribute to the maintenance of neurogenesis and spatial learning abilities in adulthood. Nat Neurosci 9:268–275.

Zucker RS, Stockbridge N (1983) Presynaptic calcium diffusion and the time courses of transmitter release and synaptic facilitation at the squid giant synapse. J Neurosci 3:1263–1269.
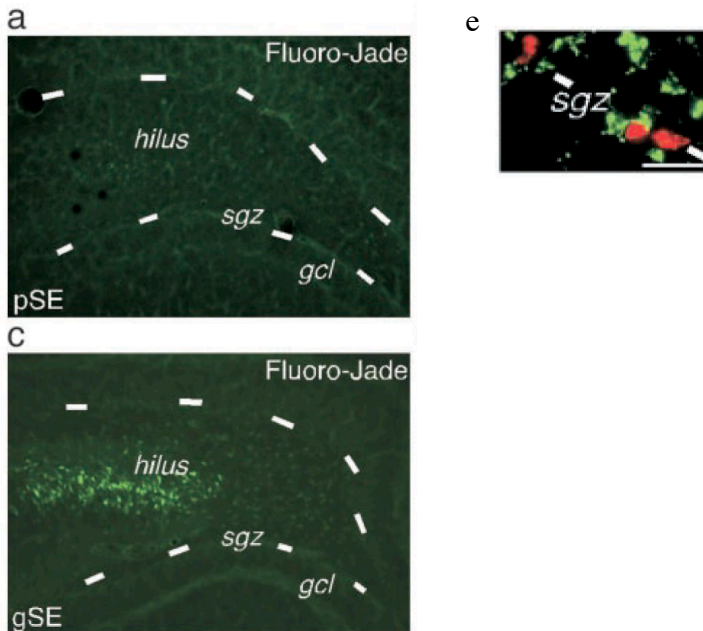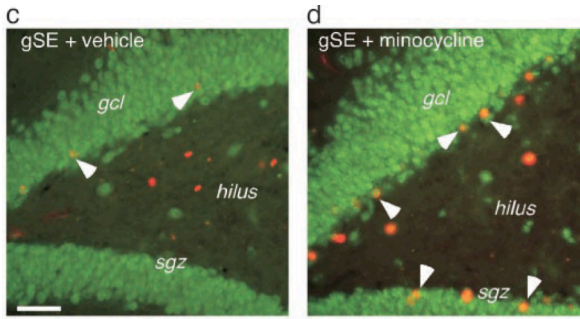
Colour plates
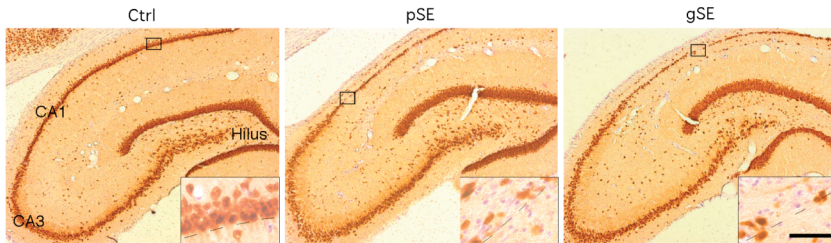
Paper A

Figur 1 d

Figur 2 a, c, e

Figur 4 c, d

Figur 4 c, d

Paper B

Figur 1 e

Figur 2

Figure 3

Iba1 ED1 Iba1 / ED1

A 5w ctrl — Hilus, SGZ, GCL

B 5w pSE — Hilus, SGZ, GCL

C 5w gSE — Hilus, SGZ, GCL

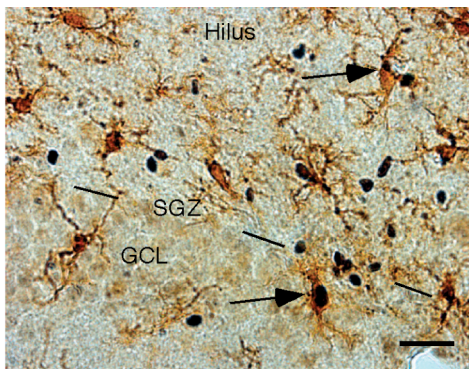D 6m ctrl — Hilus, SGZ, GCL

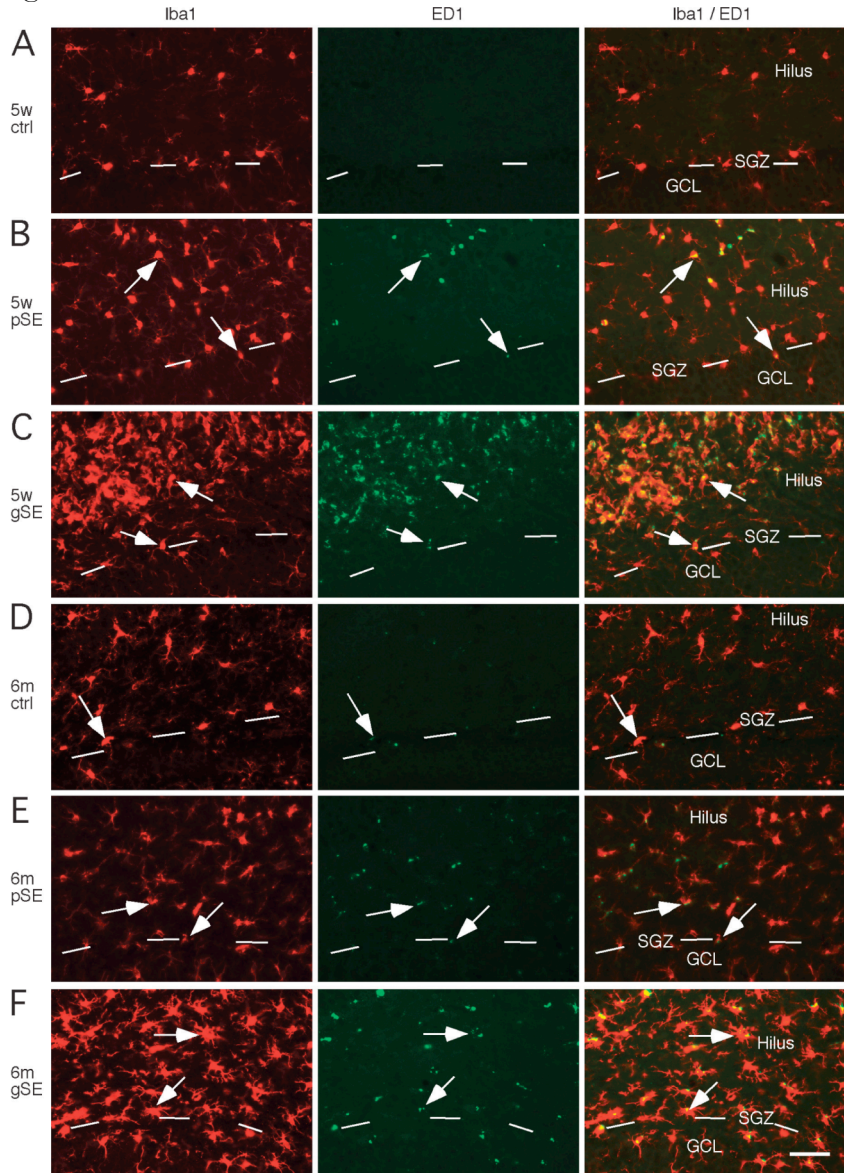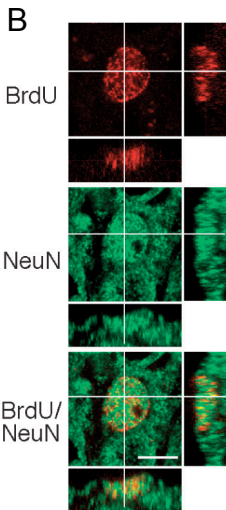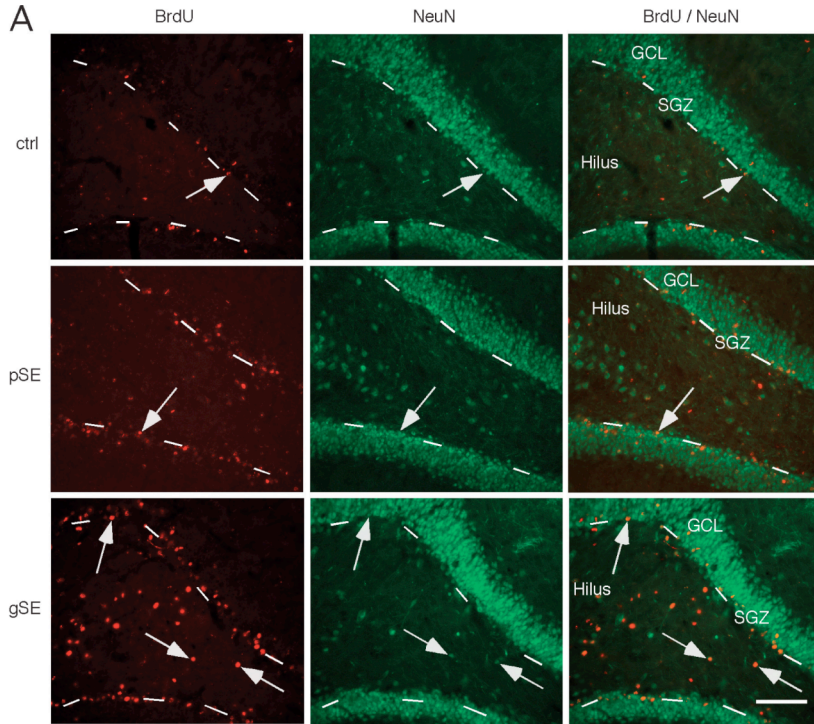E 6m pSE — Hilus, SGZ, GCL

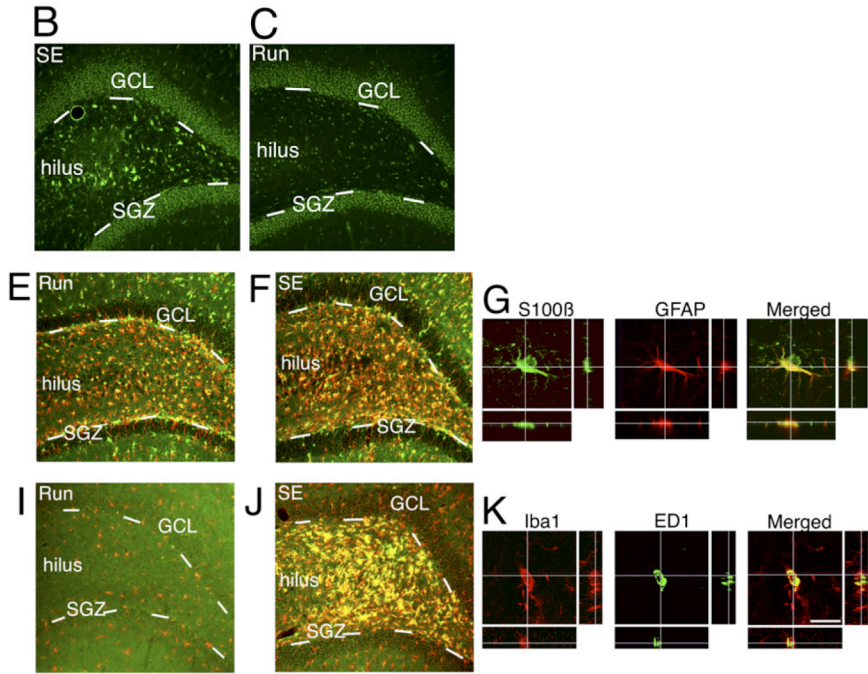F 6m gSE — Hilus, SGZ, GCL

Figure 5 a, b

Paper C
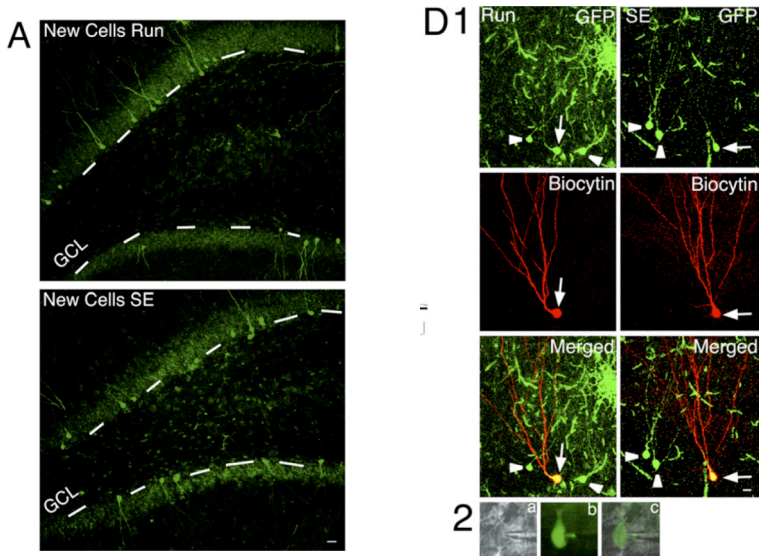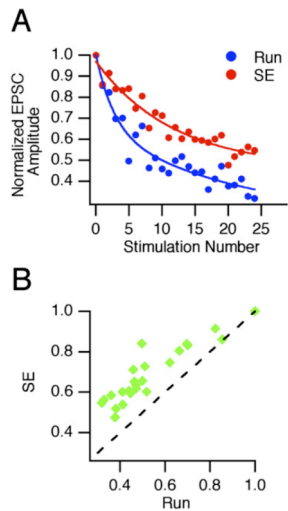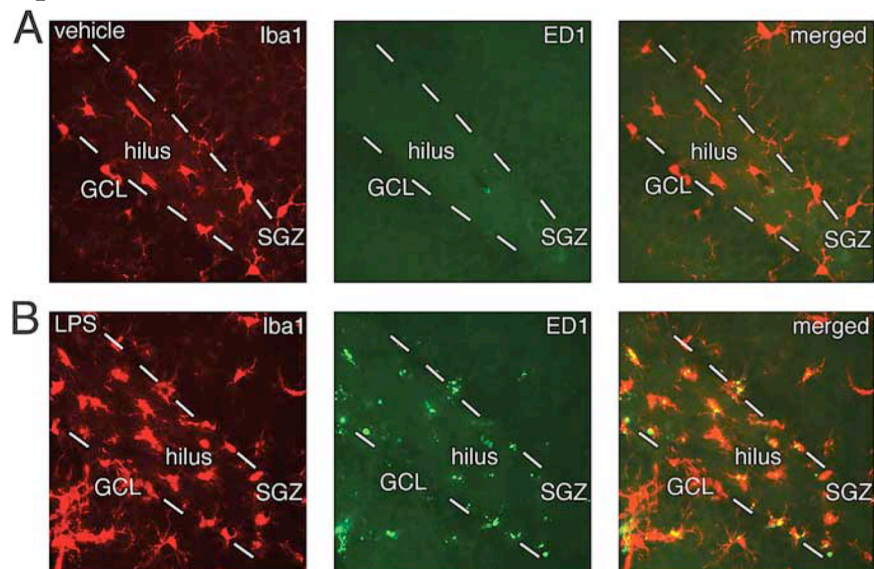
Figure b, c, e, f, g, i, j, k
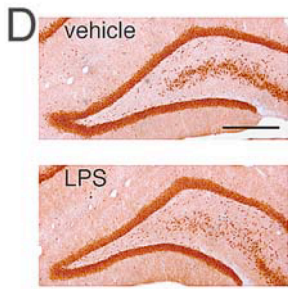

Figure 2 a, d

Figure 5 a, b

Figure 1 a, b, d

Paper D

Figure 2 a, b, c, d, e, i, j

Figure 8 a, d, e